DEVELOPMENT OF PHOTOREFRACTIVE POLYMERS:

SYNTHESIS AND CHARACTERIZATION OF POLYMERS WITH DONOR-π-ACCEPTOR GROUPS

Thesis submitted to

Cochin University of Science and Technology

in partial fulfillment of the requirements
for the award of the degree of

DOCTOR OF PHILOSOPHY
in
Polymer Chemistry
Under the Faculty of Technology

by

Dhanya R.
Department of Polymer Science and Rubber Technology
Cochin University of Science and Technology
Kochi - 682022, Kerala, India

July 2008

Development of Photorefractive Polymers: Synthesis and Characterization of Polymers with Donor-π-Acceptor Groups

Submitted by,

Dhanya R.

Dept. of Polymer Science and Rubber Technology

Cochin University of Science and Technology

Kochi - 22, Kerala, India

dhanya.ri@gmail.com

Research Supervisors

Dr. Rani Joseph

Professor, Dept. of Polymer Science and Rubber Technology

Cochin University of Science and Technology

Cochin - 682 022

rani@cusat.ac.in

Dr. K. Sreekumar

Reader, Dept. of Applied Chemistry

Cochin University of Science and Technology

Cochin - 682 022

ksk@cusat.ac.in

Dr. C. Sudha Kartha

Reader, Dept. of Physics

Cochin University of Science and Technology

Cochin - 682 022

csk@cusat.ac.in

Front cover : Molecules used for the preparation of a photorefractive system.

CERTIFICATE

Certified that the work presented in the thesis entitled "Development of Photorefractive Polymers: Synthesis and Characterization of Polymers with Donor-π-Acceptor Groups" is the bonafide record of research work done by Ms. Dhanya R. under our guidance at the Department of Polymer Science and Rubber Technology, Department of Applied Chemistry and Department of Physics, Cochin University of Science and Technology, Cochin, India - 682 022, and that it has not been included in any other thesis submitted previously for the award of any other degree/dipolma.

Kochi- 682 022
July, 2008

Prof. Rani Joseph
(Supervising Guide)

Dr. K. Sreekumar
(Co-Supervising Guide)

Dr. C. Sudha Kartha
(Co-Supervising Guide)

DECLARATION

I hereby declare that the work presented in this thesis is based on the original research work done by me under the guidance of Prof. Rani Joseph, Department of Polymer Science and Rubber Technology, Dr. K. Sreekumar, Department of Applied Chemistry and Dr. C. Sudha Kartha, Department of Physics, Cochin University of Science and Technology, Kochi, India - 682 022, and that it has not been included in any other thesis submitted previously for the award of any other degree/dipolma.

Kochi- 682 022
July, 2008

Dhanya R.

To my beloved Amma, Achan & Chettan

Acknowledgements

First and foremost, I bow before Him for the blessings showered on me.

During the course of my PhD, there have been many people who directly or indirectly motivated and inspired me. I would like to thank all of them for the support and help offered to me. First, I owe a deep debt of gratitude to my supervisor, Prof. Rani Joseph for her guidance, care, love, inspiration, encouragement, advice, solid support and prayers. I would like to extend my sincere gratitude to my co-supervisor, Dr. K. Sreekumar for his guidance, strong support, inspiration, help, scientific advice and valuable suggestions. I would also like to extend my sincere gratitude to my co-supervisor Dr. C. Sudha Kartha for her guidance, advice, support and help.

I would like to thank Dr. Thomas Kurian, Head, Department of PS&RT, Prof. K. E. George, Dr. Philip Kurian, Dr. Eby Thomas Tachil, Dr. Sunil K. Narayanankutty and Dr. Jayalatha for their encouragement and support during my research. I also like to thank the office staff and technical staff of PS&RT for their timely help and cooperation.

I would also like to thank Prof. Godfrey Louis, Head, Department of Physics and Prof. Vijaykumar for the cooperation and providing the necessary facilities in the Department. I am grateful to Dr. Girish Kumar, Head, Department of Applied Chemistry, for giving the permission to carry out cyclic voltammetric measurements in his lab.

I am indebted to the Department of Science and Technology (DST), Government of India, for the financial support through the research project.

I would also like to thank Sophisticated Analytical Instrument Facility, Punjab, Sophisticated Test and Instrumentation Center, Cochin and Central Drug Research Institute, Lucknow, India, for elemental, DSC, NMR and Mass spectral analysis.

I would like to express my heartfelt thanks to all the FIP teachers Sreenivasan sir, Jude sir, Dr. Lovely Mathew, Parameshwaran sir, Dr. Shiny Palaty, Bhuvaneshwary teacher, Joshi sir, Raju sir, Prema teacher, Mary teacher, Dr. Lakshmykutty Amma, Renjana teacher, Dr. Benny, Dr. Unnikrishnan and Suma teacher. I would like to thank Saritha, Dr. Anoop, Dr. Priya, Sinto, Nimmy, Abhilash, Ansu, Vijaylakshmi, Dr. Aswathy, Dr. Nisha, Dr. Rinku, Dr. Sreekala, Leny, Neena, Anna, Vidya, Ajeelesh and Reshmi for their love and support. I would like to thank Deepa, Anitha, Beena, Pramitha, Tina, Angel, Poornima, Ajimsha, Jayakrishnan, Sreeku-

mar, Vimal, Sreeroop, Sreekanth, Rajesh Menon, Rajesh C. S., Sajeesh, Jafar, Subrahmanyan, Rajesh Mon and Amarnath from the Department of Physics. I also thank Dr. Daly, Rajesh, Sindhu and Sreesha from the Department of Applied Chemistry. I am thankful to my seniors Dr. Soney, Dr. Ushamani, Dr. Lity, Dr. Thomas and Dr. Vipin for sharing their research experience and providing me valuable advice.

I would like to express my sincere gratitude to five of my close friends Dr. Maya, Dr. Honey, Bipin, Prayank and Newsun. I will never forget the inspiring words, affection and love offered to me at difficult times.

I profoundly thank Kishore for the strong support, care and help extended to me. Your friendship is very valuable to me. I learned a lot from you and I appreciate your experimental skills. I would like to extend my gratitude to my sister-in-law, Surekha for her love and affection. Finally, I would like to express my deepest gratitude to Amma, Achan and Chettan for their unwavering love, constant care, emotional support, encouragement and patience.

Dhanya R.

Preface

The photorefractive effect was first studied in inorganic crystalline materials in 1966. The phenomenon which makes photorefractive effect different from other mechanisms of grating formation is the energy transfer between two incident beams. The dephasing between the refractive index modulation and the initial light distribution are responsible for the above phenomenon. This effect is unique to photorefractive materials. In 1991, the photorefractive effect was first reported in polymers. High figure-of-merit, low dielectric constant and large electro-optic coefficients make polymers favorable for photorefractive device fabrication compared to inorganic crystals which are usually accompanied by high bulk dielectric constant and small figure-of-merit. In addition, low cost, ease of fabrication and structural flexibility of polymers have attracted technological interest.

The thesis is divided into seven chapters.

In **Chapter 1**, an introduction to photorefractive polymers is presented. The fundamentals and necessary requirements for photorefractivity are described. The various classes of photorefractive polymers with special emphasis on photoconducting and electro-optic molecules are discussed in detail.

Chapter 2 describes studies on two types of polymeric photoconductors. The first class involves those in which low molecular weight chromophores are dispersed in an inert polymer matrix, called molecularly doped polymers and the second in which photoconducting moiety is a part of the polymer. For the present study on molecularly doped polymers, 2,4,6-trinitrophenol was selected as the electron acceptor, aniline as electron donor and poly(methyl methacrylate) (PMMA) as inert polymer matrix. The electronic absorption spectra of molecules alone and in the dispersed state were recorded. The spectral dependence of photoconductivity was also studied. The main drawback with this class of materials is the possibility of phase separation due to large number of dopants in the polymer matrix which limits its application towards photorefractivity.

The second type of polymer system synthesized and studied was a non-conjugated copolymer, poly(2-methacryloyl-1-(4-azo-1'-phenyl)aniline-co-styrene). The structure of the polymer was confirmed by (^{1}H and ^{13}C) nuclear magnetic resonance (NMR) and fourier transform infra-red (FT-IR) spectroscopy. The number average ($\overline{M}_n$) and weight average ($\overline{M}_w$) molecular weight was determined using size exclusion chromatography (SEC). The

glass transition temperature, thermal stability and the degradation behavior was studied using differential scanning calorimetry (DSC) and thermogravimetry (TG). The lowest unoccupied molecular orbital (LUMO) and the highest occupied molecular orbital (HOMO) of the polymer were evaluated using cyclic voltammetry. A lock-in technique was used to study the spectral dependence of photocurrent. The effect of C_{60} as electron acceptor on the optical absorption and photocurrent behavior of the polymer was also studied.

The synthesis and characterization of a series polybenzoxazines is described in **Chapter 3**. Polybenzoxazines are non-conjugated polymers synthesized by Mannich condensation of phenol, formaldehyde and an amine. The Mannich base bridge characterizes the structure of the polymer. The structure of the synthesized polymer was confirmed by (^{1}H & ^{13}C) NMR and FT-IR spectroscopy. The molecular weight was determined using SEC. The glass transition temperature, thermal stability and the degradation behavior was studied using DSC and TG analysis. The electrochemical behavior of the polymer was studied using cyclic voltammetry. The spectral dependence of photocurrent was recorded on thin polymer film using lock-in technique. The effect of C_{60} as electron acceptor on the optical absorption and photoconductivity was also investigated. The polymer showed photocurrents in the visible region without any sensitizers. The polymer with highest photocurrent was selected for photorefractive studies.

The synthesis and characterization of electro-optic molecules based on a series of alkyl substituted p-nitroaniline possessing high ground state dipole moment are explained in **Chapter 4**. The length of the alkyl chain was varied by changing the number of alkyl spacers (n= 2-6). The structure of the synthesized chromophores was confirmed by elemental analysis, (^{1}H & ^{13}C) NMR, FT-IR and mass spectroscopy. The ground state dipole moment of the chromophores was determined using Debye-Guggenheim method and the excited state dipole moment by solvatochromic method. The chromophores with large figure-of-merit were selected and subjected to electro-optic studies. For electro-optic studies, the chromophores were embedded in PMMA matrix. The glass transition temperature of PMMA doped with the chromophores was studied using DSC. The electro-optic coefficient was measured using a transmission ellipsometric technique.

Chapter 5 deals with the synthesis and characterization of electro-optic copolymer, poly(3-methacryloyl-1-(4'-nitro-4-azo-1'-phenyl) phenylalanine-

co-methyl methacrylate). The structure of the polymer was confirmed using elemental analysis, (^{1}H & ^{13}C) NMR and FT-IR spectroscopy. The polymer comes under the class : Nonlinear Optical Chromophore Functionalized Side-Chain Polymers. In this system, the nonlinear optical chromophores are covalently bonded as a pendant group to the polymer backbone via spacers. The main advantage of nonlinear optical chromophore functionalized side chain polymers over guest-host systems is the absence of phase separation and greater stability towards orientational relaxation processes. The molecular weight was determined using SEC. The glass transition temperature, thermal stability and the degradation behavior was studied using DSC and TG analysis. The optical absorption spectrum of the polymer was also recorded. The electro-optic coefficient of the synthesized copolymer was measured using a transmission technique.

In **Chapter 6**, a novel photorefractive system based on the photoconductor, poly(6-tertiary-butyl-3-phenyl-3,4-dihydro-2H-1,3-benzoxazine), sensitized with C_{60} and the nonlinear optical molecule, 4-[N-ethyl-N-(2-hydroxyethyl)]amino-4-nitroazobenzene (Disperse Red 1, DR1), have been developed. N-ethylcarbazole was used as the plasticizer to lower the glass transition temperature of the photorefractive system. Attempts were made to develop several photorefractive systems using the nonlinear optical chromophore based on alkyl substituted p-nitroaniline and the electro-optic polymer, poly(3-methacryloyl-1-(4'-nitro-4-azo-1'-phenyl) phenylalanine-co-methacrylate). The glass transition temperature of the system was determined using DSC analysis. Photoconductivity and electro-optic studies were done on the sample. The photorefractive properties of this system was characterized by two-beam coupling.

The important conclusions drawn from various investigations are presented in **Chapter 7**. References are given towards the end of each chapter.

CONTENTS

CHAPTER

ONE

Photorefractive Polymers

1.1 Introduction

The term "*photorefractive*" literally means light-induced refractive index change. The photorefractive effect combines photoconductivity and electro-optic effect. It is a nonlocal process arising from physical motion of charges in the material. The spatial phase shift between the refractive index grating and the light intensity pattern is an important consequence of this effect which results in an asymmetric energy transfer between two mutually coherent laser beams interacting inside a photorefractive medium, called asymmetric two beam coupling.[1–3]

The photorefractive effect was first observed by Askin et al.[4] in 1966 in an inorganic $LiNbO_3$ crystal. Since then photorefractive materials have attracted tremendous attention due to potential applications in reversible holography, optical image processing, novelty filtering, phase conjugation and optical computing.[5–7] Today a wide range of inorganic crystals, such as $KNbO_3$, $BaTiO_3$, GaAs, $Bi_{12}SiO_{20}$ etc., are found to exhibit photorefractive effect.[8] The parameters (photoconductive sensitivity, and charge transport) which are required for photorefractive effect in these crystals strongly depend on the concentration of the impurities.[9] The high cost and the difficulty in growing crystals with high photorefractive perfor-

mance prevents their use in widespread technological applications.

In 1990, Sutter et al.[10,11] made first observation of photorefractive effect in an organic crystal, 2-cyclooctylamino-5-nitropyridine doped with tetracyanoquinodimethane. Growth of such doped organic crystals with high-quality was a difficult process since most dopants were expelled during the crystal preparation. Due to difficulty in high-quality crystal growth, research was focused on finding materials with ease of fabrication, good transparency and better cost effectiveness. In 1991, after the discovery of photorefractive effect in polymers, various research groups worked towards designing a wide variety of efficient photorefractive polymer systems. The first polymeric photorefractive system developed consists of bisphenol-A-diglycidyldiether-4-nitro-1,2-phenylenediamine, as nonlinear epoxy polymer and (diethylamino)benzaldehyde diphenylhydrazone, as hole-transport agent.[12]

To be photorefractive, the polymer must have charge generating, charge transporting and electro-optic properties. The mechanism of grating formation in photorefractive polymers is similar to that of inorganic crystals.[1] When two mutually coherent laser beams are made to interact in a material, light intensity pattern is created. In the bright areas of the fringes, mobile charge carriers are generated. Under the influence of an external field, the charge carriers migrate and eventually get trapped in the dark areas of the fringes. The resulting charge redistribution creates the space charge field in the material. This space charge field changes the refractive index of the material via electro-optic effect.[13]

In most of the photorefractive polymer systems, poly(N-vinyl carbazole) (PVK), was selected as charge transporting polymer due to high photogeneration efficiency and good charge transport properties. PVK was usually sensitized with suitable electron acceptors. The electron acceptor forms charge-transfer complex with PVK thereby showing high level of photoconductivity.[14,15] The linear electro-optic effect was provided by doping the photoconductor with dipolar molecules called nonlinear optical (NLO) chromophores. More than 200 cm^{-1} net two-beam coupling gain and near 100 % diffraction efficiency was observed in some PVK based photorefrac-

tive systems.[16] Apart from PVK, many other photoconducting polymers have been synthesized as good hosts with better charge-transporting properties for the development of photorefractive systems.

1.2 Requirements for Photorefractivity

1.2.1 Charge Generating Molecules

The first requirement of photorefractivity is the generation of mobile charge carriers in response to the spatially varying illumination. This can be achieved by the addition of suitable charge generating molecules. Charge generating molecules (electron acceptors) are species which when added to charge transport polymer generate mobile charge carriers at suitable long wavelengths. The chemical structures of some electron acceptors, tetracyanoquinodimethane (A1), 2,4,7-trinitrofluorenone (TNF), (A2), C_{60} (A3) and squaryllium dye (A4) are shown in Figure 1.1.

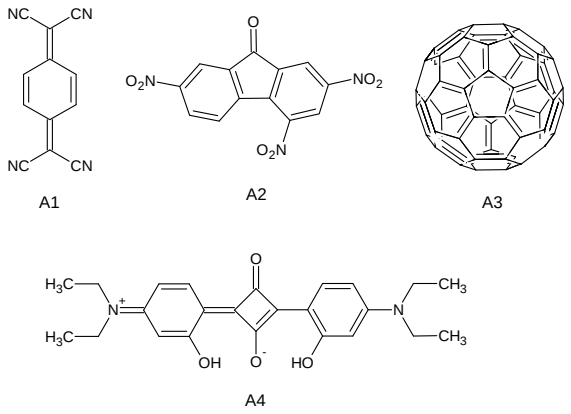

Figure 1.1: Chemical Structures of Charge Generating Molecules.

Most of the charge transporting polymers are photoconductive only in the UV region. The addition of electron acceptor shifts the absorption to the visible region of the spectrum by the formation of a charge transfer complex.[17] The formation of charge transfer complex arises from the partial transfer of charges from the HOMO of the electron donor to the LUMO

of the electron acceptor.[18] Aromatic systems with hetero atom behaves as electron donors and they can form molecular complexes with electron acceptor species. Electron donors are species with a low ionization potential and electron acceptors are species with high electron affinity. The applicability of an electron acceptor depends strongly on the ability of the electron acceptor to form a charge transfer complex with the electron donating unit of the photoconducting polymer or on the ability to transfer a hole to the charge transporting unit.

Silence et al.[19] evaluated the effect of electron acceptors on the performance of a photorefractive polymer system and found C_{60} as superior due to large enhancement in steady-state diffraction efficiency and initial rate of grating growth. Long wavelength absorption, low reduction potential and high triplet yield make C_{60} act as a good hole generator for polymeric photoconductors.

1.2.2 Charge Transporting Molecules

The second requirement for photorefractivity is transport of photogenerated charge carriers. The charge carriers move within the bulk of the polymer under the influence of an electric field until they are trapped. These traps are readily available in organic molecules as defect sites. Photoconductivity in polymers was first discovered in 1957 by H. Hoegl.[15] The first observation of photoconductivity was made on PVK and is the most widely studied organic photoconductor. PVK is usually obtained by the polymerization of N-vinylcarbazole (NVK). PVK is good photoconductor in the UV region. Addition of suitable electron acceptor to PVK enhances photoconductivity. In 1970, IBM introduced Copier I series, in which the organic photoconductor PVK sensitized with 2,4,7-trinitrofluorenone was used for the first time.[20] Since then a variety of other polymers with aromatic and heteroaromatic units were designed and synthesized as organic photoconductors. The photoconducting polymers are generally synthesized by cationic, anionic, free-radical, charge-transfer, ring-opening, co-ordination and electrochemical polymerization techniques.

Polymeric photoconductor used in practise are generally categorized

into five types of systems. The first class comprise molecularly doped polymers, in which charge generating and charge transporting molecules are dispersed in an inert polymer matrix. Examples of some commonly used inert polymer matrices such as PMMA (B1), polyvinylalcohol (B2), polyvinylchloride (B3), polystyrene (B4), bisphenol-A-polycarbonate (B5), etc.[21,22] are shown in Figure 1.2.

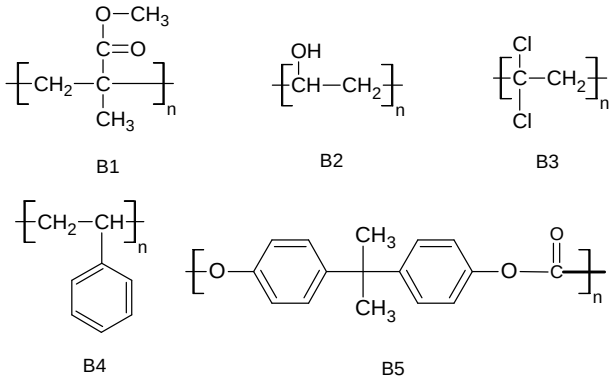

Figure 1.2: Chemical Structures of Inert Polymer Matrices.

Charge generating molecules are electron acceptors. For these type of molecules, the electron density on the ring system is very low due to the presence of strong electron withdrawing groups such as -NO_2, -CN, etc. The examples of some commonly used charge generator molecules are shown in Figure 1.1. Charge transporting molecules are strong electron donors. The electron density on the ring system in these type of molecules is very high due to the presence of strong electron donating amino groups. Examples of some charge transport molecules, N-ethylcarbazole (ECZ), (C1), 4-(N, N'-diethylamino)benzaldehydediphenyl hydrazone (C2) and N,N'-diphenyl-N,N'-bis(3-methylphenyl)-[1,1'-biphenyl]-4,4'-diamine (C3), are shown in Figure 1.3. Charge transport in molecularly doped polymers is a hopping process among the donor and acceptor species.[23,24] The electron donor species forms charge-transfer complex with the electron acceptor species.[14,25] The degree of charge transport determines the conducting and insulating behavior of molecularly doped polymers.

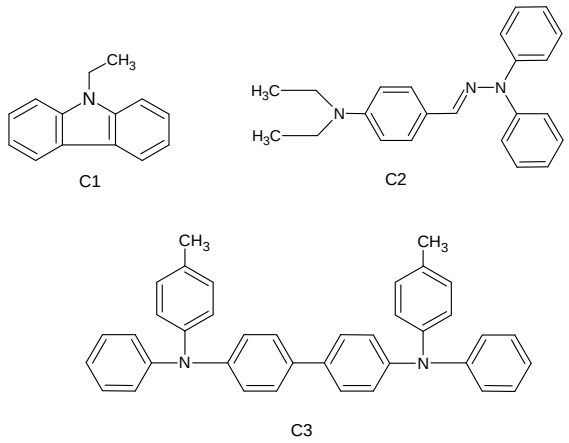

Figure 1.3: Chemical Structures of Charge Transport Molecules.

The second class consists of polymers with pendant or in-chain electronically isolated photoactive groups. In this class of polymers, the charge transporting unit is a part of the polymer chain. PVK, is the first known polymeric photoconductor with relatively stable radical cations and high charge carrier mobility.[15] After the discovery of photoconductivity in PVK, a wide variety of charge transporting polymers with carbazole units were synthesized and their photoconducting behavior was studied. The ease of introducing different substituent into the carbazole ring, low cost, high thermal and photochemical stability make carbazole based compounds attractive as charge transporting polymers. PVK was first synthesized in 1934 by the polymerization of NVK.[26] The polymerization of NVK can be initiated by cationic, free-radical, charge-transfer, co-ordination and electrochemical process.[27] Attempts were made to copolymerize N-vinylcarbazole with styrene, alkyl methacrylates, vinyl acetate and divinyl benzene.[28] All copolymers exhibit substantially lower photoconductivity than PVK. Photoconductivity in carbazole containing polymers was enhanced by introducing pendant dimeric carbazole units, in the side chain and main chain. The polymers were prepared by cationic and step growth polymerization of corresponding monomers. The photoconducting properties were studied both in the presence and absence of 2,4,7-

trinitrofluorenone and found to exhibit better photoconductivity than PVK-TNF system.[29] In order to enhance the charge carrier mobility, a series of polyacrylates and poly methacrylates, with pendant carbazole groups were prepared using radical polymerization. The high charge carrier mobility in these polymers could be attributed to the lack of excimer forming sites in it.[30,31]

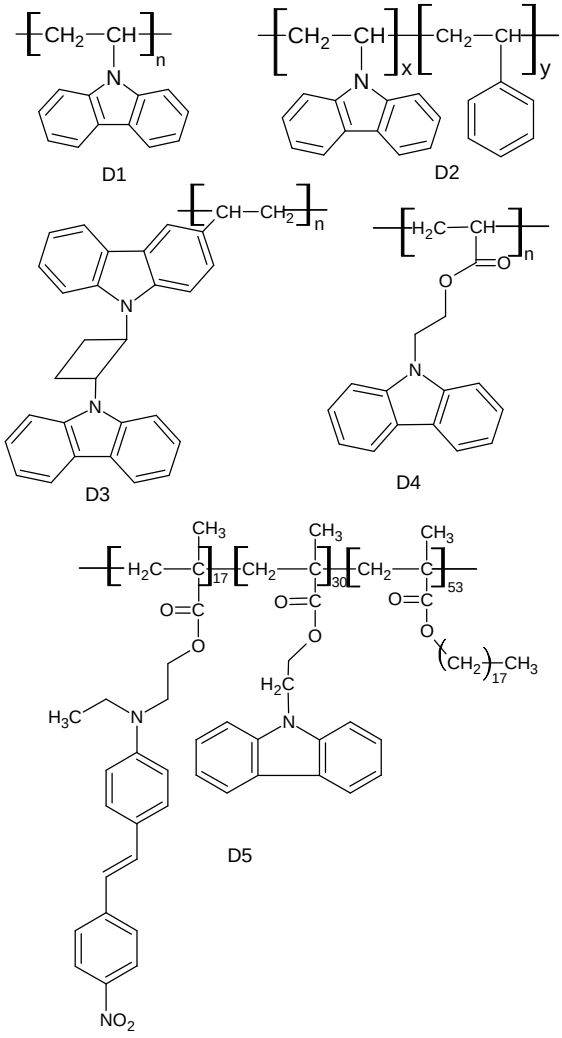

Figure 1.4: Chemical Structures of Pendant or In-chain Electronically Isolated Photoconducting Polymers.

Wada et al.,[32,33] synthesized a series of multi-functional polymers and oligomers having carbazole moieties in the main chain. The approach involves the synthesis of a fully-functional polymer, which combines all necessary functions, i.e. photoinduced charge generation, charge transport, and electro-optic nonlinearity, required for the development of a photorefractive system. Some examples of in-chain electronically isolated photoconducting polymers PVK (D1), poly(N-vinylcarbazole-co-styrene) (D2), poly(trans-1-(3-vinyl)carbazolyl)-2-(9-carbazolyl)cyclobutane) (D3), poly-(N-(2-carbazolyl)ethyl acrylate) (D4), and a fully functionalized carbazole containing polymer (D5), are shown in Figure 1.4.

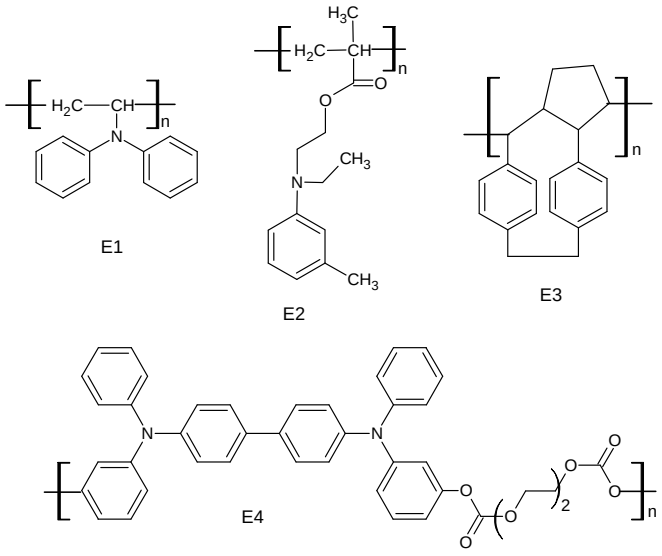

Figure 1.5: Chemical Structures of Non-Conjugated Photoconducting Polymers.

The third class consists of charge transporting polymers with non-conjugated main chain. The non-conjugated photoconducting polymers were synthesized via free radical, anionic, cationic and step growth polymerization techniques. Some of the examples of such type of polymers are poly(N-vinyldiphenylamine), poly(vinylarylamines) and polymers containing triphenyldiamine moieties.[34–36] These polymers were found to exhibit

charge carrier mobilities that exceed the values of PVK. The chemical structures of some of the non-conjugated polymers, poly(N-vinyl diphenylamine) (E1), poly(E,E-[6,2]-paracyclophane-1,5-diene) (E2), poly(2-(N-ethyl-N-3-tolylamino)ethyl methacrylate) (E3) and triphenyldiamine containing condensation polymer (E4), are shown in Figure 1.5.

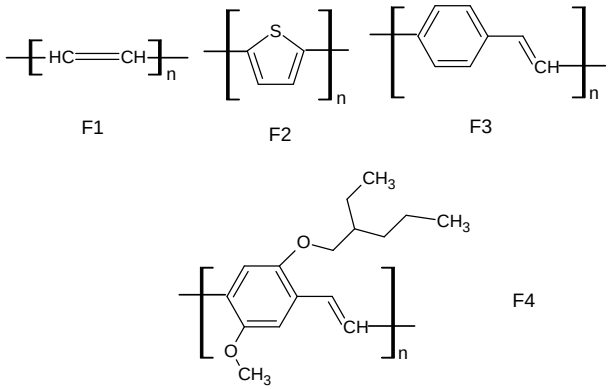

Figure 1.6: Chemical Structures of π- Conjugated Photoconducting Polymers.

The fourth class consists of photoconducting polymers with extended π-conjugated double bonds in the main chain. They are novel class of materials that combines optical and electronic properties of semiconductors. Now a days they are used as active components in photovoltaic cells, light-emitting diodes, photodiodes, solar cells, etc.[37–39] The ease of processing, low cost, good strength and flexibility make these class of polymers superior compared to conventional inorganic semiconductors. Examples of π-conjugated polymers are polyacetylene, poly(phenylenevinylene) and its derivatives, polythiophene, poly(3-alkylthiophenes), polybenzothiazoles, etc. The chemical structures of some of these polymers, polyacetylene (F1), polythiophene (F2), poly(p-phenylenevinylene) (F3) and poly(2-methoxy-5-(2'-ethyl)hexyloxy-p-phenylenevinylene) (F4), are shown in Figure 1.6. Conjugated polymers have band gaps in the range of 1-4 eV. In recent years, considerable research have been focused on designing conjugated polymers with low-band gap. The energy gap between HOMO and LUMO

determines the conducting properties of conjugated polymers. The energy band gap in conjugated polymers depends on the extent of conjugation. Greater the extent of conjugation, lower will be the band gap and hence better the electrical conductivity. These class of polymers are generally prepared by chemical or electrochemical oxidation methods.[40]

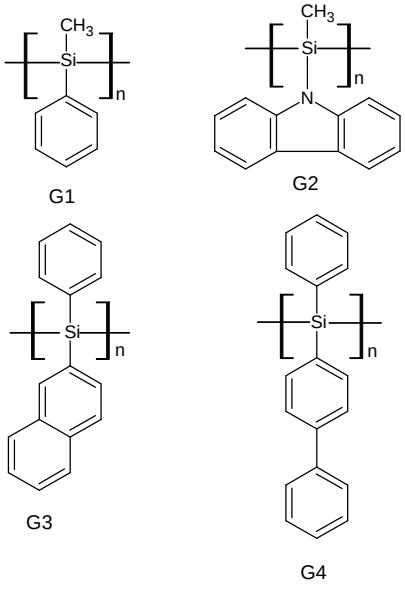

Figure 1.7: Chemical Structures of σ-Conjugated Photoconducting Polymers.

The fifth class consists of polymers with σ-conjugated main chain. Polysilanes comes under this category with a silicon backbone and carbon based side groups. They are p-type organic semiconductors with luminescence in the UV region of the spectra.[41,42] The charge carrier transport in these class of polymers proceeds predominantly along the σ-conjugated Si backbone. Some of the examples of polymers under this class are poly(methylphenylsilane) (G1), poly(methylcarbazolesilane) (G2), poly(2-naphtylphenylsilane) (G3), poly(phenyl-p-biphenylsilane) (G4). The chemical structure of these polymers are shown in Figure 1.7. Photoconductivity measurements on these polymer were performed by several groups.[43] The photoconductivity of polysilanes can be improved by the addition

of suitable charge generators such as C_{60}, TNF, etc. The drift mobility of polysilanes were found to be three orders of magnitude higher than PVK at room temperature. The photoconductivities and hole mobilities of polysilanes are largely influenced by the molecular weight, orientation, solid state properties and pendants on silicon atoms.[44,45] They are proved useful for a wide range of applications such as UV-photoresists, electrophotography, photorefractive devices etc. Several photorefractive composites with polysilane as photoconductor were studied in detail.[46] However, poor solubility of chromophores in the polysilane matrix resulted in low performance of photorefractive system. Attempts were made to design multifunctionalized polysilane photorefractive polymers.[47]

1.2.3 Electro-optic Molecules

The third requirement for photorefractivity is electro-optic effect. In recent years, organic electro-optic materials have been reported to offer several advantages over inorganic crystals due to low dielectric constant, high electro-optic coefficients and ease of synthesis.[48,49] They are promising candidates for a variety of applications such as optical memory, electro-optic modulator, frequency doubling, optical parametric amplification, polarization holography, nonlinear optical generator, etc.[50,51]

Electro-optic effect is defined as the change in the refractive index of a material in response to an electric field. In photorefractive polymer systems, the modulation in refractive index is achieved by electro-optic chromophores. Photorefractive polymer systems can be prepared either by dispersing charge transporting molecules into an electro-optic polymer or by dispersing electro-optic chromophores into a charge transport polymer.[52,53] Another approach is to design and synthesize fully-functionalized polymers with all active components needed for photorefractivity.[54]

Electro-optic chromophores are push-pull molecules possessing an electron donor group connected to an electron acceptor group through a π-conjugated bridge. The second-order optical nonlinearity in these chromophores arise from the intramolecular charge transfer between two groups of opposite nature.[55] Therefore, a typical NLO molecule can be repre-

sented as shown in Figure 1.8.

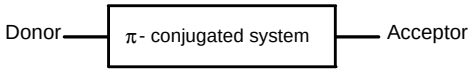

Figure 1.8: Chemical Structures of NLO Molecules.

The π-conjugated system could be benzene, azobenzene, stillbene, biphenyl, heterocycle, polyenes, tolans, etc. The electron acceptor groups attached to the π-conjugated system are NO_2, NO, CN, COOH, $CONH_2$, CONHR, $CONR_2$, CHO, SO_2R, COR, CF_3, $COCH_3$, $CH{=}C(CN)_2$, SO_2NH_2, $N_2{}^+$, $NH_2{}^+$, etc. and electron donor groups are NH_2, $NHCH_3$, $N(CH_3)_2$, NHR, N_2H_3, F, Cl, Br, I, SH, SR, OR, CH_3, OH, $NHCOCH_3$, OCH_3, SCH_3, OC_6H_5, $COOCH_3$, etc. A typical example of NLO molecule is p-nitroaniline, in which the electron donor NH_2 group is connected to electron acceptor NO_2 group by a aromatic benzene ring. One of the major challenges in this area of research is to design and synthesize NLO chromophores exhibiting large first molecular hyperpolarizability, good transparency and high thermal stability. There are four main classes of electro-optic molecules.

The first class comprises of guest-host polymer systems. The NLO chromophore with large molecular hyperpolarizability is incorporated into an amorphous host polymer matrix. Meredith et al.[56] reported one of the first guest-host systems in which the NLO chromophore, 4-(dimethylamino)-4'-nitrostilbene was incorporated into a side chain thermotropic nematic liquid crystalline polymer. Since then, a wide variety of NLO chromophores have been investigated as guests in a number of polymer hosts. One such thoroughly studied guest-host polymer system is PMMA dispersed with azo dye, 4-[N-ethyl-N-(2-hydroxyethyl)]amino-4-nitroazobenzene (Disperse Red 1, DR1).[57] The dipolar alignment of the chromophore in host polymer matrix was achieved by applying an electric field for a period of few minutes to several hours. Low dielectric constant, ease of processing into thin films, high mechanical strength, optical transparency, etc. are some of the advantages of guest-host systems. Two of the major problems encountered with these systems are: Fast decay of the NLO prop-

erties and the low concentration of NLO chromophores in the host polymer matrix. The chemical structures of some of the NLO chromophores such as 4-(dimethylamino)-4'-nitrostilbene (H1), Disperse Red 1, (H2), 1-(2'-ethylhexyloxy)-2,5-dimethyl-4-(4'-nitrophenylazo)benzene (H3), N,N-diethyl substituted para-nitroaniline (H4), 2,5-dimethyl-4-(p-nitrophenylazo)anisole (H5), 4-piperidin-4-ylbenzylidenemalononitrile (H6), (E)-4-N, N-diethylaminocinnamonitrile (H7), 3-fluoro-4-N,N-diethylamino-β-nitrostyrene (H8), etc., are shown in Figure 1.9.

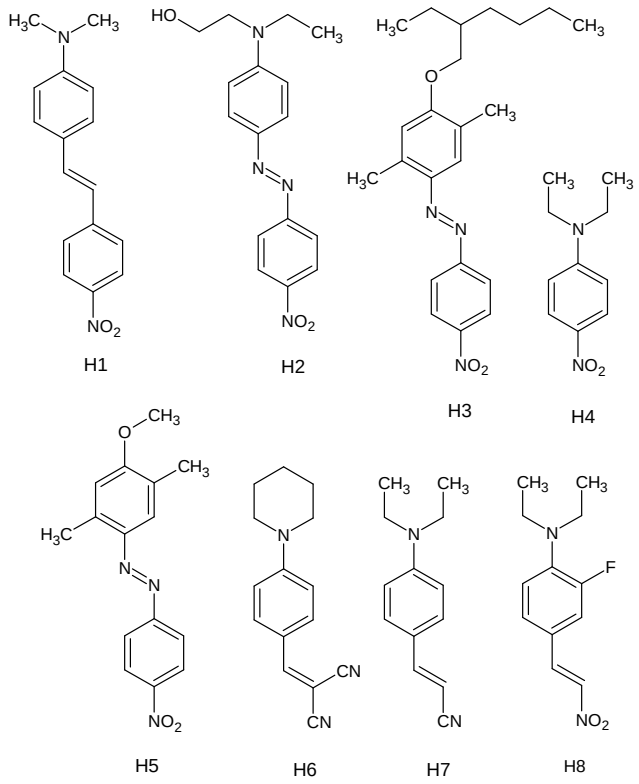

Figure 1.9: Chemical Structures of Electro-optic Molecules.

The second class consists of side-chain polymers. These are linear polymers with covalently attached NLO-active side groups. The NLO chromophores were attached to the polymer backbone via spacers. In this way, a high concentration of the NLO chromophores can be incorporated into

the polymer system without phase separation and crystallization. A number of side-chain polymers and copolymers of styrene, acrylic acid, methyl methacrylate, methacrylic acid, etc., were synthesized by chemically attaching the NLO chromophores.

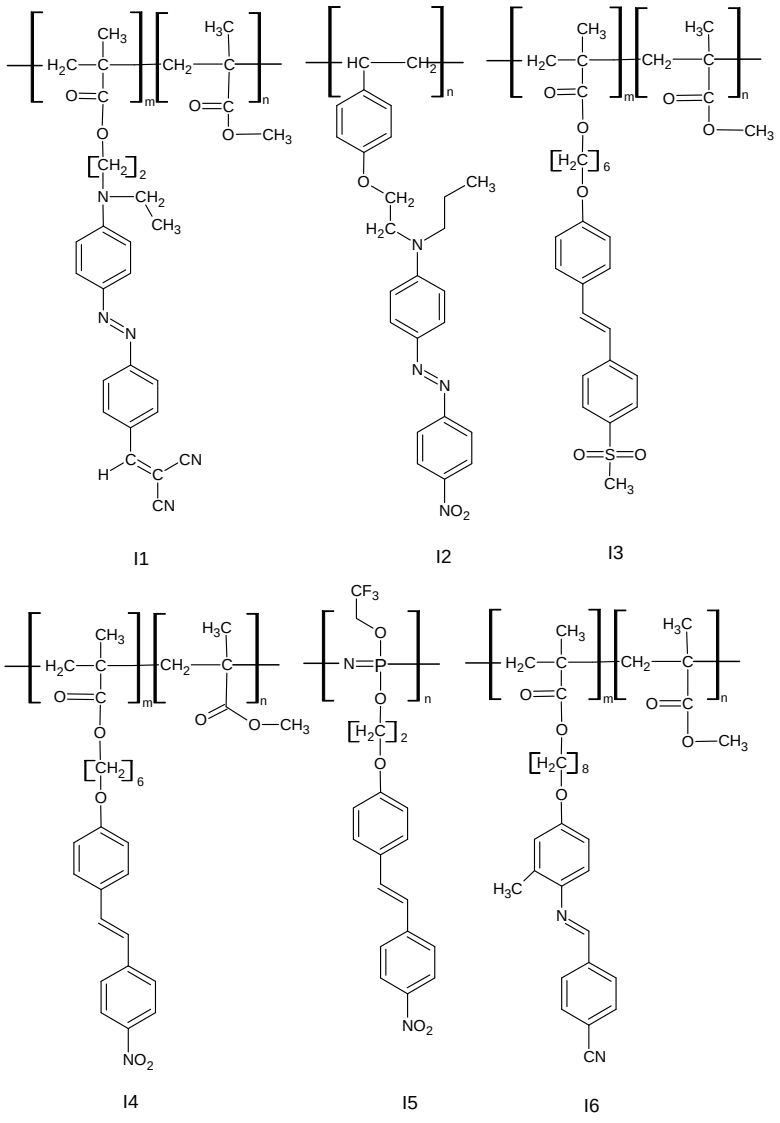

Figure 1.10: Chemical Structure of NLO-Functionalized Side-Chain Polymers.

Katz et al.,[58] reported the first side-chain system based on a random copolymer of methyl methacrylate and 4-(dicyanovinyl)-4'-(dialkylamino)-azobenzene-co-methacrylate (I1). The electro-optic coefficient (r_{33}) of the polymer was found to be 18 pm/V, measured at 799 nm. A wide variety of copolymers of disperse red 1 substituted methacrylate with methyl methacrylate have been synthesized for second-order nonlinear optics. Ye et al.,[59] has functionalized polystyrene with disperse red 1 (I2). Eich et al.,[60] covalently bonded the p-nitroaniline moieties to polyethylene type backbone. The side-chain polymers containing nitrostilbene moiety covalently linked to phosphazene backbone were reported by Allcock et al.[61] The nitrostilbene chromophores were attached to the polymer backbone through a tris(ethylene oxide) spacer group. (I5) Phosphazene polymers with different types of NLO dyes were synthesized. These polymers have low glass transition temperature below room temperature.

Singer et al.,[62] synthesized a copolymer of methyl methacrylate and dicyanovinyl terminated azo-dye by random copolymerization. Side-chain copolymers with a methacrylate backbone and sulfonyl-substituted alkoxy stilbenes (I3) as the NLO chromophores were reported by Philips Research Laboratories.[63] Recently, Chen et al.,[64] reported the synthesis of comb-shaped polymer containing methyl methacrylate and 4-[4-(methylacryloxy) octyloxy-2-methylphenyliminomethyl]cyanobenzene. (I6) The side-chain polymers having one aromatic ring NLO chromophores covalently attached to styrene and methacrylate (I4) backbone were reported by Hayashi et al.[65] The polymer showed slow decay of polar order. Some of the examples of NLO-functionalized side-chain polymers and copolymers are shown in Figure 1.10. NLO-functionalized side-chain polymer system showed enhanced stability towards orientational relaxation process compared to guest-host systems, because, the motion of the NLO chromophore is hindered as it is attached to the polymer. The orientational relaxation process can be further restricted by chemically attaching the NLO chromophores to the main-chain. The thermal stability and glass transition temperature for this system is higher than the guest-host system containing the same concentration of chromophore molecules.

The third class consists of NLO-chromophore functionalized main-chain polymers. The main-chain polymers can be divided into three groups with respect to the chromophore dipole arrangements along the polymer main chains, namely, head-to-tail, head-to-head, and random configuration. The head-to-tail or tail-to-head arrangement of the molecular dipoles might result in enhanced second order NLO activity. The T_g of the main-chain polymers ranges from 62 to 132 ^{o}C. The loading density of NLO chromophores in the main-chain polymer is high compared to side-chain polymers. Xu et al.[66] reported main-chain NLO polymer containing aminosulfone azobenzene chromophores (J1) randomly incorporated into the polymer backbone. A series of such polymers with polyurethane, polyester (J2) and polyacrylate backbone were synthesized and their NLO properties were investigated.

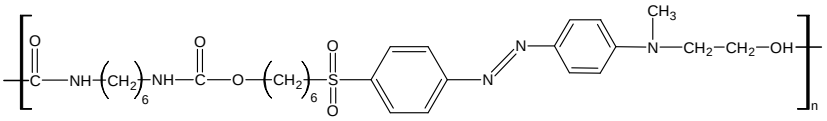

J1

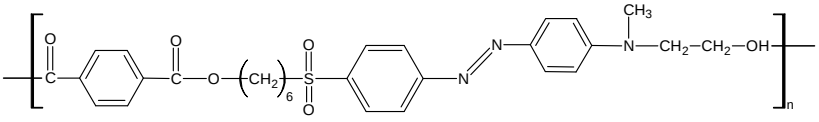

J2

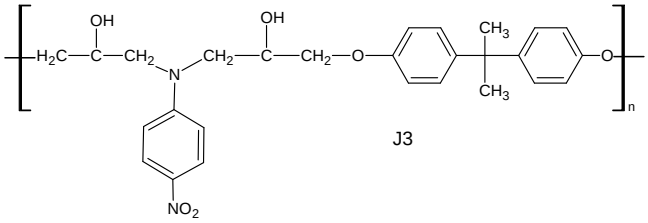

J3

Figure 1.11: Chemical Structures of NLO-Functionalized Main-Chain Polymers.

Main-chain polymers with the NLO chromophores perpendicular to the polymer backbone were also synthesized. Two of the examples of such type of polymers are: bisphenol-A-4-amino-4'-nitrotolan and bisphenol-

A-4-nitroaniline (J3).[67] The reported nonlinear optical coefficients of the poled main-chain polymers were significantly lower than those achieved for side-chain polymers. The difficulty in structure design, synthesis in head-to-tail fashion and low solubility are the disadvantages of these class of polymers which limits their wide spread use. The examples of NLO-functionalized main-chain polymers are shown in Figure 1.11.

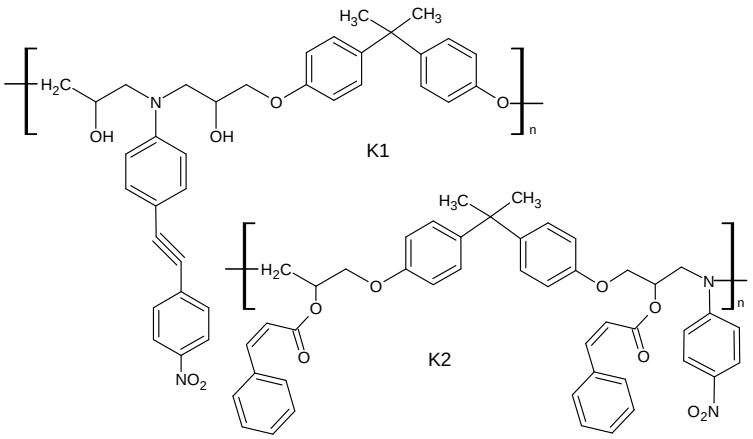

Figure 1.12: Chemical Structures of Crosslinked Polymers.

The fourth class consists of thermally crosslinked NLO polymers. In this class, polymers with side-chain or main-chain chromophores are transformed into a crosslinked network polymer via crosslinking agents. NLO-functionalized side-chain and main-chain polymers suffer from orientational and thermal stability. The interaction between the polymer chains can be minimized via formation of inter-chain chemical bonds or crosslinking. Several designing strategies (thermal and photochemical) were employed to develop crosslinked polymer systems. IBM group designed and synthesized various epoxy based crosslinked NLO polymers. The crosslinked polymers were synthesized by reacting bifunctional epoxy monomers with tetrafunctional nitro-substituted diamines.[68] The system with 20 % NLO loading exhibited no decay after three weeks at room temperature. Jungbauer et al.,[69] reported the crosslinking polymer containing 4-amino-4'-nitrotolane (K1). The polymer contains diglycidylbisphenol-A backbone.

Mandel et al.,[70] reported the synthesis of crosslinked polymer based on poly(vinyl cinnamate) with the NLO chromophore, 3-cinnamoyloxy-4-[4-(N,N-diethyamino)-2-cinnamoyloxyphenylazo]nitrobenzene via photochemical reaction. Zhu et al.,[71] reported photocrosslinked polymers containing cinnamoyl (K2) and styrylacrylol groups. The r_{33} values obtained for these systems were between 2-5 pm/V and are very stable compared to side-chain and main-chain polymers. Dalton et al.,[72] synthesized crosslinked polymer containing isocyanate groups. The polymer exhibited, r_{33} = 40-60 pm/V. Robello et al.,[73] reported the use of polyfunctional acrylates and methacrylates for photochemical crosslinking. Polymerization was initiated by using a variety of photochemical electron transfer sensitizer-activator combinations. Low solubility, brittleness, poor adhesion, etc., are some of the disadvantages of these class of polymers. Some of the examples of crosslinked NLO polymers are shown in Figure 1.12.

1.2.4 Plasticizers

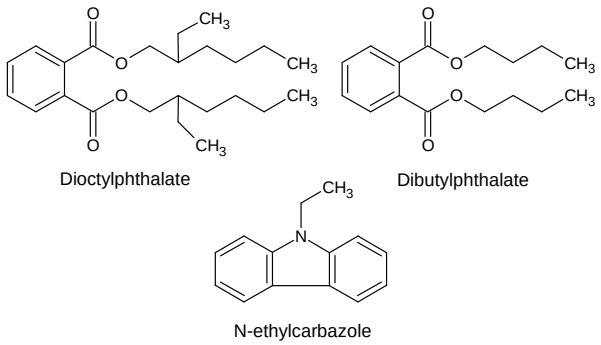

Figure 1.13: Chemical Structures of Inert and Charge-Transporting Plasticizers.

Plasticizers are organic molecules of moderate molecular weight and high boiling points. They are miscible with polymers. Addition of very small quantity of plasticizer to a polymer lowers the glass transition temperature (T_g) and enhances the flexibility. The effect of plasticizer in reducing T_g can be interpreted in several ways. Plasticizers function through a vary-

ing degree of solvating action on the polymer. They are inserted between polymer chains to increase intermolecular distance, thereby reducing the intensity of intermolecular bonding forces. Plasticizers are added to photorefractive polymer systems to lower the T_g. The lowering of T_g increases the orientational mobility of the NLO chromophores, resulting in large increase of electro-optic effect and photorefractive performance. There are two kinds of plasticizers, inert plasticizer and charge-transport plasticizer, used to lower the T_g of the photorefractive polymer system.[74–76] The chemical structure of the plasticizers are shown in Figure 1.13.

1.3 Photorefractive Polymer Systems

There are several methods for developing photorefractive polymer systems. Ducharme et al.,[12] reported the first observation of photorefractive effect in an electro-optic polymer, bisphenol-A-diglycidyldiether-4-nitro-1,2-phenylenediamine (Bis-A-NPDA), (70 wt%) doped with hole transport agent, (diethy1amino)benzaldehyde diphenylhydrazone (DEH), (30 wt%).

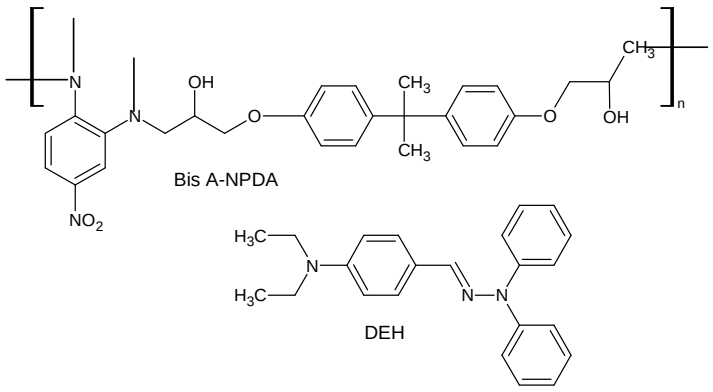

Figure 1.14: Photorefractive Polymer System with Electro-optic Polymer as Host for Charge Transport Molecules.

The photorefractive nature of this system was demonstrated by two-beam coupling. The photorefractive system was stable against phase separation. The tedious synthesis route and the difficulty in orienting the NLO

chromophores at room temperature, resulted in small electro-optic effect, hence their applicability to photorefractive systems was limited.

The simplest and thoroughly studied photorefractive polymer system is the guest-host system in which low molecular weight molecules with all desired properties are dispersed in an inert polymer matrix. Yokoyama et al.,[77] reported a guest-host photorefractive system with PMMA as a host for the charge transporting agent, DEH (30 wt%), a second-order NLO chromophore, (S)-(-)-1-(4-nitrophenyl)-2-pyrrolidinemethanol (NPP), (30 wt-%) and a charge generation sensitizer, squaryllium (SQ), (0.1 wt%). The chemical structure of the molecules are shown in Figure 1.15. The photorefractive effect was confirmed by the formation of a refraction grating with a phase-shift of 90^o in two beam coupling measurements. One of the drawbacks with guest-host systems is the phase separation due to the presence of large amount of low molecular weight dopants.

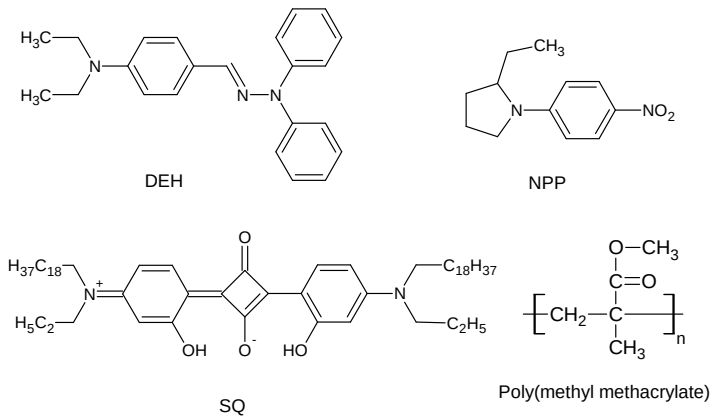

Figure 1.15: Guest-Host Photorefractive Polymer System.

One way to reduce large amount of low molecular weight dopants is to use bifunctional molecules. In bifunctional molecules, the charge transport and electro-optic functionality are present in a single molecule. They are more stable compared to guest-host systems due to lesser concentration of dopants in the inert polymer matrix.

Bolink et al.,[78] reported a novel bifunctional photorefractive poly-

mer system based on the charge-transport molecule N,N'-diphenyl-N,N'-bis(3-methylphenyl)-[1,1'-biphenyl]-4,4'-diamine (TPD). The bifunctional molecule, N-(4-[2,2-dicyanoethenyl)phenyl)-N'-phenyl-N, N'-bis(4-methyl phenyl)-[1,1'-biphenyl]-4,4'-diamine (MDCETPD), was found to be amorphous with a T_g of 110 ^{o}C. Dioctylphthalate (DOP) was used as plasticizer to decrease the T_g, C_{60} as charge generation sensitizer and polystyrene as inert polymer matrix. The study showed the bifunctional system to be photorefractive with a phase shift of approximately 90^0 between the illumination pattern and the refractive index grating. A diffraction efficiency of 6 % and a gain coefficient of 45 cm^{-1} was observed upon addition of small amounts of N,N,N',N'-tetramethyl-4-phenylenediamine (TMPD), as trap molecule.

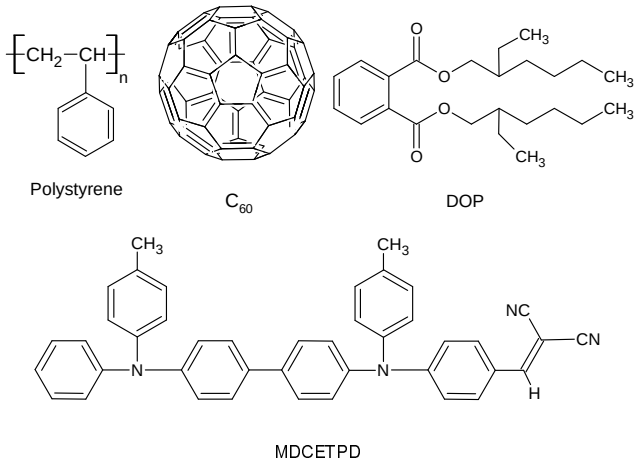

Figure 1.16: Bifunctional Photorefractive Polymer System.

Polymer systems with charge transporting polymer as host matrix for electro-optic and charge generating molecules, offered the best photorefractive performance. Several photorefractive systems with PVK as charge transporting polymer host for electro-optic molecules has been of interest. Zhang et al.,[79] reported the first PVK based photorefractive system with C_{60} (0.48 wt%) as charge generation molecule and 4-N,N-diethylamino-β-nitrostyrene (DEANST) (32 wt%) as a second-order NLO chromophore.

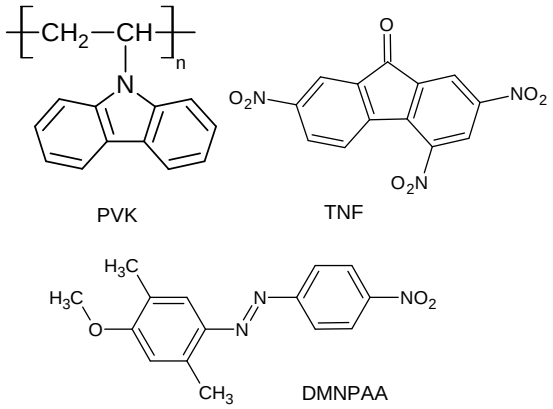

Figure 1.17: Photorefractive Polymer System with Charge Transport Polymer as Host for Electro-optic Molecules.

The high performance of the photorefractive effect was observed on a system based on PVK doped with the electro-optic chromophore 2,5-dimethyl-4-(p-nitrophenylazo)anisole (DMNPAA), with the photosensitizer TNF and plasticizer ECZ. The photorefractive polymer composite exhibited a steady-state diffraction efficiency near 100% and a two-beam coupling gain coefficient of more than 200 cm^{-1}.[80]

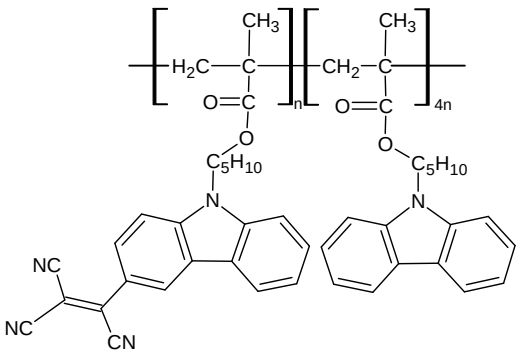

Figure 1.18: Multifunctional Photorefractive Polymer System.

Tamura et al.,[81] reported the first fully-functionalized photorefractive polymer. In this polymer, the carbazole group substituted with tricyanovinyl group has dual functions, charge generation and second-order nonlinear-

ity. Carbazole with no tricyanovinyl group offers a charge transporting function. The photorefractive polymer exhibited a photoconductivity of 9.8 X 10^{-10} Ω^{-1} cm^{-1} and an electro-optic coefficient of 6.1 pm V^{-1}. The evidence of photorefractive grating formation was confirmed by four-wave mixing experiments. The main advantage of multi-functional photorefractive polymer system is the stability towards phase separation.

1.4 Objective and Outline of the Thesis

The two major requirements for photorefractivity are photoconductivity and electro-optic effect. The main objective of the study was to synthesize and characterize a series of photoconducting polymers and electro-optic molecules and to develop a photorefractive system.

Chapter 2 starts with an initial study done on molecularly doped PMMA for photoconductivity. It also discuss synthesis, characterization, electrochemical and photoconductivity studies on a non-conjugated copolymer, poly(2-methacryloyl-1-(4-azo-1'-phenyl)aniline-co-styrene). The effect of C_{60} as electron acceptor on the optical absorption, and photocurrent behavior was also studied.

Chapter 3 focuses on synthesis and characterization, electrochemical and photoconductivity studies on a series of non-conjugated polybenzoxazines. The effect of C_{60} as electron acceptor on the optical absorption and photoconductivity was also investigated. The polymer with highest photoconductive sensitivity was selected for photorefractive studies.

In **Chapter 4**, the synthesis, characterization and electro-optic studies on a series of alkyl substituted p-nitroaniline are discussed. The ground state, excited state dipole moments and first hyperpolarizability of the chromophores were also determined.

Chapter 5 deals with synthesis and characterization of electro-optic copolymer, poly(3-methacryloyl-1-(4'-nitro-4-azo-1'-phenyl) phenyl-alanine-co-methyl methacrylate).

In **Chapter 6**, a novel photorefractive system based on the photo-

conductor poly(6-tertiary-butyl-3-phenyl-3,4-dihydro-2H-1,3-benzoxazine) sensitized with C_{60} and the NLO molecule disperse red 1 has been developed. Photoconductivity and electro-optic studies were done on the sample. The two-beam coupling gain coefficient of the photorefractive system was measured using the two-beam coupling technique.

The important conclusions drawn from various investigations are presented in **Chapter 7**.

References

[1] W. E. Moerner, S. M. Silence, Chem. Rev. 94 (1994) 127.

[2] A. V. Vannikov, A. D. Grishina, Russ. Chem. Rev. 72 (2003) 471.

[3] Y. Zhang, T. Wada, H. Sasabea, J. Mater. Chem. 8 (1998) 809.

[4] A. Ashkin, G. D. Boyd, J. M. Dziedzic, R. G. Smith, A. A. Ballmann, K. Nassau, Appl. Phys. Lett. 9 (1966) 72.

[5] C. Hohle, U. Hofmann, S. Schloter, M. Thelakkat, P. Strohriegl, D. Haarerb, S. J. Zilkerb, J. Mater. Chem. 9 (1999) 2205.

[6] E. Mecher, C. Brauchle, H. H. Horhold, J. C. Hummelenc, K. Meerholz, Phys. Chem. Chem. Phys. 1 (1999) 1749.

[7] B. Kippelen, F. Meyers, N. Peyghambarian, S. R. Marder, J. Am. Chem. Soc. 119 (1997) 4559.

[8] A. M. Glass, A. M. Johnson, D. H. Olson, W. Simpson, A. A. Ballman, Appl. Phys. Lett. 44 (1984) 948.

[9] E. Kratzig, H. Kurz, Opt. Acta 24 (1977) 475.

[10] K. Sutter, J. Hullinger, P. Gunter, Solid State Commun. 74 (1990) 867.

[11] K. Sutter, P. Gunter, J. Opt. Soc. Am. B 7 (1990) 2274.

[12] S. Ducharme, J. C. Scott, R. J. Twieg, W. E. Moerner, Phys. Rev. Lett. 66 (1991) 1846.

[13] O. Ostroverkhova, W. E. Moerner, Chem. Rev. 104 (2004) 3267.

[14] W. D. Gill, J. Appl. Phys. 43 (1972) 5033.

[15] H. Hoegl, J. Phys. Chem. 69 (1965) 755.

[16] A. Grunnet-Jepsena, C. L. Thompson, R. J. Twieg, W. E. Moerner, Appl. Phys. Lett. 70 (1997) 1515.

[17] G. Weiser, H. Seki, IBM .I. Res. Develop (1972) 598.

[18] A. El-Sayed, H. F. Mohamed, A. A. Boraei, Rad. Phys. Chem. 58 (2000) 791.

[19] S. M. Silence, C. A. Walsh, J. C. Scott, W. E. Moerner, Appl. Phys. Lett. 61 (1992) 2967.

[20] M. D. Schattuck, U. Vahtra, U.S. Pat. 3 (1969) 327.

[21] V. C. Kishore, R. Dhanya, C. S. Kartha, K. Sreekumar, R. Joseph, J. Appl. Phys. 101 (2007) 0631021.

[22] H. Tokuhisa, M. Era, T. Tsutsui, Synth. Met. 85 (1997) 1161.

[23] Y. Kanemitsu, J. Appl. Phys. 71 (1992) 3033.

[24] G. Juska, K. Genevicius, K. Arlauskas, R. Osterbacka, H. Stubb, Phys. Rev. B 65 (2002) 2332081.

[25] S. M. Teleb, A. S. Gaballa, Spectrochim. Acta, Part A 62 (2005) 140.

[26] W. Reppe, E. Keyssner, E. Dorrer, DRP 664 (1934) 231.

[27] J. Grazulevicius, P. Strohriegl, J. Pielichowski, K. Pielichowski, Prog. Polym. Sci. 28 (2003) 1297.

[28] M. Stolka, D. M. Pai, Adv. Polym. Sci. 29 (1978) 1.

[29] T. Inoue, S. Tazuke, J. Polym. Sci. 19 (1981) 261.

[30] R. Oshima, T. Uryu, M. Seno, Macromolecules 18 (1985) 1043.

[31] T. Uryu, H. Okhawa, R. Oshima, Macromolecules 20 (1987) 712.

[32] Y. D. Zhang, M. Yamamoto, T. Wada, H. Sasabe, J. Photopolym. Sci. Technol. 6 (1993) 201.

[33] Y. Zhang, L. Wang, T. Wada, H. Sasabe, Macromolecules 29 (1996) 1569.

[34] M. Stolka, D. M. Pai, D. S. Refner, J. C. Yanus, J. Polym. Sci. Polym. Chem. Ed. 21 (1983) 969.

[35] E. Bellmann, S. E. Shaheen, R. H. Grubbs, S. R. Marder, B. Kippelen, N. Peyghambarian, Chem. Mater. 11 (1999) 399.

[36] J. Kido, K. Harada, G. and. Nagai, Polym. Adv. Tecnnol. 7 (1996) 31.

[37] A. C. Arias, M. Granström, D. S. Thomas, K. Petritsch, R. H. Friend, Phys. Rev. B. 60 (1999) 1854.

[38] T. K. Daubler, D. Neher, H. Rost, H. H. Horhold, Phys. Rev. B 59 (1999) 1964.

[39] M. M. Alam, S. A. Jenekhe, Chem. Mater. 16 (2004) 4647.

[40] A.Ajayaghosh, Chem. Soc. Rev. 32 (2003) 181.

[41] H. Tang, Y. Liu, B. Huang, J. Qin, C. Fuentes-Hernandez, B. Kippelen, S. Lid, C. Ye, J. Mater. Chem 15 (2005) 778.

[42] W. Y. Ching, Y. N. Xu, R. H. French, Phys. Rev. B 54 (1996) 13546.

[43] H. Bassler, Adv. Mater. 5 (1993) 662.

[44] R. G. Kepler, J. M. Zeigler, L. A. Harrah, S. R. Kurtz, Phys. Rev. B35 (1987) 2818.

[45] K. A. Klingensmith, J. W. Downing, R. F. Miller, J. Michl, J. Am. Chem. Soc. 108 (1986) 7438.

[46] R. D. Miller, J. Michl, Chem. Rev. 89 (1989) 1359.

[47] D. Wright, U. Gubler, W. E. Moerner, M. S. DeClue, J. S. Siegel, J. Phys. Chem. B 107 (2003) 4732.

[48] Y. Cui, Y. Zhang, P. N. Prasad, J. S. Schildkraut, D. J. Williams, Appl. Phys. Lett. 61 (1992) 2132.

[49] B. Kippelen, K. Tamura, N. Peyghambarian, A. B. Padias, J. H. K. Hall, J. Appl. Phys. 74 (1993) 3617.

[50] Y. Zhang, C. A. Spencer, S. Ghosal, M. K. Casstevens, R. Burzynski, J. Appl. Phys. 76 (1994) 671.

[51] K. Khand, D. J. Binks, D. P. West, M. D. Rahn, J. Mod. Opt. 48 (2001) 93.

[52] S. Ducharme, B. Jones, J. M. Takacs, L. Zhang, Opt. Lett. 18 (1993) 152.

[53] Y. Zhang, C. A. Spencer, S. Ghosal, M. Casstevens, R. Burzynski, Appl. Phys. Lett. 64 (1994) 1908.

[54] Z. H. Peng, Z. N. Bao, Y. M. Chen, L. Yu, J. Am. Chem. Soc. 116 (1994) 6003.

[55] T. Verbiest, S. Houbrechts, M. Kauranen, K. Clays, A. Persoons, J. Mater. Chem. 7 (1997) 2175.

[56] G. R. Meredith, J. G. Vandusen, D. J. Williams, Macromolecules 15 (1982) 1385.

[57] K. D. Singer, J. Lalama, J. E. Sohn, SPIE Proc. 578 (1985) 130.

[58] H. Katz, K. Singer, J. Sohn, C. Dirk, L. King, H. Gordon, J. Am. Chem. Soc. 109 (1987) 656.

[59] C. Ye, T. J. Marks, J. Yang, G. K. Wong, Macromolecules 20 (1987) 2322.

[60] M. Eich, A. Sen, H. Looser, G. C. Bijorklund, J. D. Swalen, R. Twieg, D. Y. Yoon, J. Appl. Phys. 66 (1989) 2559.

[61] H. Allcook, A. Dembek, C. Kim, R. Devine, Y. Shi, W. Steier, C. Spangler, Macromolecules 24 (1991) 1000.

[62] K. D. Singer, M. G. Kuzyk, W. R. Holland, J. E. Sohn, S. J. Lalama, R. B. Comizzoli, H. E. Katz, M. L. Schilling, Appl. Phys. Lett. 53 (1988) 1800.

[63] G. L. J. A. Rikken, C. J. E. Seppen, S. Nijhuis, A. H. J. Venhuzen, Appl. Phys. Lett. 58 (1991) 435.

[64] Y. Chen, M. Rahman, T. Takahashi, B. Mandal, J. Lee, J. Kumar, S. K. Tripathy, Jpn. J. Appl. Phys. 30 (1991) 672.

[65] A. Hayashi, Y. Goto, M. Nakayama, K. Kaluzynski, H. Sato, T. Watanabe, S. Miyata, Chem. Mater. 4 (1992) 555.

[66] C. Xu, B. Wu, L. R. Dalton, P. M. Ramon, Y. Shi, W. H. Steier, Macromolecules 25 (1992) 6716.

[67] I. Teraoka, D. Jungbauer, B. Reck, D. Yoon, R. Twieg, C. Willson, J. Appl. Phys. 69 (1991) 2568.

[68] B. Kippelen, K. Meerholz, N. Peyghambarian, An Introduction to Photorefractive Polymers, CRC Press, 1997.

[69] D. Jungbauer, I. Teraoka, D. Yoon, B. Reck, J. Swalen, R. Twieg, C. Willson, J. Appl. Phys. 69 (1991) 8011.

[70] B. K. Mandel, Y. M. Chen, J. Y. Lee, J. Kumar, S. K. Tripathy, Appl. Phys. Lett. 58 (1991) 2459.

[71] X. Zhu, Y. M. Chen, L. Li, R. J. Jeng, B. K. Mandel, J. Kumar, S. K. Tripathy, Opt. Commun. 88 (1992) 77.

[72] X. Chenzeng, B. Wu, L. R. Dalton, Y. Shi, P. M. Ranon, W. H. Steier, Macromolecules 25 (1992) 6714.

[73] W. Kohler, D. Robello, C. Willand, D. Williams, Macromolecules 24 (1991) 4589.

[74] H. J. Bolink, V. V. Krasnikov, G. G. Malliaras, G. Hadziioannou, J. Phys. Chem. 100 (1996) 16356.

[75] M. E. Orczyk, J. Zieba, P. N. Prasad, J. Phys. Chem. 98 (1994) 8699.

[76] B. Kippelen, Sandalphon, N. Peyghambarian, S. R. Lyon, A. B. Padias, J. H. K. Hall, Electron. Lett. 29 (1993) 1873.

[77] K. Yokoyama, K. Arishima, T. Shimada, K. Sukegawa, Japn. J. Appl. Phys. 33 (1994) 1029.

[78] H. J. Bolink, C. Arts, V. V. Krasnikov, G. G. Malliaras, G. Hadziioannou, Chem. Mater. 9 (1997) 1407.

[79] Y. Zhang, Y. Cui, P. N. Prasad, Phys. Rev. B 46 (1992) 9900.

[80] B. Kippelen, Sandalphon, K. Meerholz, N. Peyghambarian, Appl. Phys. Lett. 68 (1996) 1748.

[81] K. Tamura, A. B. Padias, J. H. K. Hall, N. Peyghambarian, Appl. Phys. Lett. 60 (1992) 1803.

CHAPTER

TWO

Synthesis and Characterization of Photoconducting Poly(2-methacryloyl-1-(4-azo-1'-phenyl)aniline-co-styrene)

2.1 Introduction

Photoconducting polymers are the subject of intense study owing to their potential applications in photorefractive devices,[1] light emitting diodes,[2] photovoltaic[3] and many other optoelectronic devices. The possibility of adjusting the properties by modifying the structure is the attractive feature of polymeric systems. Photoconductivity in polymeric systems is a complex process involving absorption of radiation, generation of charge carriers, injection, transport, recombination and trapping.[4–6]

One of the necessary requirements for photorefractivity is photoconductivity.[7–10] The polymeric photoconductor used in practise are based on two type of systems. In the first, the charge transporting unit is a part of the polymer chain[11,12] and in the second, low molecular weight charge generating and charge transporting molecules are embedded in a polymeric matrix. These are called molecularly doped polymers.[13,14] A large number of polymers with charge-transporting units in the side chain and main chain, polymers with π-conjugated and σ-conjugated main chain were extensively studied.[6,15–17] Different classes of photoconducting poly-

mers were discussed in Chapter 1.

In this Chapter, two different types of polymeric photoconductors are described. The first one is a molecularly doped polymer. For the present study, 2,4,6-trinitrophenol (TNP) was selected as electron acceptor, aniline as electron donor and PMMA as inert polymer matrix. The second photoconducting polymer system is a copolymer of 2-methacryloyl-1-(4-azo-1'-phenyl)aniline and styrene. The synthesis and characterization of this copolymer are also described in this chapter.

2.2 Molecularly Doped Polymers

Systems with charge generating and charge transporting molecules dispersed in an inert polymer matrix, known as molecularly doped polymers, have been the subject of numerous investigations.[14] The charge generating units are usually electron acceptors or charge transfer complexes of acceptors with donor type molecules.[13,18–21] In molecularly doped polymers, charge transport is a hopping process among the donor–acceptor molecules.[22,23] The energetic disorder between the donor and acceptor plays an important role in hopping charge transport.[24,25] The inert polymer matrix affects the energetic disorder of hopping sites during charge transport.[24]

2.3 Experimental Section

2.3.1 Materials

Aniline (Merck, AR Grade) and methanol (Sd fine, AR Grade) were purified, dried and distilled by the standard procedures.[26] Chloroform (98%, Merck, Spectroscopic Grade) was used as received. 2,4,6-trinitrophenol (Sd Fine Chemicals, AR grade) was purified by two fold recrystallization using ethanol and dried under vacuum over P_2O_5 for three days. Poly(methyl methacrylate) (Mw-75,000) was reprecipitated thrice from chloroform-methanol and dried under reduced pressure.

2.3.2 Instrumentation

Absorption spectra of the samples were recorded using a Jasco V-570 UV/VIS/NIR spectrophotometer. The thickness of the film samples were measured using a Stylus (Dektak 6M) profiler.

2.3.3 Sample Preparation

The samples for photocurrent measurements were prepared by drop casting a solution of PMMA (7 wt%) containing TNP and aniline in chloroform. Three types of samples were prepared with TNP:aniline mole ratio as **1:0**, **1:1** and **1:100**. The concentration of TNP (0.0873 mmol) was kept low to reduce chances of phase separation. The solution was passed through a 0.2 μm PTFE filter and deposited on indium tin oxide (ITO) coated glass substrates. Overnight evaporation of the solvent at room temperature (28 ^{0}C) and subsequent drying of the films for 12 h in vacuum chamber (at 10^{-2} Torr), resulted in good optical quality films of about 16 μm thickness, measured using a Stylus profiler. Silver top contacts of 25 mm^2 active area were vacuum deposited on the slightly yellow polymer films.

Modulated photocurrent detection method using a lock-in-amplifier (Stanford SR830) coupled with a chopper (Stanford SR540) was used for the measurement of the photogenerated voltage across a load resistance connected in series with the sample and a high voltage DC power supply (Stanford PS350).[13] The spectral dependence of photocurrent was measured using the dispersed output of a Fluoromax-3 fluorimeter. The samples were irradiated from the ITO side.

2.4 Results and Discussion

Aromatic amines with unshared pair of electrons generally act as electron donors. Electron acceptors on the other hand are electron deficient species.[27] The molecularly doped polymer (MDP) system chosen for the present study contains aniline as electron donor and TNP as electron acceptor. Aniline and TNP were dispersed in PMMA. The molecular structures

of PMMA, aniline and TNP are shown in Figure 2.1. A charge transfer complex formation was evident from the optical absorption spectra of the MDP compared to individual molecules.

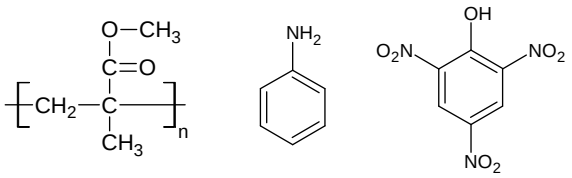

Figure 2.1: Chemical Structures of Poly(methyl methacrylate), Aniline and 2,4,6-trinitrophenol.

2.4.1 Optical Absorption

The absorption spectra of aniline, TNP, TNP: aniline (**1:1**) and TNP:aniline (**1:100**) dispersed in PMMA are shown in Figure 2.2.

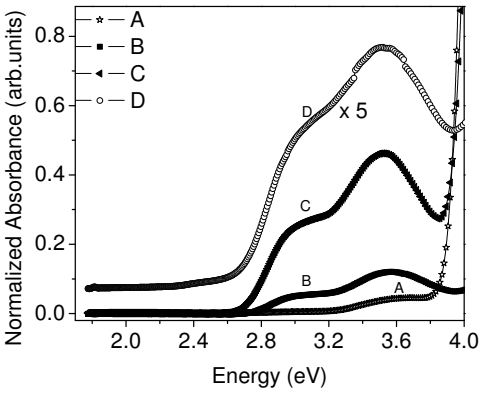

Figure 2.2: UV-Vis Absorption Spectra of Aniline (A), 2,4,6-trinitrophenol (B), 2,4,6-trinitrophenol:Aniline (1:1),(C) and 2,4,6-trinitrophenol:Aniline (1:100),(D) in Poly(methyl methacrylate) Matrix.

The absorption spectrum of TNP:aniline in **1:1** mole ratio showed bathochromic and hyperchromic shifts compared to neat samples indicating formation of a charge-transfer complex between aniline and TNP.[13] The spectrum of TNP:aniline in **1:100** mole ratio showed an increase in absorbance,

implying a strong dependence on the concentration of the donor molecules.

2.4.2 Photocurrent Action Spectrum

The photocurrent action spectra of TNP:aniline in **1:1** mole ratio and **1:100** mole ratio in PMMA at an electric field of 20 V/μm are shown in Figure 2.3.

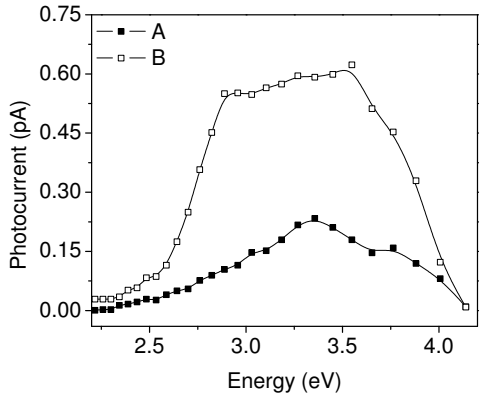

Figure 2.3: Photocurrent Action Spectra of 2,4,6-trinitrophenol: Aniline (1:1), (A) and 2,4,6-trinitrophenol: Aniline (1:100), (B) in Poly(methyl methacrylate) Matrix.

The sample with **1:1** mole ratio of TNP and aniline showed a maximum photocurrent of 0.23 pA (at 3.35 eV). Further addition of aniline molecules as a **1:100** resulted in considerable increase of photocurrent. The maximum photocurrent observed for TNP and aniline in **1:100** sample was 0.6 pA (at 3.35 eV). In the visible region (at 2.9 eV), the maximum photocurrent observed was 0.10 pA (**1:1**) and 0.55 pA (**1:100**) respectively. The decrease of photocurrent in TNP:aniline complex with **1:1** ratio may be due to the release of lesser number of free charge carriers. Photocurrent as function of applied electric field and intensity are studied and reported in detail elsewhere.[13] An increase was observed in photocurrent upon increasing the electric field. The intensity dependence of photocurrent showed linear behavior indicating absence of bimolecular recombination and heating effects. The system showed a photoconductive sensitivity of the order

of 10^{-13} S cm/W. The main drawback with this system was the phase separation upon addition of excess dopants. Also, the photoconductive sensitivity of this system was very low.

2.5 Photoconducting Poly(2-methacryloyl-1-(4-a-zo-1'-phenyl)aniline-co-styrene)

Molecularly doped systems have attracted great attention because of their importance in the construction of transport theories in amorphous photoconductors.[22] The main drawback with these systems is phase separation due to the presence of large number of low molecular dopants in the inert polymer host matrix.[28] Hence the application of molecular doping towards stable photorefractive polymer systems is limited. In order to decrease the chances of phase separation, polymers were synthesized with charge transporting units chemically attached to the main chain or as side chain.[29–31] Most of the photorefractive systems studied to date consist of charge transporting polymers as host for a wide variety of electro-optic chromophores.[5,32,33]

In this section, the synthesis and characterization of a non-conjugated photoconducting copolymer, poly(2-methacryloyl-1-(4-azo-1'-phenyl)aniline-co-styrene) is described in detail. The LUMO and the HOMO levels of the polymer were evaluated using cyclic voltammetry. The lock-in technique described earlier was used to study the spectral dependence of photocurrent. The effect of C_{60} as electron acceptor on the optical absorption and photocurrent behavior of the polymer was also studied.

2.6 Experimental Section

2.6.1 Materials

Styrene (Alfa Aesar, 97 %) was shaken with a 10 % sodium hydroxide solution to remove the inhibitor, washed with distilled water, dried over anhydrous calcium chloride and distilled under reduced pressure. Tetrahy-

drofuran (THF) (Rankem, AR Grade), methanol (S.d. Fine, AR Grade) and toluene (Rankem, AR Grade) were purified, dried and distilled by the standard procedures.[26] Fullerene (Alfa Aesar, 97 %) was dried under vacuum over P_2O_5 for three days. The following were used as received: Concentrated hydrochloric acid (Merck, AR Grade), sodium nitrite (Merck, AR Grade), crystallized sodium acetate (Merck, AR Grade), petroleum ether (Merck, AR Grade), diethylether (Rankem, AR Grade), glacial acetic acid (Merck, AR Grade), carbontetrachloride (Merck, AR Grade), pyridine (Alfa Aesar, 97 %), methacryloyl chloride (Alfa Aesar, 97 %), sodium carbonate (S.d. Fine, AR Grade), anhydrous sodium sulfate (Alfa Aesar, 97 %), methylene chloride (Alfa Aesar, 97 %), azobisisobutyronitrile (Spectrochem, 97 %), dimethyl formamide (DMF) (Spectrochem, Spectroscopic Grade, 98 %) and chloroform (Merck, Spectroscopic Grade, 98 %).

2.6.2 Instrumentation

NMR spectra were recorded with Bruker Advance II NMR spectrometer operating at 400 MHz for ^{1}H and at 100 MHz for ^{13}C. FT-IR spectra of the samples were taken on a Bruker 550 spectrometer. Absorption spectra of the samples were recorded using a Jasco V-570 UV/VIS/NIR spectrophotometer. A Fluoromax-3 fluorimeter was used to record the fluorescence spectra of the samples. CHN estimations were taken from Elementar Vario EL III CHNSO elemental analyzer. The molecular weight of the synthesized polymers was determined by SEC, (Waters 2414) using a column packed with polystyrene gel beads. Toluene was used as the eluent and the molecular weight was calibrated using polystyrene standards. The molecular weight was further estimated with Jeol SX 102 mass spectrometer. Glass transition temperature was determined from DSC, (Q-100, TA Instruments) under nitrogen at heating rate of 10 ^{o}C/min. Thermal stability was determined from TGA, (Q-50, TA Instruments) under nitrogen at a heating rate of 20 ^{o}C/min. Electrochemical measurements were performed in a three electrode BASi Epsilon electrochemical workstation.

2.6.3 Synthesis

2.6.3.1 Synthesis of Diazoaminobenzene

Aniline (14 g, 150 mmol) dissolved in hydrochloric acid (4 M) was cooled to 0^0 C. The solution was kept in an ice-bath under magnetic stirring. A solution of sodium nitrite (5.2 g, 75.36 mmol) in distilled water (12 mL) was cooled to 0^0 C. This cold solution was added drop wise to aniline solution with constant stirring. Crushed ice (50 g) was introduced into the system to keep the temperature at 0^0 C. Crystallized sodium acetate (21 g, 256 mmol) dissolved in distilled water (40 mL) was added to the above mixture, upon which a yellow solid precipitated. The solid was collected via filtration and washed with cold distilled water (250 mL). The compound was recrystallized from light petroleum.

Yield: 89 %; mp: 95-96 ^{o}C. FTIR (KBr) ν cm^{-1}: 3332 (aromatic NH st), 1454 (-N=N st), 3201 (aromatic CH st), 1600-1545 (aromatic C=C st). ^{1}H NMR (400 MHz $CDCl_3$) δ: 4.77 (s, 1H), 9.71 (m, 1H), 7.24-7.49 (m, 2H) 7.14-7.53 (m, 2H), 7.99 (m, 1H). ^{13}C NMR (100 MHz $CDCl_3$) δ: 117.93, 130.72, 121.11, 129.59, 117.93, 125.24, 122.78. Mass (m/e): 197 (molecular ion peak). Anal. Calcd for: $C_{12}H_{11}N_3$ - C, 73.07; H, 5.62; N, 21.30. Found: C, 73.15; H, 5.60; N, 21.25.

2.6.3.2 Synthesis of p-Aminoazobenzene

At first, aniline hydrochloride was prepared by treating aniline (2 g, 21.50 mmol) with HCl (3 mL, 12 M) and this mixture was cooled to 0^0 C. Upon cooling, the off white solid precipitated out was filtered and washed with diethylether.

Finely crushed diazoaminobenzene (5 g, 25.38 mmol) was dissolved in aniline (15 g, 161.29 mmol). Aniline hydrochloride (2.5 g, 19.37 mmol) was added to it. The reaction mixture was heated at 40-45 ^{o}C for 1 h and the reaction was allowed to stand for further 30 min. The aniline present in excess was removed as a soluble acetate by treating with glacial acetic acid (15 mL) diluted with distilled water (15 mL). The mixture was stirred for 15 min, during which, precipitation of p-aminoazobenzene

was observed. The precipitate was filtered and washed several times with distilled water. The orange-yellow solid obtained was recrystallized from carbontetrachloride.

Yield: 68 %; mp: 125 ^{o}C. FTIR (KBr) ν cm^{-1}: 3323, 3315 (aromatic NH_2 st), 1452 (-N=N st), 3207 (aromatic CH st), 1600-1540 (aromatic C=C st). ^{1}H NMR (400 MHz $CDCl_3$) δ: 2.21 (s, 2H), 9.71 (m, 1H), 7.24-7.49 (m, 2H) 7.14-7.53 (m, 2H), 7.99 (m, 1H). ^{13}C NMR (100 MHz $CDCl_3$) δ: 114.54, 130.72, 121.11, 129.59, 117.93, 125.24, 122.78, 145.17, 149.74. Mass (m/e): 197 (molecular ion peak). Anal. Calcd for: $C_{12}H_{11}N_3$ - C, 73.07; H, 5.62; N, 21.30. Found: C, 73.10; H, 5.62; N, 21.28.

2.6.3.3 Synthesis of 2-Methacryloyl-1-(4-azo-1'-phenyl)aniline

p-Aminoazobenzene (2.0 g, 10.16 mmol) was dissolved in 25 mL dry THF under N_2. To the solution, pyridine (0.1 g, 1.26 mmol) and methacryloyl chloride (1 mL, 10.26 mmol) were added drop wise simultaneously. The reaction was carried out at 0^0 C with magnetic stirring for 3 h and then at room temperature for 48 h. The resulting mixture was washed with HCl (0.1 M), Na_2CO_3 (5 %) and finally with distilled water. The excess solvent was evaporated under reduced pressure. The organic layer was dried over anhydrous Na_2SO_4. The reaction product obtained was purified by column chromatography using methylene dichloride.

Yield: 72 %; mp: 128 ^{o}C. FTIR (KBr) ν cm^{-1}: 1454 (-N=N st), 3332 (aromatic NH st), 3207 (aromatic CH st), 1600-1545 (aromatic C=C st), 1715 (C=O st), 1674 (H_2C=C), 2958, 2849 (sy & ay C-H st). ^{1}H NMR (400 MHz $CDCl_3$) δ: 1.72 (s, 1H), 9.71 (m, 1H), 7.24-7.49 (m, 2H), 7.14-7.53 (m, 2H), 7.99 (m, 1H), 1.59 (s, 3H), 4.15 (s, 2H). ^{13}C NMR (100 MHz $CDCl_3$) δ: 160.73, 130.72, 121.11, 129.59, 117.93, 125.24, 122.78, 145.17, 149.74, 24.36, 114.54. Mass (m/e): 265 (molecular ion peak). Anal. Calcd for: $C_{16}H_{15}N_3O$ - C, 72.43; H, 5.70; N, 15.84. Found: C, 72.45; H, 5.73; N, 15.82.

2.6.3.4 Polymerization

2-methacryloyl-1-(4-azo-1'-phenyl)aniline (1 g, 3.77 mmol), styrene (0.39 g, 3.75 mmol) and azobisisobutyronitrile (2 g, 12.19 mmol) were dissolved in dry DMF (35 mL). The reaction was carried out at 110 ^{o}C for 72 h, under N_2. The resulting solid was dissolved in DMF and reprecipitated from methanol. Polymer was collected by filtration, dried under vacuum, and obtained as a dark brown powder.

Yield: 68 %. FTIR (KBr) ν cm^{-1}: 1460 (-N=N st), 3332 (aromatic NH st), 3207 (aromatic CH st), 1600-1545 (aromatic C=C st), 1715 (C=O st), 2924 (H_2C), 2958, 2849 (sy & ay C-H st, -CH_3). ^{1}H NMR (400 MHz $CDCl_3$) δ: 2.21 (s, 1H), 9.71 (m, 1H), 7.24-7.49 (m, 2H), 7.14-7.53 (m, 2H), 7.99 (m, 1H), 0.40 (s, 3H), 2.21, 2.17 (s, 4H). ^{13}C NMR (100 MHz $CDCl_3$) δ: 160.73, 130.72, 121.11, 129.59, 117.93, 125.24, 122.78, 145.17, 149.74, 21.54, 44.21, 40.43.

2.6.4 Sample Preparation

The samples for photocurrent measurements were prepared by drop casting an 8 wt% solution (7 mL) of the polymer and DOP (1 wt%) in chloroform. The polymer:C_{60} composite was prepared by dissolving of C_{60} (6.55 x 10^{-6} moles) and dioctylphthalate (1 wt%) in 8 wt% solution (7 mL) of the polymer in chloroform. The concentration of C_{60} molecules were kept at 10^{-5} moles/litre. The solution was passed through a 0.45 μ Nylon filter and deposited on ITO coated glass substrates. Overnight evaporation of the solvent at room temperature (28 ^{0}C) and subsequent drying of the films for 12 h in vacuum chamber (at 10^{-2} Torr), resulted in good optical quality films of about 15 μm thickness, measured using a Stylus profiler. Silver top contacts of 36 mm^2 active area were deposited on the polymer films. Photoconductivity measurements were done using the modulated photocurrent technique.[13]

2.7 Results and Discussion

2.7.1 Synthesis and Characterization

Poly(2-methacryloyl-1-(4-azo-1'-phenyl)aniline-co-styrene), comes under the class of polymers with side chain electronically isolated photoconducting groups discussed in Section 1.2.2. It is a copolymer of 2-methacryloyl-1-(4-azo-1'-phenyl)aniline and styrene. The polymer was synthesized via radical initiated polymerization of 2-methacryloyl-1-(4-azo-1'-phenyl)aniline and styrene, using solution polymerization technique.

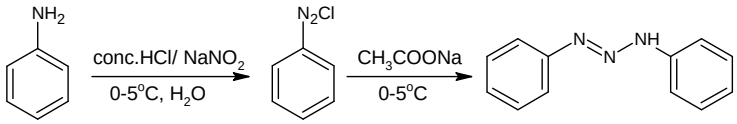

Figure 2.4: Synthesis Route of Diazoaminobenzene.

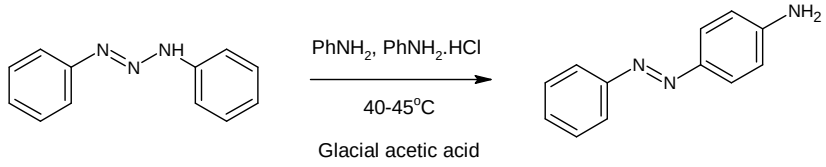

Figure 2.5: Synthesis Route of p-Aminoazobenzene.

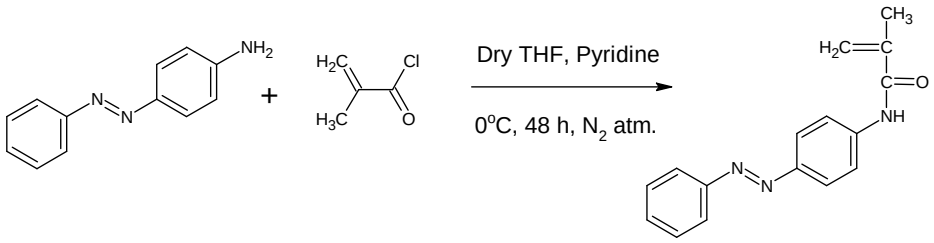

Figure 2.6: Synthesis Route of 2-Methacryloyl-1-(4-azo-1'-phenyl)aniline.

The synthesis route of monomers diazoaminobenzene, p-aminoazobenzene and 2-methacryloyl-1-(4-azo-1'-phenyl)aniline are shown in Figure 2.4, Figure 2.5 and Figure 2.6. Diazoaminobenzene and p-aminoazobenzene were

obtained by the standard diazotization of benzenamine. The synthesis of 2-methacryloyl-1-(4-azo-1'-phenyl)aniline was carried out by reacting p-aminoazobenzene and methacryloyl chloride. The monomers were obtained in acceptable yields. The monomers have good solubility in common organic solvents such as THF, DMF, chloroform, acetone and acetonitrile. The structure of monomers were confirmed using elemental analysis, FT-IR, (^{1}H & ^{13}C) NMR and mass (FAB-MS) spectral analysis.

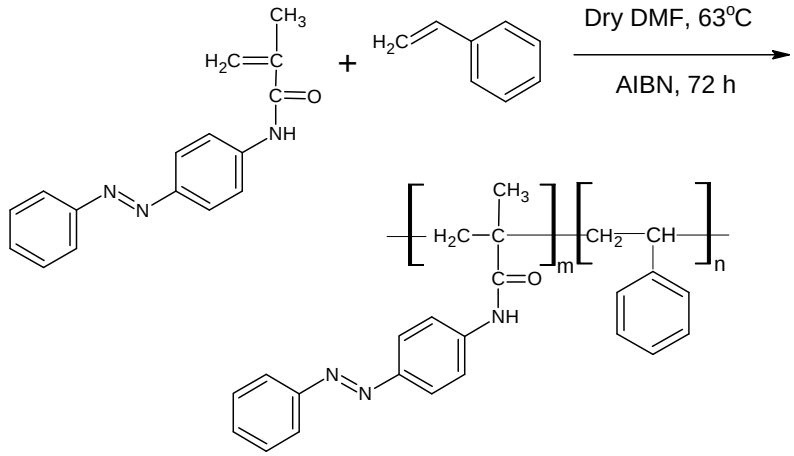

Figure 2.7: Synthesis Route of the Polymer.

The synthesis route of poly(2-methacryloyl-1-(4-azo-1'-phenyl)aniline-co-styrene) is shown in Figure 2.7. Copolymerization of 2-methacryloyl-1-(4-azo-1'-phenyl)aniline was carried out in dry DMF using azobisisobutyronitrile (AIBN) as a radical initiator. The polymer was obtained in moderate yield (68 %) with good solubility in common organic solvents such as chloroform, acetone, THF, DMF, toluene and acetonitrile. The structure of the polymer was confirmed using FT-IR and (^{1}H & ^{13}C) NMR spectroscopy. The average molecular weight and polydispersity index of the polymer were determined using SEC. The polymer can be processed into thin transparent films. The polymer has a deep brown color.

The ^{1}H NMR spectrum of the polymer is shown in Figure 2.8. The detailed spectral values of monomers and polymer are given in the section 2.6.3. The resonance peak at 2.21 ppm correspond to proton of the

NH group. The peaks at 7.82, 7.10, 7.91, 7.92, 7.48 and 7.50 ppm are assigned to the aromatic protons. The resonance at 4.40 ppm correspond to vinyl proton (H_2C=C-) and the peak at 1.59 ppm to methyl proton of the monomer 2-methacryloyl-1-(4-azo-1'-phenyl)aniline.

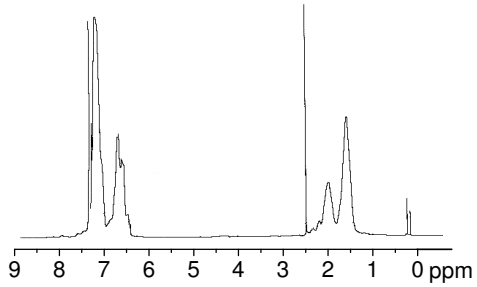

Figure 2.8: ^{1}H NMR Spectrum of the Polymer.

The absence of peak at 4.40 ppm and the shift of resonance peak of the methyl proton from 1.59 ppm to higher field (0.40 ppm) in the NMR spectrum of poly(2-methacryloyl-1-(4-azo-1'-phenyl)aniline-co-styrene) indicated polymerization. In addition, the NMR spectrum of the polymer displayed peaks corresponding to methylene protons in the main chain (2.17 and 2.21 ppm).

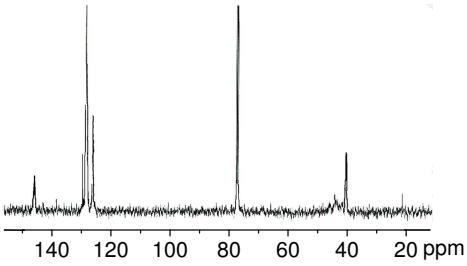

Figure 2.9: ^{13}C NMR Spectrum of the Polymer.

The structure of the polymer was further confirmed with ^{13}C NMR. The ^{13}C NMR spectrum of the polymer is shown in Figure 2.9. The resonance peaks at 149.71, 145.33, 136.86, 132.13, 121.22, 117.66 and 117.92 ppm are assigned to aromatic carbon. The resonance signal at 152.95 and 145.40 ppm correspond to the aromatic carbon (C-N=N-C). The peak at 114.54 ppm due to vinyl carbon is absent in the NMR spectrum of the polymer.

The resonance peak at 24.36 ppm of methyl carbon is shifted to 21.54 ppm in the spectrum of poly(2-methacryloyl-1-(4-azo-1'-phenyl)aniline-co-styrene). Two new peaks found at 44.21 and 40.43 ppm in the spectrum were attributed to methylene carbons of 2-methacryloyl-1-(4-azo-1'-phenyl)aniline and styrene, which confirmed copolymerization.

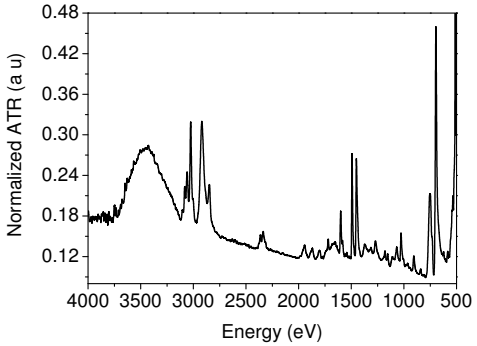

Figure 2.10: FT-IR Spectrum of the Polymer.

FT-IR spectrum of the polymer is sihown in Figure 2.10. The band at 3424 cm^{-1} is associated with the NH group. The band at 1454 cm^{-1} is the symmetric stretching of N=N group. The disappearance of band around 1647 cm^{-1}, stretching vibration of aliphatic double bond of the monomer, and the presence of new band at 2857 and 3019 cm^{-1} are attributed to methylene aliphatic single bond asymmetric and symmetric C-H stretching vibration.

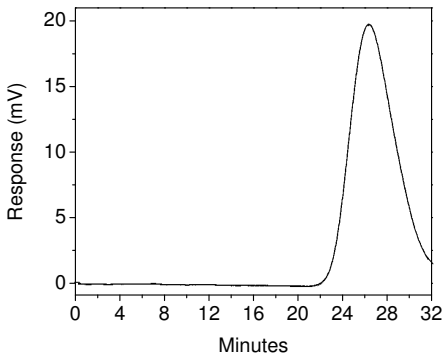

Figure 2.11: Size Exclusion Chromatogram of the Polymer.

Figure 2.11 shows SEC of the polymer. The number average molecular mass ($\overline{M}_n$) was 4987 and weight average molecular mass ($\overline{M}_w$) was 12326. The polydispersity index ($\overline{M}_w/\overline{M}_n$) obtained was 2.47. The polymer exhibited a broad molecular weight distribution.

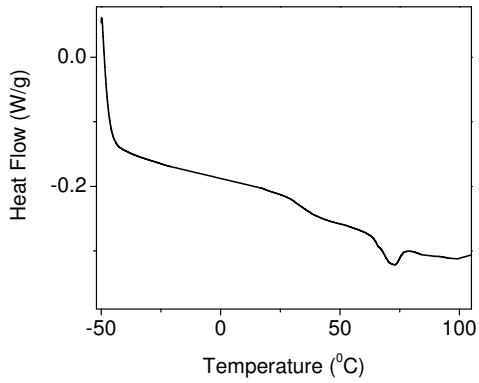

Figure 2.12: Differential Scanning Calorimetric Curve of the Polymer.

The DSC curve of the polymer is shown in Figure 2.12. The glass transition temperature of the polymer was 46.85 ^{o}C. The polymer showed well defined melting point at 72.98 ^{o}C.

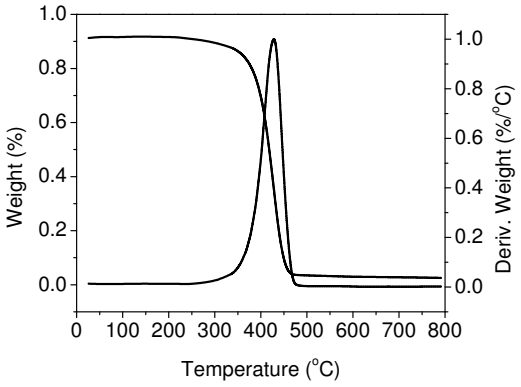

Figure 2.13: Thermogram of the Polymer.

The thermogram of the polymer is shown in Figure 2.13. The degradation process started at around 273.72 ^{o}C and reached maximum degradation

at 426.12 ^{o}C. The polymer showed good thermal stability indicating occurrence of strong inter- and intramolecular dipolar interactions originated by the presence of high charge delocalization in the macromolecular side chain.[34]

2.7.2 Electrochemical Properties

The conducting and semiconducting properties of polymers generally depend on the extent of separation between the HOMO and LUMO energy levels.[35,36] The lower the energy gap, better the semiconducting properties. Polymers with increased conjugation have lower energy gap between the HOMO-LUMO levels.[37,38]

The electrochemical behavior of the polymer was studied using cyclic voltammetry. The measurement was carried out at 25^{o}C in dimethylformamide solution containing 0.1 M tetrabutylammonium chloride as supporting electrolyte with a glassy carbon working electrode. Ag/AgCl was used as the reference electrode. The experiment was calibrated with the standard ferrocene/ferrocenium redox system. The potential was cycled between 0 to 2 V at a constant sweep rate of 25 mVs^{-1}. The cyclic voltammogram is shown in Figure 2.14.

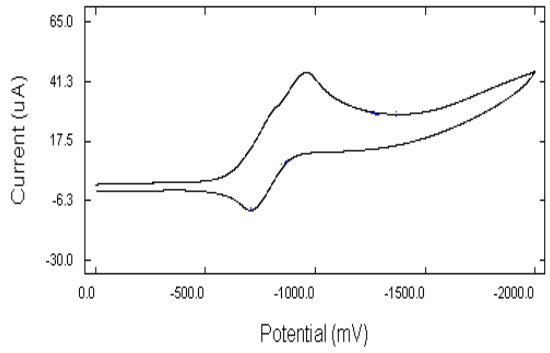

Figure 2.14: Cyclic Voltammogram of the Polymer.

The polymer showed the onset of reduction at -0.626 eV. The onset potential was used to calculate the LUMO level, according to the equation,

$E_{LUMO} = [E^{red}_{(onset)} + 4.4\ eV]$.[39] The LUMO energy level was estimated as 3.77 eV. The actual single particle LUMO position is higher by the exciton binding energy (~ 0.5 eV). The HOMO level for the polymer was obtained from the optical gap calculated from the absorption edge. The HOMO energy level of the polymer was 5.75 eV. The optical gap of the polymer was 1.98 eV. The values are calculated based on 4.4 eV for ferrocenium redox system with respect to zero vacuum level.[40]

2.7.3 Optical Absorption

The optical absorption spectra of the polymer films with and without C_{60}, are shown in Figure 2.15. The spectrum of C_{60} in chloroform is also given, which showed all characteristic bands in the range 4.5-1.9 eV. The polymer showed two absorption bands centered in the 3.62-1.63 eV and 4.39-3.66 eV spectral regions. The intense band appeared in the low energy region is related to the combined contributions of the n-π^*, first π-π^* and internal charge transfer electronic transitions of azobenzene chromophores.[41] The band in the high energy corresponds to the π-π^* electronic transition of the aromatic ring. Upon addition of C_{60} to the polymer, no additional absorption bands appeared in the spectrum, which could be due to weak mixing of the ground state electronic wave functions.[42]

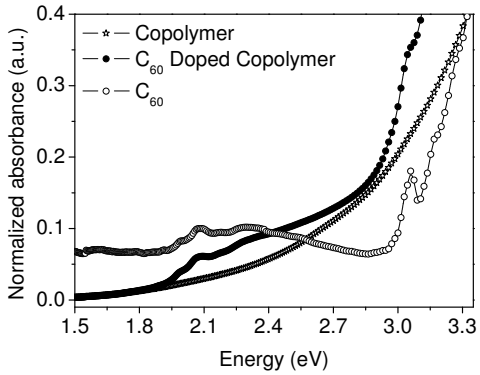

Figure 2.15: Optical Absorption Spectra of the Polymer, C_{60} and C_{60} Doped Copolymer.

The photoluminescence studies were carried out on undoped and C_{60} doped polymer samples.[43] Fluorescence quenching was observed upon doping with C_{60}. The addition of 0.00487 mmol of C_{60} quenches the photoluminescence (PL) intensity of polymer by 66%. Enhanced photoconductivity was observed in C_{60} doped polymer samples. The efficient quenching of PL intensity and enhanced photocurrent on addition of C_{60} may possibly be due to photoinduced charge transfer of electrons from the polymer to the acceptor molecule.[44]

2.7.4 Photocurrent Action Spectrum

Photocurrent action spectrum of undoped and C_{60} doped samples at an electric field of 10 V/μm with ITO biased positive is shown in Figure 2.16.

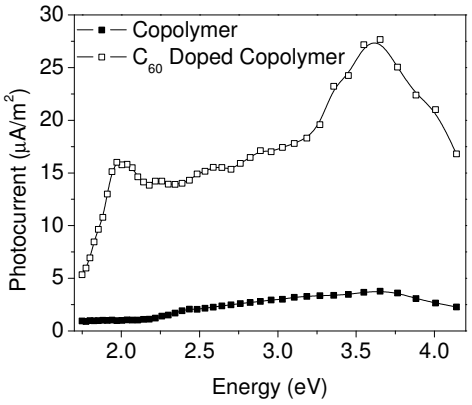

Figure 2.16: Photocurrent Action Spectra of the Polymer and C_{60} Doped Copolymer.

The polymer showed maximum photocurrent of 2.25 μA/m^2 at 2.5 eV and 3.84 μA/m^2 at 3.6 eV. The photocurrent of the polymer was significantly enhanced upon addition of small amount of C_{60}. The polymer doped with C_{60} showed a maximum photocurrent of 15.79 μA/m^2 (1.99 eV), 15.14 μA/m^2 (2.5 eV) and 27.31 μA/m^2 (3.6 eV) respectively. The enhanced photoconductivity could be due to the electron transfer reaction between C_{60} and the polymer.

The photoconductive sensitivity of the polymer was found to be 10^{-12} S cm/W. The C_{60} doped polymer showed enhanced photoconductive sensitivity. The photoconductive sensitivity observed was 22.9 x 10^{-12} S cm/W at 630 nm.

2.8 Conclusions

Photoconductivity studies were done on molecularly doped PMMA with aniline as electron donor and TNP as electron acceptor. Bathochromic shift was observed in the absorption spectrum in dispersed state indicating formation of charge transfer complex between aniline and TNP, similar to TNF-PVK system. A maximum photocurrent of 0.6 pA (3.35 eV) was observed at an electric field of 20 V/ μm. The photoconductive sensitivity of the molecularly doped system was found to be 10^{-13} S cm/W.

Non-conjugated photoconducting copolymer, poly(2-methacryloyl-1-(4-azo-1'-phenyl)aniline-co-styrene) was synthesized via radical initiated polymerization of 2-methacryloyl-1-(4-azo-1'-phenyl)aniline and styrene, using solution polymerization technique. The structure of the polymer was confirmed using (^{1}H and ^{13}C) NMR and FT-IR spectroscopy. The polymer showed broad distribution of molecular weights. Quenching of photoluminescence and enhancement of photoconductivity upon addition of C_{60} were observed. The polymer showed maximum photocurrent of 2.25 μA/m^2 (at 2.5 eV) at an electric field of 10 V/ μm. The photoconductive sensitivity of the polymer was found to be 10^{-12} S cm/W. The C_{60} doped polymer showed a maximum photocurrent of 15.14 μA/m^2 (at 2.5 eV) at 10 V/ μm. The photoconductive sensitivity of the C_{60} doped polymer was 22.9 x 10^{-12} S cm/W.

References

[1] H. J. Bolink, C. Arts, V. V. Krasnikov, G. G. Malliaras, G. Hadziioannou, Chem. Mater. 9 (1997) 1407.

[2] W. Huang, W.-L. Yu, H. Meng, J. Pei, S. F. Y. Li, Chem. Mater. 10 (1998) 3340.

[3] A. C. Arango, S. A. Carter, P. J. Brock, Appl. Phys. Lett. 74 (1999) 1698.

[4] O. Ostroverkhova, W. E. Moerner, Chem. Rev. 104 (2004) 3267.

[5] T. K. Daubler, L. Kulikovsky, D. Neher, V. Cimrova, J. Hummelen, E. Mecher, R. Bittner, K. Meerholz, Proc. of SPIE 4462 (2002) 206.

[6] J. Grazulevicius, P. Strohriegl, J. Pielichowski, K. Pielichowski, Prog. Polym. Sci. 28 (2003) 1297.

[7] Y. Zhang, T. Wada, H. Sasabea, J. Mater. Chem. 8 (1998) 809.

[8] E. Mecher, C. Brauchle, H. H. Horhold, J. C. Hummelenc, K. Meerholz, Phys. Chem. Chem. Phys. 1 (1999) 1749.

[9] M. S. Bratcher, M. S. DeClue, A. Grunnet-Jepsen, D. Wright, B. R. Smith, W. E. Moerner, J. S. Siegel, J. Am. Chem. Soc. 120 (1998) 9680.

[10] K. Yokoyama, K. Arishima, T. Shimada, K. Sukegawa, Japn. J. Appl. Phys. 33 (1994) 1029.

[11] D. Yang, L. Li, C. Wang, Mater. Chem. Phys. 87 (2004) 114.

[12] S. Shim, M. Suh, S. Suh, X.-L. Huang, E. Suh, Polymer 41 (2000) 467.

[13] V. C. Kishore, R. Dhanya, C. S. Kartha, K. Sreekumar, R. Joseph, J. Appl. Phys. 101 (2007) 0631021.

[14] H. Tokuhisa, M. Era, T. Tsutsui, Synth. Met. 85 (1997) 1161.

[15] Z. Y. Wang, Y. Qi, J. P. Gao, G. G. Sacripante, P. R. Sundararajan, J. D. Duff, Macromolecules 31 (1998) 2075.

[16] S. C. Suh, S. C. Shim, Synth. Met. 114 (2000) 91.

[17] M. S. Ho, C. Barrett, J. Paterson, M. Esteghamatian, A. Natansohn, P. Rochon, Macromolecules 29 (1996) 4613.

[18] E. El-Mossalamy, Spectrochim. Acta, Part A 60 (2004) 1161.

[19] S. M. Teleb, A. S. Gaballa, Spectrochim. Acta, Part A 62 (2005) 140.

[20] W. D. Gill, J. Appl. Phys. 43 (1972) 5033.

[21] M. S. Subhani, N. K. Bhatti, M. Mohammad, A. Y. Khan, Turk. J. Chem. 24 (2000) 223.

[22] Y. Kanemitsu, H. Funada, Y. Masumoto, Appl. Phys. Lett. 59 (1991) 697.

[23] L. B. Schein, A. Peled, D. Glatz, J. Appl. Phys. 66 (1989) 686.

[24] Y. Kanemitsu, J. Appl. Phys. 71 (1992) 3033.

[25] G. Juska, K. Genevicius, K. Arlauskas, R. Osterbacka, H. Stubb, Phys. Rev. B 65 (2002) 2332081.

[26] A. I. Vogel, A Text-Book of Practical Organic Chemistry including Qualitative Organic Analysis, 3rd Edition, Longman, 1956.

[27] A. El-Sayed, H. F. Mohamed, A. A. Boraei, Rad. Phys. Chem. 58 (2000) 791.

[28] L. Yu, Y. M. Chen, W. K. Chan, J. Phys. Chem. 99 (1995) 2797.

[29] K. Ogino, T. Nomura, T. Shichi, S.-H. Park, H. Sato, Chem. Mater. 9 (1997) 2768.

[30] H. Chun, I. K. Moon, D.-H. Shin, N. Kim, Chem. Mater. 13 (2001) 2813.

[31] K. Okamoto, T. Nomura, S.-H. Park, K. Ogino, H. Sato, Chem. Mater. 11 (1999) 3279.

[32] D. Wright, M. A. Diaz-Garcia, J. D. Casperson, M. DeClue, W. E. Moerner, R. J. Twieg, Appl. Phys. Lett. 73 (1998) 1490.

[33] W. G. Jun, M. J. Cho, D. H. Choi, J. Korean Phys. Soc. 47 (2005) 620.

[34] L. Angiolini, T. Benelli, L. Giorgini, E. Salatelli, Polymer 46 (2005) 2424.

[35] C. Lô, K.-I. Chane-Ching, F. Maurel, J. J. Aaron, B. Kosata, J. Svoboda, Synth. Met. 156 (2006) 256.

[36] E. Sahin, P. Camurlu, L. Toppare, V. M. Mercore, I. Cianga, Y. Yağci, J. Electroanal. Chem. 579 (2005) 189.

[37] J. A. Mikroyannidis, I. k Spiliopoulos, A. P. Kulkarni, S. A. Jenekhe, Synth. Met. 142 (2004) 113.

[38] M. Toba, Y. Takeoka, M. Rikukawa, K. Sanui, Synth. Met. 152 (2005) 197.

[39] F. Ç. Cebeci, E. Sezer, A. S. Sarac, Electrochim. Acta 52 (2007) 2158.

[40] M. A. Loi, E. J. W. List, C. Gadermaier, W. Graupner, G. Leising, G. Bongiovanni, A. Mura, J.-J. Pireaux, K. Kaeriyama, Synth. Met. 111 (2000) 519.

[41] L. Angiolini, D. Caretti, L. Giorgini, E. Salatelli, Polymer 42 (2001) 4005.

[42] C. H. Lee, D. M. G. Yu, K. Pakbaz, C. Zhang, N. S. Sariciftci, A. J. Heeger, F. Wudl, Phys. Rev. B 48 (1993) 15425.

[43] V. C. Kishore, Development of photorefractive polymers: Evaluation of photoconducting and electro-optic properties, Ph.D. Thesis, Cochin University of Science and Technology, India, 2008.

[44] L. Smilowitz, N. S. Sariciftci, R. Wu, C. Gettinger, A. J. Heeger, F.Wudl, Phys. Rev. B 47 (1993) 13835.

CHAPTER

THREE

Synthesis and Characterization of Photoconducting Polybenzoxazines

3.1 Introduction

Macromolecular materials with unique combination of both electronic and optical properties have attracted tremendous technological interest in the past few decades due to increasing need for low cost materials with structural flexibility.[1–5] Various designing methods have been employed to achieve efficient semiconducting properties in polymers with potential applications in the field of optical storage media,[6] dynamic holography,[7] xerography,[8] photorefractive composites,[9] photovoltaic devices,[10] light emitting diodes[11] and many other photonic systems. The extend of π- conjugation and the presence of aromatic amino group in the polymer structure are the common structural features of charge transporting materials.[4,12–14] The charge transport and the semiconducting properties of these materials depend mainly on the structure and morphology of the polymer chains.

Lot of reports are there in the literature about the synthesis and properties of conjugated polymer systems.[15–21] However, less attention was given to non-conjugated polymers. In non-conjugated polymers, the semiconducting property is based on the charge hopping from one localized site to another in the direction of electric field.[22] In this chapter, the

synthesis and characterization of a series of Mannich phenolic type polybenzoxazines are discussed. These low molecular weight polymers can be synthesized via thermally activated cationic ring opening polymerization.[23] The thermally activated polymerization of benzoxazines with and without initiators or catalyst, in the presence and absence of solvent have been studied in detail.[23] The structure of the polymers were confirmed by FT-IR, (^{1}H & ^{13}C) NMR, mass spectral and thermal analysis. The spectral dependence of photocurrent was studied using lock-in technique.[24] The effect of fullerene (C_{60}) as electron acceptor on the photoconductivity of polybenzoxazines was also investigated.

Polybenzoxazines are non-conjugated polymers with good thermal, mechanical and physical properties.[23,25,26] These polymers were synthesized via heterocyclic ring opening polymerization of benzoxazine monomers at elevated temperatures.[23,25] Benzoxazines are obtained by Mannich condensation of a phenol, formaldehyde and an amine.[26–29] The Mannich base bridge (-CH_2-NR-CH_2-) characterizes the structure of the polymer,[25] with the reaction taking place preferentially at the ortho position of free phenolic group.[30] The oxygen and nitrogen atom in the heterocyclic ring as well as the unobstructed ortho position in the benzene ring with respect to the phenolic group are preferred sites for ring opening.[31] Depending upon the reaction condition, the polymerization leads to Mannich phenoxy type and Mannich phenolic type polybenzoxazines.[31]

3.2 Experimental

3.2.1 Materials

Poly(methyl methacrylate) (Mw-75,000) was reprecipitated thrice from chloroform-methanol and dried under reduced pressure. Toluene (Rankem, AR Grade) was dried over sodium and distilled before use. The following chemicals were used as received without further purification: 4-tertiary butyl phenol (97 %, Acros Organics), buckminister fullerene (C_{60}) (98 %, Alfa Aesar), dioctyl phthalate (DOP) (98 %, Alfa Aesar), formaldehyde solution (97%, Merck) (37-41 % w/v), ammonia solution (AR, Sd Fine)

(25 %), methyl amine (98 %, Spectrochem, AR GRade) chloroform (99 %, Merck, Spectroscopic Grade), toluene (98 %, Merck, Spectroscopic Grade) and dimethylformamide (DMF), (98 %, Merck, Spectroscopic Grade). The electron acceptor was dried under vacuum over P_2O_5 for three days.

3.2.2 Instrumentation

The instrumentation techniques employed for the study of molecules are described in detail in section 2.6.2.

3.2.3 Synthesis of Poly(6-tertiary-butyl-3,4-dihydro-2H-1,3-benzoxazine) (P1)

A mixture of 4-tertiary butyl phenol (10.4 g, 69.0 mmol) and formaldehyde solution (11.02 mL, 175 mmol, 38%) were heated to 40 ^{0}C. Ammonium solution (5.49 mL, 80.6 mmol, 25%) was added drop wise to the above mixture. The solution was stirred at 120 ^{o}C for 6 h and then cooled to room temperature. The bright yellow solid product obtained was dissolved in chloroform (25 mL) and reprecipitated from methanol. The precipitated polymer was isolated by filtration, washed with distilled water and dried at room temperature. The polymer was further purified by soxhlet extraction with methanol. The purified polymer was dried under vacuum at 40 ^{o}C for 72 h.

Yield: 86.5 %. FTIR (KBr) ν cm^{-1}: 1483 (tetra-substituted benzene), 1121 (C-N-C ay st), 3320 (-NH st). ^{1}H NMR (400 MHz $CDCl_3$) δ: 1.27 (s, 9H), 2.35 (s, 1H), 3.82 (2H), 4.23 (s, 2H), 4.29 (s, 2H), 4.35 (s, 4H), 4.63 (s, 2H), 5.23 (s, 2H), 6.75-7.15 (m, 2H). ^{13}C NMR (100 MHz $CDCl_3$) δ: 33.99, 43. 53, 46.80, 49.72, 113.15-153.28.

3.2.4 Synthesis of Poly(6-tertiary-butyl-3-methyl-3,4-dihydro-2H-1,3-benzoxazine), (P2)

A mixture of 4-tertiary butyl phenol (10.4 g, 69.0 mmol) and formaldehyde solution (11.02 mL, 175 mmol, 38%) were heated to 40 ^{0}C. Methyl amine (3.95 mL, 82.29 mmol, 25%) was added drop wise to the above mixture.

The solution was stirred at 85 ^{o}C for 6 h and then cooled to room temperature. The pale yellow solid product obtained was dissolved in chloroform (25 mL) and reprecipitated from methanol. The precipitated polymer was isolated by filtration, washed with distilled water and dried at room temperature. The polymer was further purified by soxhlet extraction with methanol. The purified polymer was dried under vacuum at 40 ^{o}C for 72 h.

Yield: 82 %. FTIR (KBr) ν cm^{-1}: 1484 (tetra-substituted benzene), 1120 (C-N-C ay st). ^{1}H NMR (400 MHz $CDCl_3$) δ: 1.27 (s, 9H), 2.61 (s, 3H), 3.70 (s, 4H), 6.71-7.25 (m, 2H). ^{13}C NMR (100 MHz $CDCl_3$) δ: 31.70, 33.25, 41.78, 114.12-154.25.

3.2.5 Synthesis of Poly(6-tertiary-butyl-3-phenyl-3,4-dihyd-ro-2H-1,3-benzoxazine), (P3)

A mixture of 4-tertiary butyl phenol (10.4 g, 69.0 mmol) and formaldehyde solution (11.02 mL, 175 mmol, 38%) were heated to 40 ^{0}C. Aniline (7.53 mL, 82.29 mmol, 25%) was added drop wise to the above mixture. The solution was stirred at 180 ^{o}C for 6 h and then cooled to room temperature. The bright orange solid product obtained was dissolved in chloroform (25 mL) and reprecipitated from methanol. The precipitated polymer was isolated by filtration, washed with distilled water and dried at room temperature. The polymer was further purified by soxhlet extraction with methanol. The purified polymer was dried under vacuum at 40 ^{o}C for 72 h.

Yield: 92 %. FTIR (KBr) ν cm^{-1}: 1481 (tetra-substituted benzene), 1117 (C-N-C ay st). ^{1}H NMR (400 MHz $CDCl_3$) δ: 1.27 (s, 9H), 3.76 (s, 2H), 4.08 (s, 2H), 4.96 (s, 4H), 6.73-7.25 (m, 2H). ^{13}C NMR (100 MHz $CDCl_3$) δ: 31.28, 49.54, 55.02, 56.14, 78.83, 114.13-155.19.

3.2.6 Sample Preparation

The samples for photocurrent measurements were prepared by drop casting a 8 wt % solution (7 mL) of the polymer (**P1, P2, P3**) and DOP (1 wt %)

in chloroform. The polymer:C_{60} composites were prepared by dissolving C_{60} (0.00487 mmol) in 7.5 wt% solution of the polymer in chloroform. The concentration of C_{60} molecules were kept at 10^{-5} moles/litre. The solution was passed through a 0.2 μm PTFE filter and deposited on indium tin oxide (ITO) coated glass substrates. Overnight evaporation of the solvent at room temperature (28 ^{0}C) and subsequent drying of the films for 12 h in vacuum chamber (at 10^{-2} Torr), resulted in good optical quality films of about 15 μm thickness, measured using a Stylus profiler. Silver top contacts of 36-42 mm^2 active area were deposited on to the polymer films. Photoconductivity measurements were done using the modulated photocurrent technique.[32]

3.3 Results and Discussion

3.3.1 Synthesis and Characterization

Poly(6-tertiary-butyl-3,4-dihydro-2H-1,3-benzoxazine) (**P1**), poly(6-tertiary-butyl-3-methyl-3,4-dihydro-2H- 1,3-benzoxazine) (**P2**) and poly(6-tertiary-butyl-3-phenyl-3,4-dihydro-2H-1,3-benzoxazine) (**P3**) were synthesized via thermally activated cationic ring opening polymerization. The route of polymer synthesis is depicted in Figure 3.1.

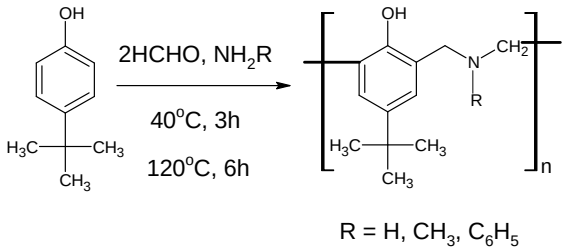

Figure 3.1: Synthesis route of the Polymers.

The reaction was carried out in single stage by reacting stoichiometric amounts of tertiary butyl phenol, formaldehyde and amine (ammonia solution for **P1**, methylamine for **P2** and aniline for **P3**) without isolating the benzoxazine monomer. The formation of benzoxazine monomer was

confirmed by spectral analysis. At first, the temperature was maintained at 40 ^{0}C. The reaction temperature was then slowly raised and the reaction medium was refluxed for 6 h (120 ^{0}C for **P1**, 85 ^{0}C for **P2** and 180 ^{0}C for **P3**).

The polymerization of benzoxazine proceeded via the formation and propagation of oxonium ion centers. The reaction involves nucleophilic attack of benzoxazine monomer on the oxonium ion. The presence of hetero atom in the ring provides potential sites for initiation and propagation of reaction by ring opening. If the monomer contains two different types of hetero atoms, the preferred site will be the one with high negative charge distribution. Ishida et al., reported a highly strained distorted semi-chair conformation for benzoxazine monomer.[31] The strained conformation makes the monomer to undergo cationic ring opening polymerization. The benzoxazine monomer carries both oxygen and nitrogen atoms in its structure. Hence, polymerization involves nucleophilic attack of monomer on either the oxygen or nitrogen sites. The attack on the oxygen and nitrogen propagation sites lead to phenolic type polybenzoxazine structure. The attack on unobstructed ortho position in the benzene ring with respect to the phenolic group leads to phenoxy type polybenzoxazine structure.[31] The phenolic and phenoxy type structures can be differentiated by the chemical environment of the two methylene groups between adjacent aromatic rings.[31] The FT-IR and (^{1}H & ^{13}C) NMR spectra of **P1, P2** and **P3** confirm the presence of Mannich phenolic type base bridge in the repeating unit of the polymer.

The polymers are soluble in organic solvents such as chloroform, DMF, THF, toluene and acetone. They can be processed into thin transparent films also. The molecular mass of **P1, P2** and **P3** were determined using SEC. The introduction of different amines in the polymer chain leads to change in the color from yellow to bright orange. The polymer **P1** has bright yellow, **P2** has light yellow and **P3** has a bright orange color.

The ^{1}H NMR spectrum of **P1** is shown in Figure 3.2. The peaks at 2.35 and 1.28 ppm correspond to the proton attached to the nitrogen atom of the Mannich bridge and the tertiary butyl group. The resonance

peaks at 3.82, 4.23, 4.29 and 4.35 ppm are assigned to methylene protons of oligomeric and open bridge Mannich base compounds. The resonance peaks at 4.63 and 5.23 ppm correspond to methylene protons in the oxazine ring.

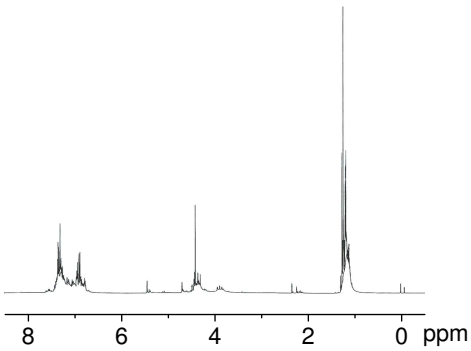

Figure 3.2: ^{1}H NMR spectrum of Poly(6-tertiary-butyl-3,4-dihydro-2H-1,3-benzoxazine.

The intense resonance signal at 4.30 ppm indicated that both the methylene groups in the repeating unit were chemically equivalent. Assignment of protons was done assuming that the two tertiary butyl phenol units are connected through methylene-secondary amine-methylene linkage at the ortho-position as shown in the structure in Figure 3.1. Aromatic signals of the tertiary butyl phenol unit appeared from 6.75 to 7.15 ppm.

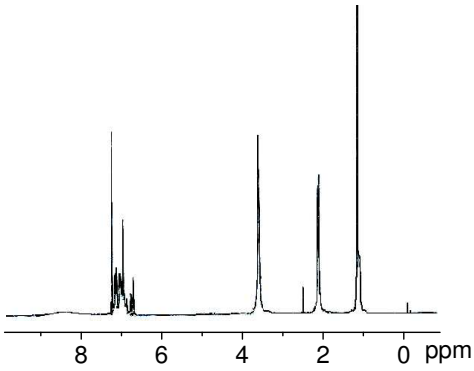

Figure 3.3: ^{1}H NMR spectrum of Poly(6-tertiary-butyl-3-methyl-3,4-dihydro-2H-1,3-benzoxazine).

The ^{1}H NMR spectrum of **P2** is shown in Figure 3.3. The peak at 2.61 ppm correspond to the proton of the methyl group attached to the nitrogen atom in the Mannich bridge structure. The intense resonance signal at 3.70 ppm indicated that both the methylene groups in the repeating unit are chemically equivalent. Methyl protons of tertiary butyl unit resonate at 1.27 ppm. Aromatic signals of the tertiary butyl unit appeared from 6.71 to 7.25 ppm.

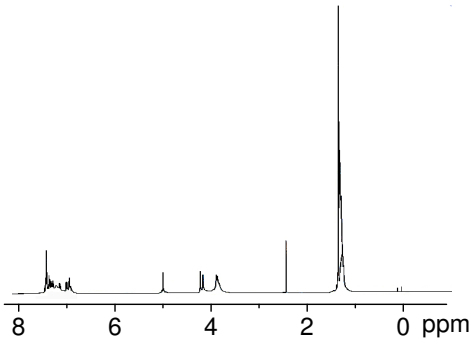

Figure 3.4: ^{1}H NMR spectrum of Poly(6-tertiary-butyl-3-phenyl-3,4-dihydro-2H-1,3-benzoxazine).

The ^{1}H NMR spectrum of **P3** is shown in Figure 3.4. The peak at 1.27 ppm corresponds to methyl protons of the tertiary butyl group. The resonance peaks at 3.76, 4.08 and 4.26 ppm are assigned to methylene protons of oligomeric and oxazine ring Mannich base bridge. The intense resonance signal at 4.96 ppm indicated that both the methylene groups in the repeating unit are chemically equivalent. Aromatic signals of the tertiary butyl phenol unit appear from 6.73 to 7.25 ppm.

The ^{13}C NMR spectrum of **P1** is shown in Figure 3.5. The resonance at 33.99 ppm is assigned to the methyl carbons of the tertiary butyl group. The resonance at 46.80 ppm is assigned to methylene carbon of the open Mannich base. The resonances between 113.15 and 153.28 ppm are assigned to the aromatic carbons. The resonance around 43.53, 46.80 and 49.72 ppm are assigned to methylene carbons of oligomeric and oxazine

ring compounds.

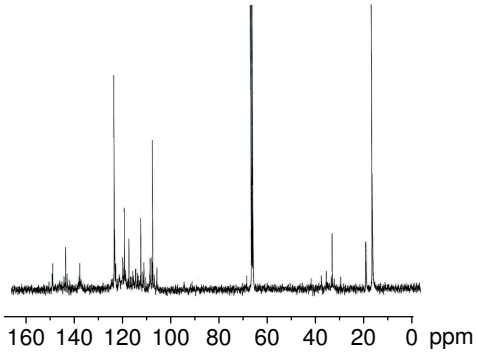

Figure 3.5: ^{13}C NMR spectrum of Poly(6-tertiary-butyl-3,4-dihydro-2H-1,3-benzoxazine.

The ^{13}C NMR spectrum of **P2** is shown in Figure 3.6. The resonance at 31.70 ppm is assigned to methyl carbons of the tertiary butyl group and at 33.25 ppm to methyl carbon attached to the nitrogen of the Mannich base bridge. The resonance at 41.78 ppm is assigned to methylene carbon of the open Mannich base. The resonances between 114.12 and 154.25 ppm are assigned to the aromatic carbons.

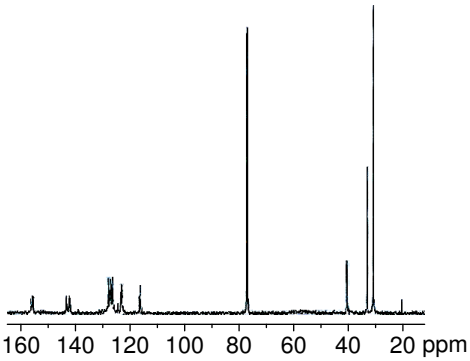

Figure 3.6: ^{13}C NMR spectrum of Poly(6-tertiary-butyl-3-methyl-3,4-dihydro-2H- 1,3-benzoxazine).

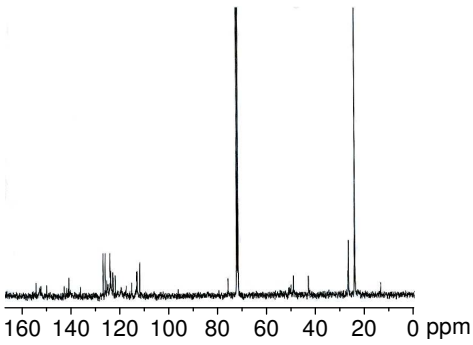

Figure 3.7: ^{13}C NMR spectrum of Poly(6-tertiary-butyl-3-phenyl-3,4-dihydro-2H- 1,3-benzoxazine).

The ^{13}C NMR spectrum of **P3** is shown in Figure 3.7. The resonance at 31.28 ppm is assigned to methyl carbons of the tertiary butyl group. The resonance at 49.54 ppm is assigned to methylene carbon of the open Mannich base. The resonance between 114.13 and 155.19 ppm are assigned to the aromatic carbons. The resonance around 55.02, 56.14 and 78.83 ppm are assigned to methylene carbons of oligomeric and oxazine ring compounds. Thus it appeared that the final product contained trace amounts of monomer and dimers, which could be due to the fact that the reaction was carried out without isolating the monomer.

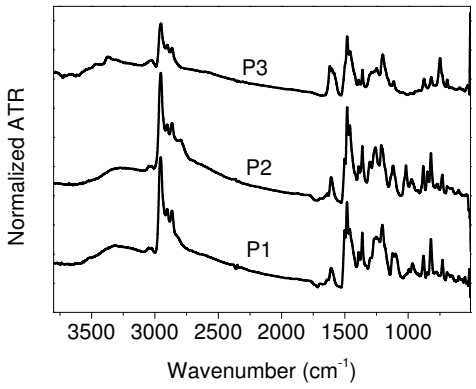

Figure 3.8: FT-IR spectrum of the Polymers.

FT-IR spectra of the **P1, P2** and **P3** were compatible with the assigned structure of the polymer. FT-IR spectrum of **P1, P2** and **P3** are shown in Figure 3.8. Vibrational assignments of similar benzoxazine substituted polymers have been reported earlier.[31] The band centered around 966 cm^{-1} associated with the oxazine ring indicated the presence of oxazine ring compounds. The band around 1123 cm^{-1} is assigned to C-N-C asymmetric stretching vibration. The band around 1481 cm^{-1} is attributed to tetra-substituted benzene ring with methylene-amine-methylene bridge at the ortho position. The band around 1251 cm^{-1} is assigned to aromatic C-O stretching frequency of phenols. The broad peak centered around 3324cm^{-1} is attributed to hydrogen bonded hydroxyl groups.[33]

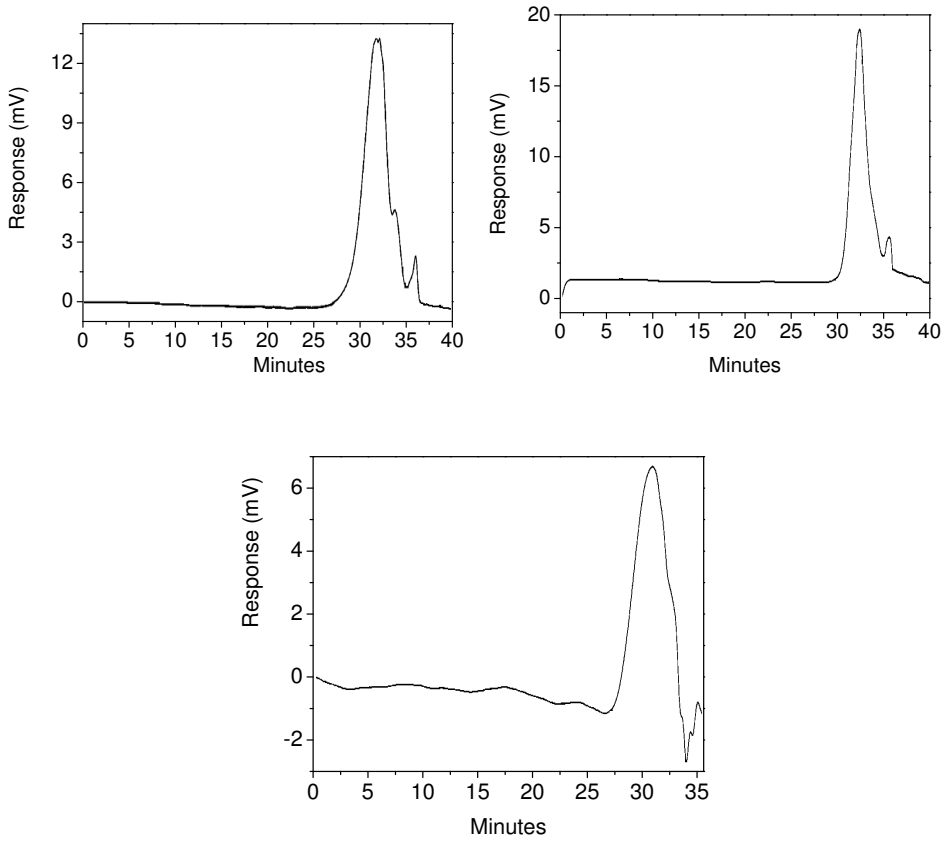

Figure 3.9: SEC of the Polymers.

The molecular weight of **P1**, **P2** and **P3** were estimated using SEC and the chromatograms are shown in Figure 3.9. The chromatogram showed two peaks, a broad peak centered at 31.2 min and a shoulder peak at 33.5 min. The shoulder peak was assigned to the closed-ring monomer species. The number average molecular weight ($\overline{M}_n$) of **P1**, **P2** and **P3** were 403, 239 and 268 and the weight average molecular weight were ($\overline{M}_w$) 1080, 971 and 900 respectively. The polydispersity index ($\overline{M}_w/\overline{M}_n$) of **P1**, **P2** and **P3** were 2.67, 4.06 and 3.35 respectively, which indicate a broad distribution of molecular weights.

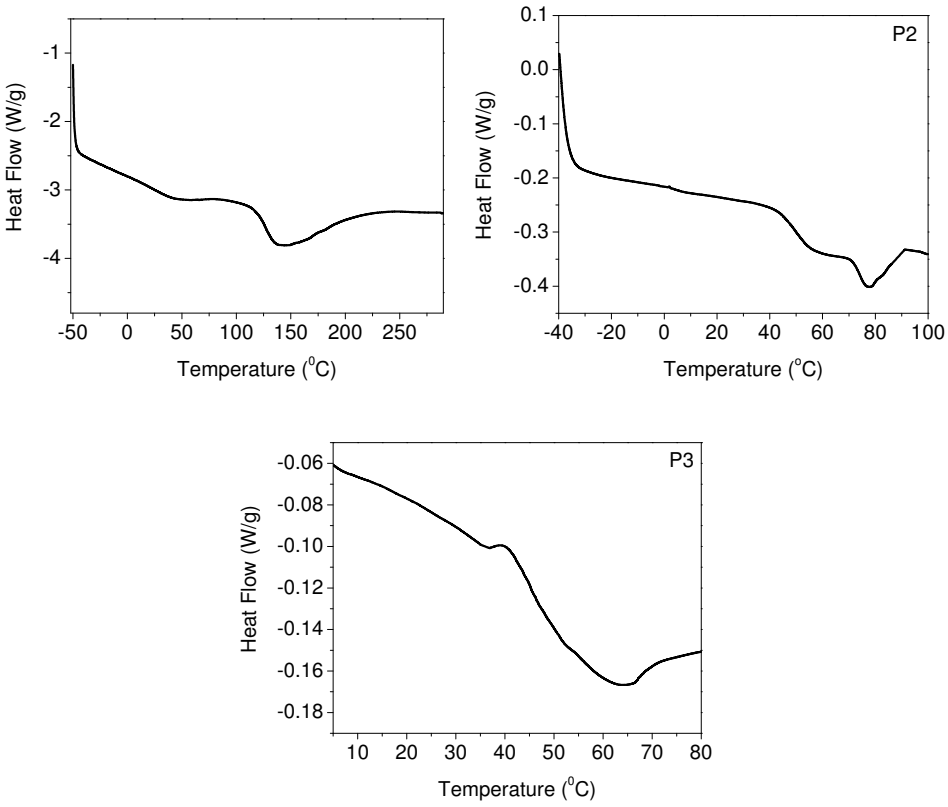

Figure 3.10: DSC Curves of the Polymers.

The DSC curves of **P1, P2** and **P3** are shown in Figure 3.10. The corresponding T_g s and the melting points of **P1, P2** and **P3** are given in Table 4.1.

Table 3.1: Glass Transition Temperature (T_g) and Melting Point of P1, P2 and P3.

Molecules	T_g (^oC)	Melting Point (^oC)
P1	46.49	144.66
P2	49.63	77.42
P3	52.45	64.28

The thermal degradation behavior of **P1, P2** and **P3** was examined by TG and the thermograms are shown in Figure 3.11.

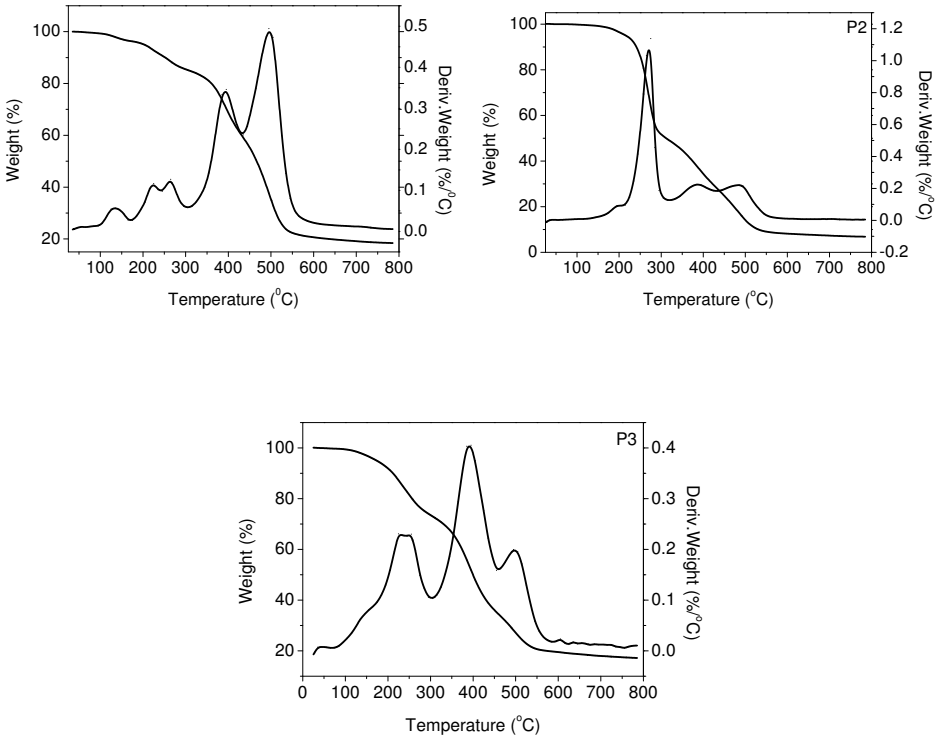

Figure 3.11: Thermogram of the Polymers.

Four well resolved degradation peaks were found in the derivative ther-

mogram of **P1, P2** and **P3**. The first and second degradation process were around 125 and 162 ^{o}C for **P1**, 127 and 213 ^{o}C for **P2**, 123 and 184 ^{o}C for **P3** and reached maximum rates of 0.05 %/^{o}C and 0.12 %/^{o}C at 132 and 220 ^{o}C (**P1**), 193 and 273 ^{o}C (**P2**), 142 and 243 ^{o}C (**P3**). These peaks could be due to the degradation of Mannich base.[34] The third major weight loss process due to the degradation of phenolic linkage started at 295 ^{o}C (**P1**), 317 ^{o}C (**P2**), 302 ^{o}C (**P3**) and reached maximum rates of 0.34 %/^{o}C at 389 ^{o}C (**P1**), 382 ^{o}C (**P2**) and 389 ^{o}C (**P3**). These degradation peaks were reported to be due to the primary decomposition products obtained from the cleavage of C-C, C-N and C-O linkages present in the polymer.[25,34] The fourth weight loss started at 425 ^{o}C (**P1**), 433 ^{o}C (**P2**), 459 ^{o}C (**P3**) with maximum rate (0.49 %/^{o}C) of degradation at 498 ^{o}C (**P1**), 490 ^{o}C (**P2**) and 495 ^{o}C (**P3**) was reported to be due to secondary decomposition product which were not present in the polymer structure.[25]

3.3.2 Electrochemical Properties

The electrochemical behavior of **P1, P2** and **P3** was studied using cyclic voltammetry. The measurement was carried out at 25 ^{o}C in dimethylformamide solution containing 0.1 M tetrabutylammonium chloride as supporting electrolyte with a glassy carbon working electrode. Ag/AgCl was used as the reference electrode. The experiment was calibrated with the standard ferrocene/ferrocenium redox system. The potential was cycled between 0 to -2 V at a constant sweep rate of 25 mVs^{-1}. The cyclic voltammogram is shown in Figure 3.14.

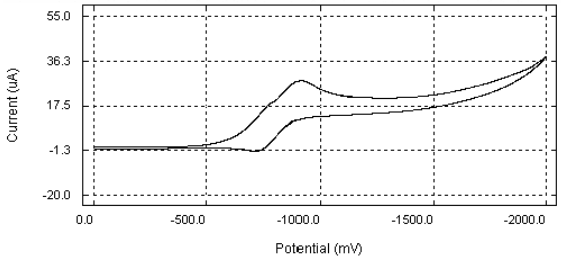

Figure 3.12: Cyclic Voltammogram of Poly(6-tertiary-butyl-3,4-dihydro-2H-1,3-benzoxazine.

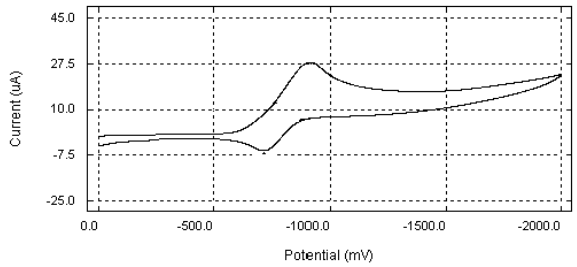

Figure 3.13: Cyclic Voltammogram of Poly(6-tertiary-butyl-3-methyl-3,4-dihyd-ro-2H- 1,3-benzoxazine).

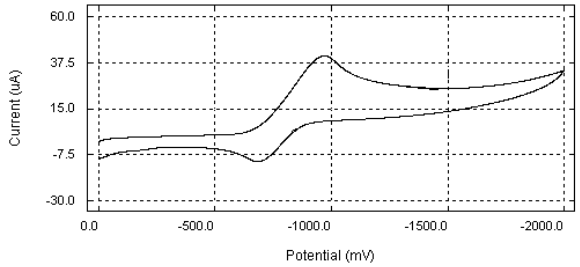

Figure 3.14: Cyclic Voltammogram of Poly(6-tertiary-butyl-3-phenyl-3,4-dihyd-ro-2H- 1,3-benzoxazine).

The polymers **P1, P2** and **P3** showed the onset of reduction at -0.54, -0.62 and -0.64 eV respectively. The onset potential was used to calculate the LUMO levels, according to the equation, $E_{LUMO} = [E^{red}_{(onset)} + 4.4$ eV$]$.[35] The LUMO energy levels of **P1, P2** and **P3** were estimated as 3.86, 3.78 and 3.76 eV respectively. The actual single particle LUMO position is higher by the exciton binding energy ($\sim$ 0.5 eV). The HOMO level of the polymers were calculated using the optical gap estimated from the absorption spectrum. The HOMO energy level of **P1**, **P2** and **P3** are 6.77, 6.91 and 6.59 eV respectively. The polymers exhibited optical gaps of 2.41, 2.63 and 2.33 eV respectively, much lower than PVK (4.0 eV). The values are calculated based on 4.4 eV for ferrocenium redox system with respect to zero vacuum level.[36]

3.3.3 Optical Absorption

The absorption spectrum of **P1, P2** and **P3** recorded in thin film samples are shown in Figure 3.15. The onset of absorption for **P1**, **P2** and **P3** were observed at 2.41, 2.63 and 2.33 eV respectively.

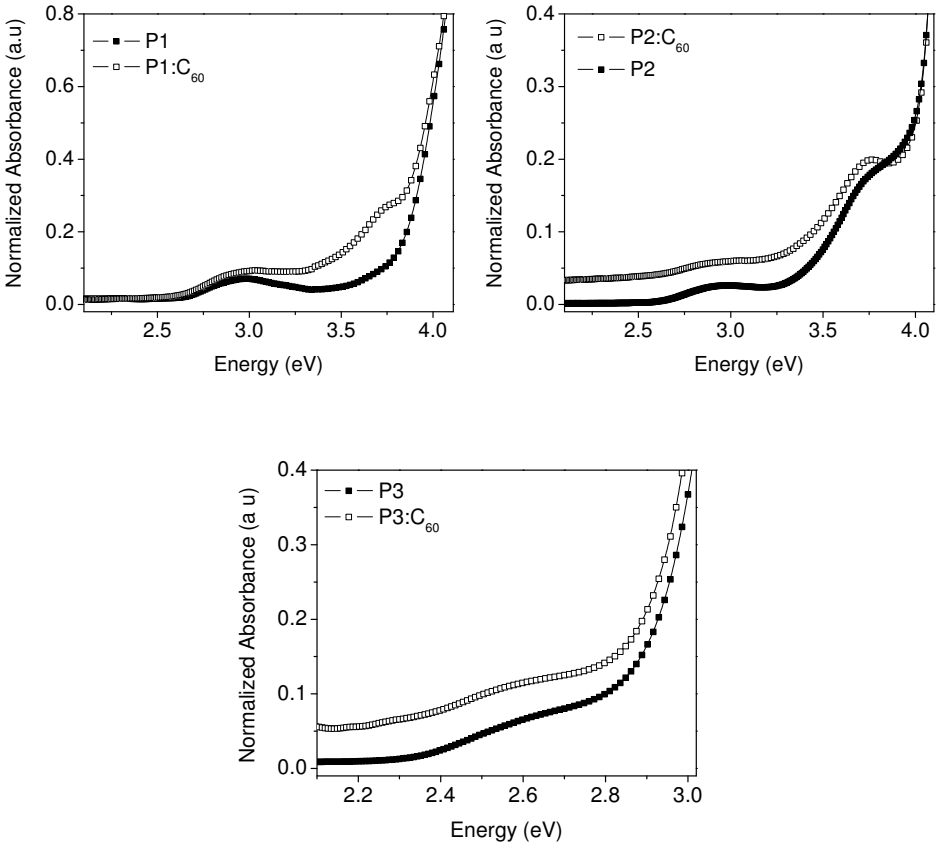

Figure 3.15: UV-Vis Absorption Spectrum of Polymers alone and with C_{60} Doped.

The absorption spectra showed two bands, low energy bands with maxima at 2.96 (for P1), 2.93 (for P2) and 2.72 eV (for P3) and high energy bands with maxima at 3.80 (for P1), 3.76 (for P2) and 3.50 eV (for P3) respectively. The intense band in the high energy region was attributed to π-π^* transition and the less intense band in the low energy region to

n-π^* transition. The n-π^* transition involves the excitation of unshared pair of electrons in the n (nonbonding) orbital of the hetero atom to the π^* (antibonding) orbital of the unsaturated group present in the polymer.

To distinguish n-π^* transition from π-π^* transition, Kasha and McConnell suggested the blue shift phenomenon.[37,38] The general solvation hypothesis and the specific hydrogen bonding hypothesis were proposed to explain the blue shift phenomenon.

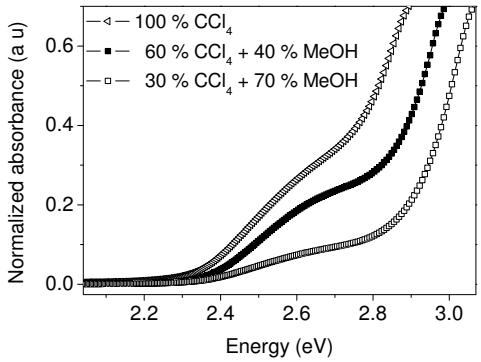

Figure 3.16: A Typical UV-Vis Spectrum of Poly(6-tertiary-butyl-3-phenyl-3,4-dihyd-ro-2H- 1,3-benzoxazine) showing n-$\pi*$ Transition.

McConnell[38] provided theoretical explanation for n-π^* transitions on the basis of general solvation hypothesis. The solvent molecules orient themselves around the solute molecules to bind with the ground state charge distribution of the solute molecule. Upon excitation, if the excited state charge distribution of the solute changed markedly from the ground state charge distribution, the solvent molecules would not have the position and orientation to bind most strongly with the excited state charge distribution. This can give rise to blue-shift phenomenon since a polar solvent (relative to a non-polar solvent) would give a greater solvation energy for the ground state of the solute than for the excited state.

Kasha et al.,[37] proposed the specific hydrogen bonding hypothesis. According to this, the specific hydrogen bonding of the solvent with the solute plays an important role in shift of n-π^* transitions on changing solvent from hydrocarbon to hydroxylic one. Hydroxylic solvents in comparison

with hydrocarbon solvents favors hydrogen bond formation with solute molecule containing lone pair of electrons. The lone pair of electrons on the oxygen and nitrogen atom present in the polymer was responsible for the n-π^* transition, which was confirmed with specific hydrogen bonding hypothesis.

In order to prove the presence of n-π^* transition in the polymer sample, we have recorded the absorption spectra in pure CCl_4 and 40% and 70% methanol in CCl_4 solution. A typical spectrum of **P3** showing n-π^* transition is shown in Figure 3.16. The addition of 40% methanol shifted the absorption spectrum considerably towards higher energy region. With the addition of 70% methanol, the absorption spectrum again shifted towards higher energy region.

3.3.4 Photocurrent Action Spectrum

The photocurrent action spectra of **P1, P2** and **P3** at an electric field of 20 and 40 V/μm with ITO biased positive are shown in Figure 3.17. The photocurrent spectra of **P1, P2** and **P3** showed two peaks, one in the low energy region and the other in the higher energy region. At an electric field of 20 V/μm, **P1** showed a maximum photocurrent of 0.56 $\mu A/m^2$ (at 2.81 eV) and 0.68 $\mu A/m^2$ (at 3.30 eV) respectively. The maximum photocurrent observed for **P1** at 40 V/μm was 1.29 $\mu A/m^2$ (at 2.81 eV) and 1.53 $\mu A/m^2$ (at 3.30 eV). For **P2**, the maximum photocurrent observed at 20 V/μm was 0.73 $\mu A/m^2$ (at 3.06 eV) and 0.88 $\mu A/m^2$ (at 3.44 eV). The maximum photocurrent obtained at 40 V/μm was 1.31 $\mu A/m^2$ (at 3.06 eV) and 1.92 $\mu A/m^2$ (at 3.44 eV). The maximum photocurrent observed for **P3** at 20 V/μm was 0.93 $\mu A/m^2$ (at 3.02 eV) and 0.88 $\mu A/m^2$ (at 3.35 eV). At an electric field of 40 V/μm, **P3** showed a maximum photocurrent of 2.25 $\mu A/m^2$ (at 3.02 eV) and 1.84 $\mu A/m^2$ (at 3.35 eV) respectively. **P3** showed higher photocurrent values compared to **P1** and **P2**, which might be due to the strong intrachain interactions between the tertiary butylphenol moiety and the phenyl ring resulting in a higher photogeneration of charge carriers.

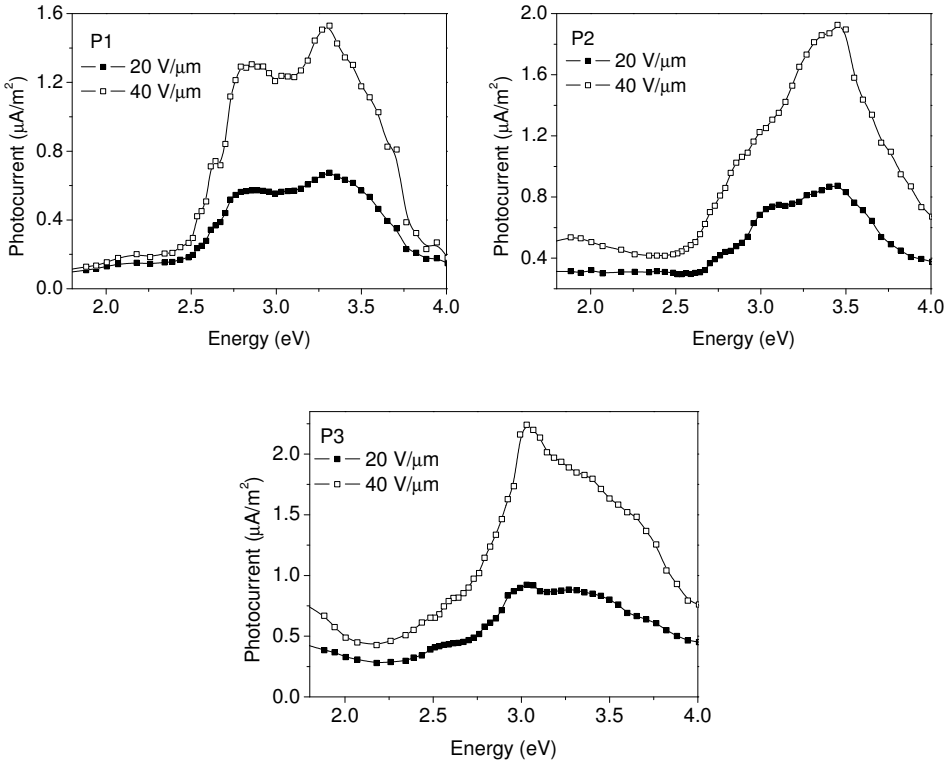

Figure 3.17: Photocurrent Action Spectrum of the Polymers.

As shown in Figure 3.17, the photocurrent values were highly dependent on the electric field, which indicates that the increase in photoconductivity on exposure to light was not due to any photochemical reactions. The photoconductive sensitivity of P1, P2 and P3 were found to be 5 x 10,$^{-14}$ 1 x 10^{-14} and 3 x 10^{-14} S cm/W respectively at 440 nm respectively.

3.3.5 Photocurrent Action Spectrum of C_{60} Sensitized Polymers

Photocurrent action spectra of C_{60} doped polymers **P1, P2** and **P3** with ITO biased positive are shown in Figure 3.18. The photocurrent spectra of **P1, P2** and **P3** doped with C_{60} showed two peaks, one in the low energy region and the other in the higher energy region. At an electric field of 30 V/μm, **P1** showed a maximum photocurrent of 40.79 μA/m^2 (at 2.53 eV)

and 37.48 μA/m^2 (at 3.35 eV) respectively. The maximum photocurrent observed for **P2** at 30 V/μm was 28.95 μA/m^2 (at 2.03 eV) and 34.30 μA/m^2 (at 3.64 eV). The maximum photocurrent observed for P3 at 10 V/μm was 1.04 mA/m^2 (at 1.99 eV) and 0.89 mA/m^2 (at 2.69 eV).

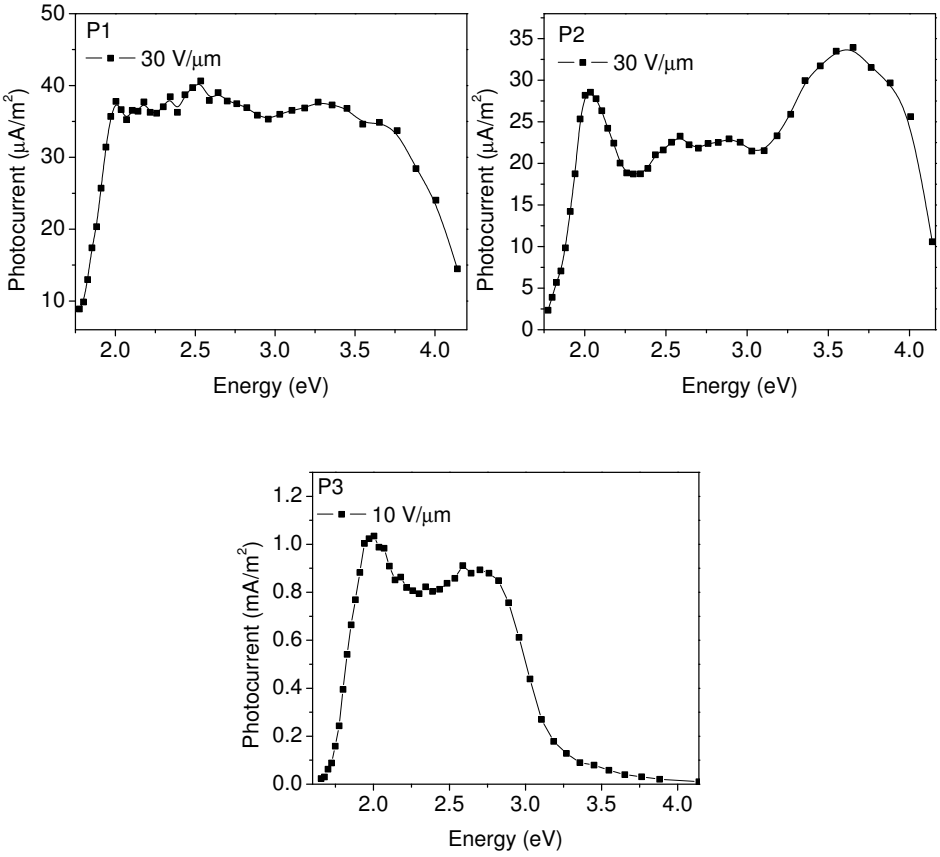

Figure 3.18: Photocurrent Action Spectrum of C_{60} Doped Polymers.

Upon doping with C_{60}, a 40 times increase in photocurrent was observed for P1 and P2 and a 1000 times increase in photocurrent was observed for P3. The enhanced photocurrent upon addition of C_{60} might be due to the electron transfer reaction between fullerene and polymer. The photoconductive sensitivity of **P1, P2** and **P3** sensitized with C_{60} was found to be 2034 x 10^{-14}, 1445 x 10^{-14} and 34100 x 10^{-14} S cm/W respectively at 630

nm respectively.

3.4 Conclusions

Polymers **P1, P2** and **P3** were synthesized by Mannich condensation of 4-tertiary butyl phenol, formaldehyde and an amine. The reaction proceeds via thermally activated cationic ring opening polymerization. Phenolic type polybenzoxazines were obtained. The structure of the polymers were characterized by elemental and spectral analysis. The polydispersity index (Mw/Mn) obtained were 2.67, 4.06 and 3.35 respectively. The reaction yielded a polymer of relatively low molecular weight exhibiting broad molecular weight distribution. The electrochemical and photocurrent spectral investigations were done. An enhanced photocurrent was observed upon addition of C_{60}. The photoconductive sensitivity of **P3** doped with C_{60} was found to be higher compared to other two polymers, hence **P3** was selected as charge transport host for fabricating the photorefractive system.

References

[1] M.-M. Shi, H.-Z. Chen, J.-Z. Sun, J. Ye, M. Wang, Chem. Phys. Lett. 381 (2003) 666.

[2] E. Kim, H. W. Lee, Mol. Cryst. Liq. Cryst. 431 (2005) 581.

[3] K.-S. Kang, W. N. Sisk, M. Y. A. Raja, F. F. J, J. Photochem. Photobiol., A 121 (1999) 133–140.

[4] K. Yoshino, A. Fujii, H. Nakayama, S. Lee, A. Naka, M. Ishikawa, J. Appl. Phys. 85 (1999) 414.

[5] O. Ostroverkhova, D. G. Cooke, S. Shcherbyna, R. F. Egerton, F. A. Hegmann, R. R. Tykwinski, J. E. Anthony, Phys. Rev. B 71 (2005) 0352041.

[6] V. P. Pham, G. Manivannan, R. A. Lessard, Trends. Polym. Sci 270 (1995) 295.

[7] C. Denz, T. Dellwig, J. Lembcke, T. Tschudi, Opt. Lett. 21 (1996) 278.

[8] K.-Y. Law, Chem. Rev. 93 (1993) 449.

[9] N. Peyghambarian, B. Kippelen, Mat. Res. Soc. Symp. Proc. 39 (1998) 488.

[10] M. Granstrom, K. Petritsch, A. C. Arias, A. Lux, R. Andersson, M. R. a Friend, Nature 395 (1998) 257.

[11] A. Greiner, Polym. Adv. Technol. 9 (1998) 371.

[12] R. Friend, G. Denton, J. Halls, N. Harrison, A. Holmes, A. Kfhler, A. Lux, S. Moratti, K. Pichler, N. Tessler, K. Towns, H. Wittmann, Solid State Commun. 102 (1997) 249.

[13] G. Iftime, F. L. Labarthet, A. Natansohn, P. Rochon, K. Murti, Chem. Mater. 14 (2002) 168.

[14] M. S. Ho, C. Barrett, J. Paterson, M. Esteghamatian, A. Natansohn, P. Rochon, Macromolecules 29 (1996) 4613.

[15] A.Ajayaghosh, Chem. Soc. Rev. 32 (2003) 181.

[16] G. Yu, J. Gao, J. C. Hummelen, F. Wudl, A. J. Heeger, Science 270 (1995) 1789.

[17] V. Dyakonov, G. Zoriniants, M. Scharber, C. J. Brabec, R. A. J. Janssen, J. C. Hummelen, N. S. Sariciftci, Phys. Rev. B 59 (1999) 8019.

[18] G. Zerza, A. Cravino, H. Neugebauer, R. Gamez, J. L. Segura, N. Martin, M. Svensson, M. R. Andersson, N. S. Sariciftci, Mat. Res. Soc. Symp. Proc. 660 (2001) 11.1.

[19] M. Wohlgenannt, W. Graupner, G. Leising, Z. V. Vardeny, Phys. Rev. B 60 (1999) 5321.

[20] M. Ranger, M. Leclerc, Macromolecules 32 (1999) 3306.

[21] V. N. Bliznyuk, S. A. Carter, J. C. Scott, G. Kla1rner, R. D. Miller, D. C. Miller, Macromolecules 32 (1999) 361.

[22] H. R. Kricheldorf, O. Nuyken, G. Swift, Hand Book of Polymer Synthesis, 2nd Edition, Marcel Dekker, Oxford, 2005.

[23] Y.-X. Wang, H. Ishida, Polymer 40 (1999) 4563.

[24] V. C. Kishore, R. Dhanya, K. Sreekumar, R. Joseph, C. S. Kartha, Spectral distribution of photcurrent in poly(6-tertiary-butyl-3-methyl-3,4-dihydro-2h-1,3-benzoxazine, Synth. Met. (2008) In press.

[25] H. Ishida, D. Sanders, Polymer 42 (2001) 3115.

[26] X. Ning, H. Ishida, J. Polym. Sci. Part A:Polym. Chem. 32 (1994) 1121.

[27] W. J. Burke, C. W. Stephens, J. Am. Chem. Soc. 74 (1952) 1518.

[28] F. W. Holly, A. C. Cope, J. Am. Chem. Soc. 66 (1994) 1875.

[29] B. Kiskan, D. Colak, A. E. Muftuoglu, I. Cianga, Y. Yagci, Macromol. Rapid. Commun. 26 (2005) 819.

[30] W. J. Burke, J. Bishop, E. L. Glennie, J. Bauer, W. N, J. Org. Chem. 30 (1965) 3423.

[31] Y. X. Wang, H. Ishida, Macromolecules 33 (2000) 2839.

[32] V. C. Kishore, R. Dhanya, C. S. Kartha, K. Sreekumar, R. Joseph, J. Appl. Phys. 101 (2007) 0631021.

[33] J. A. Macko, H. Ishida, Polymer 42 (2001) 6371.

[34] H. Y. Low, H. Ishida, Polymer 40 (1999) 4365.

[35] F. Ç. Cebeci, E. Sezer, A. S. Sarac, Electrochim. Acta 52 (2007) 2158.

[36] M. A. Loi, E. J. W. List, C. Gadermaier, W. Graupner, G. Leising, G. Bongiovanni, A. Mura, J.-J. Pireaux, K. Kaeriyama, Synth. Met. 111 (2000) 519.

[37] G. J. Brealey, M. Kasha, Abstracts of OSU International Symposium on Molecular Spectroscopy 1946-1959 77 (1955) 4462.

[38] H. McConnell, J. Chem. Phys. 20 (1952) 700.

CHAPTER

FOUR

Synthesis and Characterization of Alkyl Substituted p-Nitroaniline Derivatives for Electro-optic Effect

4.1 Introduction

The field of non-linear optics has generated considerable interest by bringing in the key elements of future photonic technologies.[1–5] Organic chromophores with efficient electron donor and acceptor groups connected by a conjugated bridge are promising candidates for photorefractive applications owing to their high electro-optic coefficient, ease of synthesis, high figure of merit (FOM) and low dielectric constant.[6,7] High electro-optic coefficient requires non-centrosymmetric alignment of molecules in the bulk[8] and an effective intramolecular charge transfer between the donor and acceptor groups.[9,10] Non-centrosymmetric molecules with large permanent dipole moment exhibit significant degree of intramolecular charge transfer. Such molecules contribute to high optical nonlinearity with applications in second harmonic generation,[11] Raman scattering,[12] and multiphoton transitions.[13] Organic molecules with permanent dipole moment have strong tendency towards centrosymmetric alignment.[14] Various approaches have been made to introduce asymmetry in the chromophore which include incorporation of bulky substituent, long alkyl chains and chirality in the chromophore.[15–17] The optical nonlinearity of these systems can be en-

hanced by modifying the dipole moment.[18] The challenges in this area of research is to design and synthesize molecules with high optical quality and high nonlinearity.[19] Therefore suitable selection and optimization of conjugate bridge and donor-acceptor pairs are needed to achieve both requirements.

The synthesis, characterization and determination of electro-optic coefficients of a series of alkyl substituted para-nitroaniline derivatives possessing high ground state dipole moment is reported in this chapter. p-Nitroaniline, a well known donor-acceptor system, with relatively high nonlinearity was commonly used to design and synthesize molecules with high electro-optic coefficients.[20] The motive to introduce lengthy alkyl chains was to increase the first hyperpolarizability without shifting the absorption into the visible region of the spectrum. The length of the alkyl chain was varied by changing the number of alkyl spacers (n= 2-6). The ground state (μ_g), excited state (μ_e) dipole moments and the first hyperpolarizability (β) of the chromophores were determined. A knowledge of dipole moment provides necessary information about the electronic excited state of the chromophore.[21] The technique chosen to explore the μ_e was based on solvatochromism.[22] The solvatochromic method involves the effect of solvent on position, shape and intensity of the electronic absorption bands of the chromophores accompanying a change in the polarity of solvent.[23]

4.2 Experimental

4.2.1 Materials

4-nitroaniline (98 %, Merck) was purified by recrystallization from ethanol. The following chemicals were used as received without further purification: 1,4-dibromobutane (99 %, Alfa Aesar), 1,3-diaminopropane (98 %, Alfa Aesar), 1,4-diaminobutane (98 %, Alfa Aesar), 1,6-diaminohexane (98+ %, Alfa Aesar), sodium hydride (60 % dispersion in mineral oil) (98 %, Avocado), 1-bromoethane (98+ %, Alfa Aesar), 1,2-diaminoethane (99 %, Merck), sodium carbonate (anhydrous) (99 %, Merck) and silica gel (60-120 mesh, pH- 7.0) (98 %, Sd fine). Benzene (Rankem, AR Grade),

tetrahydrofuran (Rankem, AR Grade), ethyl acetate (Merck, AR Grade) and diethylether (Sd fine, AR Grade) were purified, dried and distilled by the standard procedures.[24] Toluene (98 %, Merck), dimethylformamide (DMF), (98 %, Merck) chloroform (99 %, Merck) and acetonitrile (98 %, Merck) were spectroscopic grade and used without further purification.

4.2.2 Instrumentation

The instrumentation techniques employed for the study of molecules are described in detail in section 2.6.2. The refractive index of the solutions were measured using an Atago DRM2 refractometer. Measurement of the capacitance was done using a HP 4277A LCZ meter operating at a frequency of 10 KHz.

4.2.3 Synthesis

Synthesis of N,N-bis(4-bromobutyl)-4-nitrobenzenamine (1a)

p-Nitroaniline (5.0 g, 36.2 mmol) was dissolved in water (60 mL). Sodium carbonate (8.96 g, 85.3 mmol) was added to this solution. The solution was kept under stirring. The temperature was kept at 98 ^{0}C. To this solution 1,4-dibromobutane (10 mL, 83.3 mmol) was added drop wise and refluxed for 12 h under stirring. The reaction was cooled and filtered. The brown solid obtained was washed with distilled water. The crude product was washed with water and purified by column chromatography using benzene/ethyl acetate. The bright yellow crystals obtained was recrystallized from ethanol.

Yield: 89%; mp: 160.5 ^{o}C. FTIR (KBr) ν cm^{-1}: 1602, 1532, 1441, 1110. ^{1}H NMR (400 MHz $CDCl_3$) δ: 8.10 (d, 2H), 6.45 (d, 2H), 3.42 (t, 4H), 3.40 (d, 4H), 2.07 (m, 4H), 1.63 (m, 4H). ^{13}C NMR (100 MHz $CDCl_3$) δ: 151.91, 136.60, 126.42, 110.49, 77.42, 47.99, 36.32, 25.50. Mass (m/e): 408 (molecular ion peak). Anal. Calcd for: $C_{14}H_{20}Br_2N_2O_2$ - C, 41.20; H, 4.94; N, 6.86. Found: C, 41.25; H, 4.96; N, 6.82.

Synthesis of N,N-bis(4-[(2-aminoethyl)amino]butyl)-4-nitrobenzenamine (2a)

N,N-bis(4-bromobutyl)-4-nitrobenzenamine (0.2 g, 0.49 mmol) was dissolved in dry THF (25 mL). To this solution 60 % NaH dispersion in paraffin oil (0.0392 g, 1.63 mmol) in dry THF (6 mL) was added drop wise. The solution was kept at reflux for 3 h. To this solution, 1,2-diaminoethane (0.6 mL, 8.72 mmol) in dry THF (2 mL) was added drop wise and was refluxed for 6 h. The brown precipitate obtained was extracted with diethylether, washed with dilute HCl and subsequently with distilled water. The solid was dried and recrystallized from diethylether.

Yield: 80%; mp: 161.5 ^{o}C. FTIR (KBr) ν cm^{-1}: 3500, 2932, 2880,1530. ^{1}H NMR (400 MHz $CDCl_3$) δ: 8.12 (d, 2H), 6.47 (d, 2H), 3.41 (t, 4H), 2.10 (m, 8H), 2.08 (t, 4H), 2.04 (s, 4H) 1.61 (s, 2H), 1.25 (m, 8H). ^{13}C NMR (75 MHz $CDCl_3$) δ: 151.91, 136.62, 126.42, 110.50, 77.42, 77.10, 76.78, 47.99, 31.1, 25.50. Mass (m/e): 366 (molecular ion peak). Anal. Calcd for: $C_{18}H_{34}N_6O_2$ - C, 58.99; H, 9.35; N, 22.93. Found: C, 58.65; H, 9.28; N, 22.90.

Synthesis of N,N-bis(4-[(3-aminopropyl)amino]butyl)-4-nitrobenzenamine (2b)

N,N-bis(4-bromobutyl)-4-nitrobenzenamine (0.2 g, 0.49 mmol) was dissolved in dry THF (25 mL). To this solution 60 % NaH dispersion in paraffin oil (0.0392 g, 1.63 mmol) in dry THF (6 mL) was added drop wise. The solution was kept at reflux for 3 h. To this solution, 1,3-diaminopropane (0.6 mL, 8.72 mmol) in dry THF (2 mL) was added drop wise and was refluxed for 6 h. The brown precipitate obtained was extracted with diethylether, washed with dilute HCl and subsequently with distilled water. The solid was dried and recrystallized from diethylether.

Yield: 82%; mp: 163.48 ^{o}C. FTIR (KBr) ν cm^{-1}: 3500, 2950, 2875, 1525. ^{1}H NMR (400 MHz $CDCl_3$) δ: 8.13 (d, 2H), 6.47 (d, 2H), 3.42 (t, 4H), 2.10 (m, 8H), 2.07 (t, 4H), 2.04 (s, 4H), 2.01 (s, 2H), 1.63 (m, 4H), 1.25 (m, 8H). ^{13}C NMR (75 MHz $CDCl_3$) δ: 151.91, 136.60, 126.42, 110.49, 77.42, 76.79, 77.11, 47.99, 31.10, 30.52, 25.50. Mass (m/e): 394 (molecular ion peak). Anal. Calcd for: $C_{20}H_{38}N_6O_2$ - C, 60.88; H, 9.71; N, 21.30. Found: C, 60.38; H, 9.65; N, 21.15.

Synthesis of N,N-bis(4-[(4-aminobutyl)amino]butyl)-4-nitro-

benzenamine (2c)

N,N-bis(4-bromobutyl)-4-nitrobenzenamine (0.2 g, 0.49 mmol) was dissolved in dry THF (25 mL). To this solution 60 % NaH dispersion in paraffin oil (0.0392 g, 1.63 mmol) in dry THF (6 mL) was added drop wise. The solution was kept at reflux for 3 h. To this solution, 1,4-diaminobutane (0.75 mL, 8.82 mmol) in dry THF (2 mL) was added drop wise and was refluxed for 6 h. The brown precipitate obtained was extracted with diethylether, washed with dilute HCl and subsequently with distilled water. The solid was dried and recrystallized from diethylether.

Yield: 85%; mp: 162.5 ^{o}C. FTIR (KBr) cm^{-1}: 3500, 2900, 2880,1530. ^{1}H NMR (400 MHz $CDCl_3$) δ: 8.13 (d, 2H), 6.47 (d, 2H), 3.42 (t, 4H), 2.10 (m, 8H), 2.07 (t, 4H), 2.04 (s, 4H), 2.01 (s, 2H), 1.63 (m, 8H), 1.25 (m, 8H). ^{13}C NMR (75 MHz $CDCl_3$) δ: 151.91, 136.60, 126.42, 110.49, 77.42, 76.79, 77.11, 47.99, 31.10, 30.70, 30.52, 25.50. Mass (m/e): 422 (molecular ion peak). Anal. Calcd for: $C_{22}H_{42}N_6O_2$ - C, 62.52; H, 10.02; N, 19.89. Found: C, 62.48; H, 10.05; N, 19.87.

Synthesis of N,N-bis(4-[(6-aminohexyl)amino]butyl)-4-nitrobenzenamine (2d)

N,N-bis(4-bromobutyl)-4-nitrobenzenamine (0.2 g, 0.49 mmol) was dissolved in dry THF (25 mL). To this solution 60 % NaH dispersion in paraffin oil (0.0392 g, 1.63 mmol) in dry THF (6 mL) was added drop wise. The solution was kept at reflux for 3 h. To this solution, 1,6-diaminohexane (1 mL, 8.82 mmol) in dry THF (2 mL) was added drop wise and was refluxed for 6 h. The brown precipitate obtained was extracted with diethylether, washed with dilute HCl and subsequently with distilled water. The solid was dried and recrystallized from diethylether.

Yield: 72%; mp: 166.25 ^{o}C. FTIR (KBr) ν cm^{-1}: 3500, 2923, 2840, 1532. ^{1}H NMR (400 MHz $CDCl_3$) δ: 8.10 (d, 2H), 6.47 (d, 2H), 3.40 (t, 4H), 2.10 (m, 8H), 2.07 (t, 4H) 2.04 (s, 4H), 1.61 (s, 2H), 1.44 (m, 16H), 1.25 (m, 8H). ^{13}C NMR (75 MHz $CDCl_3$) δ: 151.91, 136.60, 126.42, 110.49, 77.42, 76.79, 77.11, 47.99, 31.10, 30.70, 30.52, 29.9, 25.50. Mass (m/e): 478 (molecular ion peak). Anal. Calcd for: $C_{26}H_{50}N_6O_2$ - C, 65.23; H, 10.53; N, 17.56. Found: C, 65.15; H, 10.48; N, 17.52.

Synthesis of N,N-bis(4-[2-(ethyl amino)ethylamino]butyl)-4-nitrobenzenamine (3a)

N,N-bis(4-[(2-aminoethyl)amino]butyl)-4-nitrobenzenamine (0.2 g, 0.54 mmol) was dissolved in dry THF (30 mL). To this solution 60 % NaH dispersion in paraffin oil (0.0392 g, 1.63 mmol) in dry THF (6 mL) was added drop wise. The solution was kept at reflux for 3 h. To this solution, 1-bromoethane (0.4 mL, 5.40 mmol) in dry THF (2 mL) was added drop wise and was refluxed for 8 h. The brown precipitate obtained was extracted with diethylether, washed with dilute HCl and subsequently with distilled water. The solid was dried and recrystallized from diethylether.

Yield: 68%; mp: 164^{o}C. FTIR (solid) cm^{-1}: 3500, 2900, 2880, 1600, 1530, 1480, 1330. ^{1}H NMR (400 MHz $CDCl_3$) δ: 8.12 (d, 2H), 6.47 (d, 2H), 3.41 (t, 4H), 2.10 (m, 8H), 2.08 (t, 4H), 2.04 (s, 2H), 2.01 (s, 2H), 1.61 (m, 4H), 1.25 (m, 8H), 0.88 (t, 3H). ^{13}C NMR (75 MHz $CDCl_3$) δ: 151.91, 136.62, 126.42, 110.50, 77.42, 77.10, 76.78, 47.99, 31.1, 30.08, 25.50, 21.88. Mass (m/e): 422 (molecular ion peak). Anal. Calcd for: $C_{22}H_{42}N_6O_2$ - C, 62.52; H, 10.02; N, 19.89. Found: C, 62.48; H, 10.05; N, 19.86.

Synthesis of N,N-bis(4-[3-(ethyl amino)propylamino]butyl)-4-nitrobenzenamine (3b)

N,N-bis(4-[(2-aminopropyl)amino]butyl)-4-nitrobenzenamine (0.2 g, 0.54 mmol) was dissolved in dry THF (30 mL). To this solution 60 % NaH dispersion in paraffin oil (0.0392 g, 1.63 mmol) in dry THF (6 mL) was added drop wise. The solution was kept at reflux for 3 h. To this solution, 1-bromoethane (0.4 mL, 5.40 mmol) in dry THF (2 mL) was added drop wise and was refluxed for 8 h. The brown precipitate obtained was extracted with diethylether, washed with dilute HCl and subsequently with distilled water. The solid was dried and recrystallized from diethylether.

Yield: 58%; mp= 162^{o}C. FTIR (solid) cm^{-1}: 3500, 2900, 2880, 1600, 1530, 1480, 1330. ^{1}H NMR (400 MHz $CDCl_3$) δ: 8.13 (d, 2H), 6.47 (d, 2H), 3.42 (t, 4H), 2.10 (m, 8H), 2.07 (t, 4H), 2.04 (s, 2H), 2.01 (s, 2H), 1.63 (m, 6H), 1.25 (m, 8H), 0.88 (t, 3H). ^{13}C NMR (75 MHz $CDCl_3$) δ: 151.91, 136.60, 126.42, 110.49, 77.42, 76.79, 77.11, 47.99, 31.10, 30.52,

30.50, 25.50, 21.88. Mass (m/e): 450 (molecular ion peak). Anal. Calcd for: $C_{24}H_{46}N_6O_2$ - C, 63.96; H, 10.29; N, 18.65. Found: C, 63.78; H, 10.25; N, 18.66.

Synthesis of N,N-bis(4-[4-(ethyl amino)butylamino]butyl)-4-nitrobenzenamine (3c)

N,N-bis(4-[(2-aminobutyl)amino]butyl)-4-nitrobenzenamine (0.2 g, 0.54 mmol) was dissolved in dry THF (30 mL). To this solution 60 % NaH dispersion in paraffin oil (0.0392 g, 1.63 mmol) in dry THF (6 mL) was added drop wise. The solution was kept at reflux for 3 h. To this solution, 1-bromoethane (0.4 mL, 5.40 mmol) in dry THF (2 mL) was added drop wise and was refluxed for 8 h. The brown precipitate obtained was extracted with diethylether, washed with dilute HCl and subsequently with distilled water. The solid was dried and recrystallized from diethylether.

Yield: 56%; mp: 163^{o}C. FTIR (solid) cm^{-1}: 3500, 2900, 2880, 1600, 1530, 1480, 1330. ^{1}H NMR (400 MHz $CDCl_3$) δ: 8.13 (d, 2H), 6.47 (d, 2H), 3.42 (t, 4H), 2.10 (m, 8H), 2.07 (t, 4H), 2.04 (s, 2H), 2.01 (s, 2H), 1.63 (m, 10H), 1.25 (m, 8H), 0.88 (t, 3H). ^{13}C NMR (75 MHz $CDCl_3$) δ: 151.91, 136.60, 126.42, 110.49, 77.42, 76.79, 77.11, 47.99, 31.10, 30.70, 30.52, 30.48, 25.50, 21.88. Mass (m/e): 478 (molecular ion peak). Anal. Calcd for: $C_{26}H_{50}N_6O_2$ - C, 65.32; H, 10.53; N, 17.56. Found: C, 65.28; H, 10.55; N, 17.66.

Synthesis of N,N-bis(4-[6-(ethyl amino)hexylamino]butyl)-4-nitrobenzenamine (3d)

N,N-bis(4-[(2-aminohexyl)amino]butyl)-4-nitrobenzenamine (0.2 g, 0.54 mmol) was dissolved in dry THF (30 mL). To this solution 60 % NaH dispersion in paraffin oil (0.0392 g, 1.63 mmol) in dry THF (6 mL) was added drop wise. The solution was kept at reflux for 3 h. To this solution, 1-bromoethane (0.4 mL, 5.40 mmol) in dry THF (2 mL) was added drop wise and was refluxed for 8 h. The brown precipitate obtained was extracted with diethylether, washed with dilute HCl and subsequently with distilled water. The solid was dried and recrystallized from diethylether.

Yield: 52%; mp: 167^{o}C. FTIR (solid) cm^{-1}: 3500, 2900, 2880, 1600, 1530, 1480, 1330. ^{1}H NMR (400 MHz $CDCl_3$) δ: 8.10 (d, 2H), 6.47 (d,

2H), 3.40 (t, 4H), 2.10 (m, 8H), 2.07 (t, 4H) 2.04 (s, 2H), 1.61 (s, 2H), 1.44 (m, 18H), 1.25 (m, 8H), 0.88 (t, 3H). ^{13}C NMR (75 MHz $CDCl_3$) δ: 151.91, 136.60, 126.42, 110.49, 77.42, 76.79, 77.11, 47.99, 31.10, 30.70, 30.52, 30.48, 29.9, 25.50, 21.88. Mass (m/e): 506 (molecular ion peak). Anal. Calcd for: $C_{30}H_{58}N_6O_2$ - C, 67.37; H, 10.93; N, 15.71. Found: C, 67.28; H, 10.95; N, 15.70.

4.2.4 Sample Preparation

The samples for electro-optic studies were prepared as follows: The NLO chromophores were dissolved in a 8 wt% solution poly(methyl methacrylate) in chloroform. The solution was filtered through a 0.45 μm Nylon filter and deposited on patterned ITO coated glass substrates. The films were dried at room temperature (28 ^{0}C) for 12 h and then in vacuum chamber (at 10^{-2} Torr) for 24 h. The sample was heated to 100^{o}C and the second patterned ITO substrate was placed on top of the first. The film thickness was controlled by using a 48 μm Teflon spacer between the substrates. The sandwiched sample was cooled and the ITO's were glued together using a thermally stable adhesive. No phase separation was noticed in the film up to 15 wt% loading of chromophores. Further loading (20 wt %) resulted in phase separated samples. DSC measurements (Q-100, TA instruments) under nitrogen, at a heating rate of 10 ^{o}C/min, was employed to determine the T_g of the PMMA matrix dispersed with the synthesized chromophores.

4.3 Results and Discussion

A series of p-nitroaniline derivatives having typical push-pull structure with electron donating amino functionalized alkyl groups and electron accepting nitro group connected by a benzene ring were synthesized. The length of the alkyl chain attached to the central phenyl group was varied. The structure of the chromophores (**1a, 2a-d** and **3a-d**) was confirmed by elemental analysis, FTIR, (^{1}H and ^{13}C) NMR and FAB-MS. The chromophores are soluble in common organic solvents such as acetone,

chloroform, DMF, THF, toluene, acetonitrile and ethanol. The elemental analysis values were found to be in good agreement with the calculated values for the proposed structure. The (^{1}H and ^{13}C) NMR spectrum of chromophores (**1a**, **2a-d** and **3a-d**) clearly indicated disubstitution at the donor end of p-nitroaniline moiety.

4.3.1 N,N-bis(4-bromobutyl)-4-nitrobenzenamine

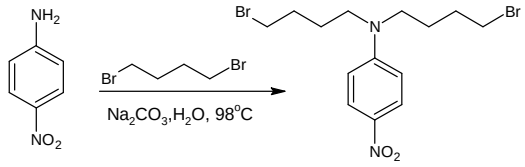

Figure 4.1: Synthesis route of N,N-bis(4-bromobutyl)-4-nitrobenzenamine.

The synthesis route of N,N-bis(4-bromobutyl)-4-nitrobenzenamine (**1a**) is shown in Figure 4.1. Chromophore **1a** was obtained in 89% yield by the standard alkylation of para-nitroaniline with 1,4-dibromobutane. The product obtained was purified by column chromatography using benzene/ethyl acetate.

4.3.2 N,N-bis(4-[(n-aminoalkyl)amino]butyl)-4-nitrobenzenamine

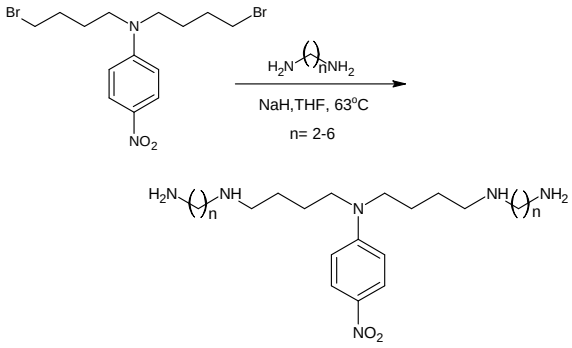

Figure 4.2: Synthesis route of N,N-bis(4-[(n-aminoalkyl)amino]butyl)-4-nitrobenzenamine.

The synthesis route of N,N-bis(4-[(n-aminoalkyl)amino]butyl)-4- nitrobenzenamine, **2(a-d)** is shown in Figure 4.2. Chromophore **2** (**a, b, c, d**) was obtained by reacting chromophore **1a** with alkyl diamines using sodium hydride. The chromophores were purified by recrystallization from diethylether. The detailed ^{1}H and ^{13}C NMR spectral interpretation of chromophores **2(a-d)** are given in 4.2.3. As an example, the ^{1}H and ^{13}C NMR spectrum of 2a are shown in Figure 4.7 and Figure 4.8.

4.3.3 N,N-bis(4-[n-(ethylamino)alkylamino]butyl)-4-nitrobenzenamine

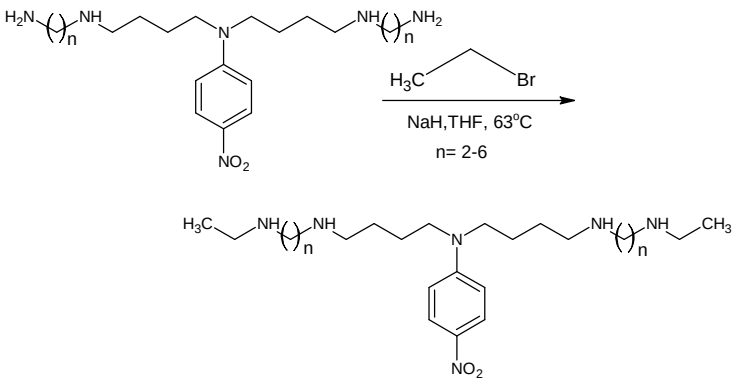

Figure 4.3: Synthesis route of N,N-bis(4-[n-(ethylamino)alkylamino]-butyl)-4-nitrobenzenamine.

The synthesis route of N,N-bis(4-[n-(ethylamino)alkylamino]butyl)- 4-nitrobenzenamine (**3a-d**) is shown in Figure 4.3. Chromophores **3** (**a, b, c, d**) were obtained by reacting chromophores **2** (**a, b, c, d**) with 1-bromoethane using sodium hydride. The donor-acceptor para-nitroaniline derivatives were obtained in moderate to good yields (48-89%) as specified in the experimental section. The detailed ^{1}H and ^{13}C NMR spectral interpretation of chromophores **3(a-d)** are given in 4.2.3. As an example, the ^{1}H and ^{13}C NMR spectrum of 3a are shown in Figure 4.10 and Figure 4.11.

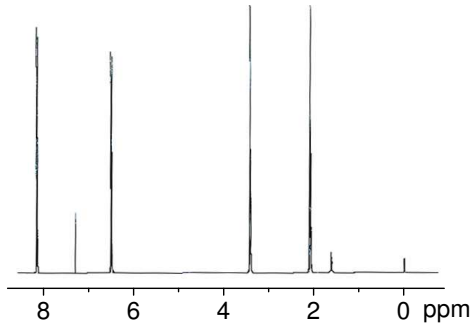

Figure 4.4: ^{1}H NMR Spectrum of N,N-bis(4-bromobutyl)-4-nitrobenzenamine.

The ^{1}H NMR spectrum of chromophore **1a** is shown in Figure 4.4. The resonance peaks at 8.10 and 6.45 ppm are attributed to the proton attached to the carbon of the aromatic ring. The peak at 3.42 ppm correspond to the methylene proton of (CH_2-Br). The resonance peaks around 2.07 and 1.63 are due to (CH_2) protons. The peak at 3.42 ppm correspond to (N-CH_2) protons substituted at the amino end of p-nitroaniline.

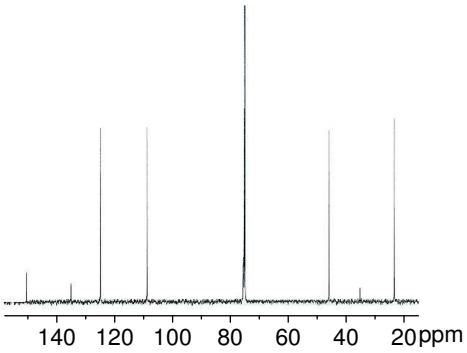

Figure 4.5: ^{13}C NMR Spectrum of N,N-bis(4-bromobutyl)-4-nitrobenzenamine.

Further the structure of chromophore **1a** was confirmed with ^{13}C NMR as shown in Figure 4.5. The resonance signals around 151.91, 136.60, 126.42 and 110.49 ppm are assigned to aromatic carbon. The peaks around 77.42 and 47.99 ppm correspond to methylene carbon of (N-CH_2) and (CH_2-Br).

The resonance signals at 36.32 and 25.50 ppm are attributed to methylene carbon.

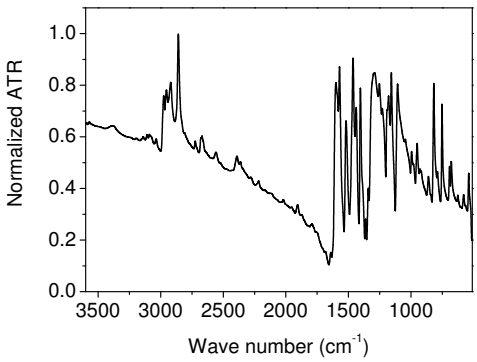

Figure 4.6: FT-IR Spectrum of N,N-bis(4-bromobutyl)-4-nitrobenzenamine.

FT-IR spectrum of chromophore **1a** is shown in Figure 4.6. The band around 671 cm^{-1} is associated with the aliphatic bromine atom. The bands at 1359 and 1110 cm^{-1} are assigned to aromatic symmetric and aliphatic asymmetric C-N stretching vibration and at 2817 cm^{-1} to N-CH_2 stretching vibration of amines. The bands at 3038, 3074 and 3093 cm^{-1} are attributed to aromatic C-H stretching and the band at 2887 cm^{-1} to aliphatic symmetric -CH_2- stretching. The bands centered around 1473 and 1601 cm^{-1} are attributed to aromatic C-NO_2 symmetric and asymmetric stretching.

Figure 4.7 shows the ^{1}H NMR spectrum of chromophore (**2a**). The resonance peaks at 8.12 and 6.47 ppm are attributed to the proton attached to carbon of the aromatic ring. The resonance peaks around 2.10, 2.08 and 1.25 ppm are assigned to the methylene protons. The peak at 3.41 ppm is attributed to methylene proton (CH_2-NH_2). The resonance peaks around 1.61 and 2.04 ppm correspond to protons attached to NH and NH_2 moiety indicated substitution of diamine.

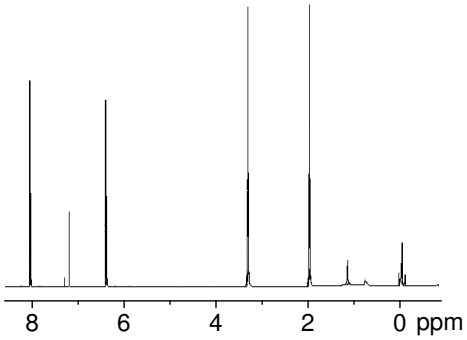

Figure 4.7: ^{1}H NMR Spectrum of N,N-bis(4-[(n-aminoethyl)amino]butyl)-4-nitrobenzenamine.

Figure 4.8 shows the ^{13}C spectrum of chromophore **2a**. The resonance signals around 151.91, 136.62, 126.42 and 110.50 ppm are of aromatic carbons. The peaks around 77.42, 77.10, 31.1 and 25.50 ppm correspond to methylene carbon. The resonance signal at 76.78 and 47.99 ppm are due to methylene protons of ethylene diamine.

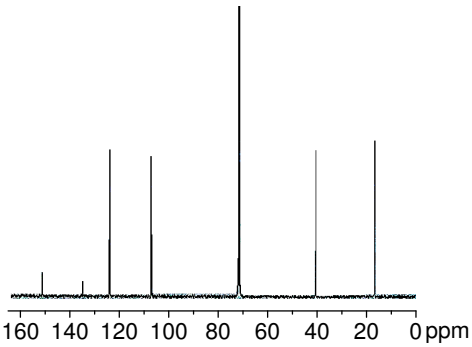

Figure 4.8: ^{13}C NMR Spectrum of N,N-bis(4-[(n-aminoethyl)amino]butyl)-4-nitrobenzenamine.

FT-IR spectrum of chromophore **2a** is shown in Figure 4.9. The disappearance of band centered around 671 cm^{-1} (aliphatic bromine atom) and the appearance of bands at 2925, 2961 and 3374 cm^{-1} (N-H symmetric stretching) indicated substitution of dialkylamines. The bands at 3325, 3318 and 3374 cm^{-1} correspond to N-H symmetric stretching of pri-

mary and secondary amines. The bands around 1259 and 1165 cm^{-1} are assigned to aromatic symmetric and aliphatic asymmetric C-N stretching vibration and the band around 2826 cm^{-1} to N-CH_2 stretching vibration of amines.

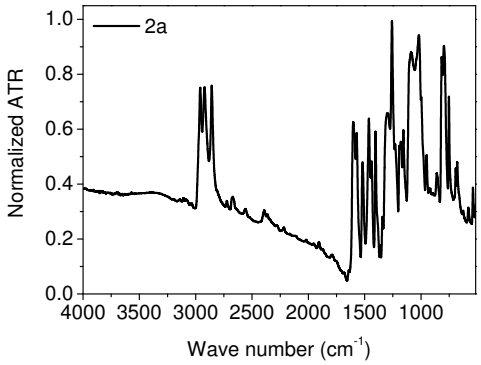

Figure 4.9: Typical FT-IR Spectrum of N,N-bis(4-[(n-aminoethyl)amino]butyl)-4-nitrobenzenamine.

The band at 3034, 3077 and 3108 cm^{-1} are attributed to aromatic C-H stretching and the band at 2862 cm^{-1} to aliphatic symmetric -CH_2 stretching. The peak centered around 1457 and 1602 cm^{-1} are attributed to aromatic C-NO2 symmetric and asymmetric stretching.

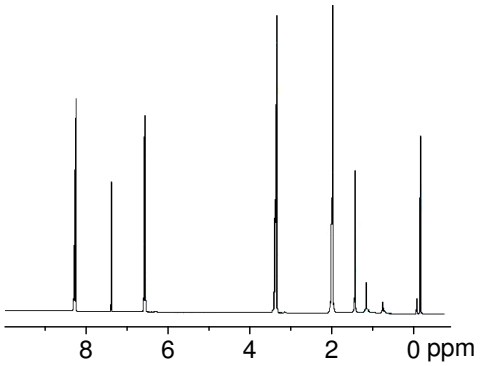

Figure 4.10: ^1H NMR Spectrum of N,N-bis(4-[n-(ethylamino)ethylamino]butyl)-4-nitrobenzenamine.

Figure 4.10 shows the ^{1}H NMR spectrum of chromophore (**3a**). The resonance peaks at 8.12 and 6.47 ppm are attributed to the proton attached to the carbon of the aromatic ring. The resonance peaks around 3.41, 2.10, 2.08, 1.61 and 1.25 ppm are assigned to the methylene protons. The peak at 0.88 ppm is assigned to methyl proton. The resonance peaks around 2.04 and 2.01 ppm correspond to protons attached to NH moiety.

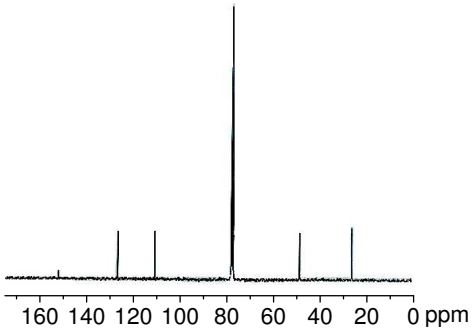

Figure 4.11: ^{13}C NMR Spectrum of N,N-bis(4-[n-(ethylamino)ethylamino]butyl)-4-nitrobenzenamine.

Figure 4.11 shows the ^{13}C NMR spectrum of chromophore (**3a**). The resonance signals around 151.91, 136.62, 126.42 and 110.50 ppm are of aromatic carbon. The peaks around 77.42, 77.10, 76.78, 47.99, 31.1, 30.08 and 25.50 ppm correspond to methylene carbon. The resonance signal at 21.88 ppm correspond to methyl carbon.

FT-IR spectrum of chromophore **3a** is shown in Figure 4.12. The disappearance of bands centered around 2925, 2961 cm^{-1} (N-H symmetric stretching of aliphatic primary amine) and the presence of singlet band at 3403 cm^{-1} (N-H symmetric stretching of secondary amines) indicated the reaction of chromophores **2** (**a, b, c, d**) with 1-bromoethane. The bands around 1257 and 1179 cm^{-1} are assigned to aromatic symmetric and aliphatic asymmetric C-N stretching vibration and the band around 2826 cm^{-1} to N-CH_2 stretching vibration of amines. The bands at 3034, 2954 and 2961 cm^{-1} are attributed to aromatic C-H stretching and the band at 2854 cm^{-1} to aliphatic symmetric -CH_2- stretching. The peak

centered around 1460 and 1602 cm^{-1} are attributed to aromatic C-NO2 symmetric and asymmetric stretching.

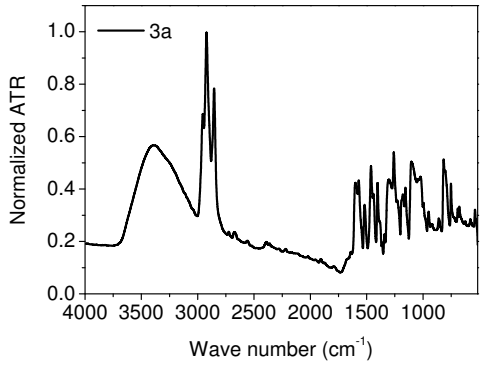

Figure 4.12: Typical FT-IR Spectrum of N,N-bis(4-[n-(ethylamino)ethylamino]butyl)-4-nitrobenzenamine.

The absorption spectrum of chromophores were recorded in 1:1 mixture of toluene and acetonitrile. The chromophore **1a** showed maximum absorption at around 3.2 eV. The chromophores **2 (a-d)** showed absorption maxima between 393-399 nm and chromophores **3 (a-d)** between 399–402 nm. There was no considerable shift observed in the absorption spectrum upon increasing the alkyl chain length. This could be due to the weak electron donating nature of alkyl groups. The maximum absorption value for the chromophores are given in Table 4.2.

4.3.4 Ground State Dipole Moment

The ground state dipole moment of the chromophores was calculated using the Debye-Guggenheim method.[25,26]

$$\mu_g^2 = \frac{3\varepsilon_0 kT}{N_A} \frac{9}{(\varepsilon^0 + 2)(n_0^2 + 2)} \frac{M}{\rho_0} \left(\frac{\partial \epsilon}{\partial \omega} \right)_o, \tag{4.1}$$

where M is the molar mass of the chromophore, N_A is the avogadro constant, ε^0 is the dielectric constant, n_0 is the refractive index, ρ_0 is the density of pure solvent, ω is the weight fraction, ε_0 is the vacuum per-

mittivity and $(\partial\epsilon/\partial\omega)_0$ is the variation of dielectric constant with weight fraction at infinite dilution.

Table 4.1: Ground state dipole moment μ_g of chromophores (1a, 2a-d and 3a-d)

Chromophores	μ_g (D)	*Chromophores*	μ_g (D)
1a	14.95	3a	4.43
2a	8.88	3b	11.75
2b	8.48	3c	16.85
2c	10.20	3d	7.47
2d	12.63		

The method involves the measurement of dielectric constant and refractive index of the chromophores with varying concentration in a non-polar solvent. Toluene was used as the non-polar solvent. The weight fraction of the chromophores was varied from 0.004 to 0.038. A detailed procedure is already reported.[27] The calculated ground state dipole moment of chromophore **1a** was 9.78 Debye. The μ_g of the chromophores (**2a-d**) were between 8-12 Debye and chromophores (3a-d) were between 9-22 Debye. The ground state dipole moment μ_g of chromophores are given in Table 4.1. The dipole moments are given in Debye (D).

4.3.5 Excited State Dipole Moment

The excited state dipole moment was measured using solvatochromic technique. The technique and method of analysis have been described in detail.[26–29] Solvatochromic technique involves the analysis of the shift in the position and intensity of spectral bands as a function of solvent polarity. The shift in the spectral band arises from the large reaction field which a solute molecule experiences due to the polarization of the surrounding solvent molecules.[30] The nature and arrangement of the surrounding solvent molecules has considerable effect on the reaction field.[23] Onsager proposed

a model in which the surrounding solvent molecule forms spherical shape cavity around the solute molecules and the dipole moment was assumed to be at the center of the cavity.[31] Various theoretical quantum level calculations provides a greater insight into the solute molecular properties with irregular shape cavities.[32] Experimentally it is not yet clear whether the solvatochromic estimation fails for molecules with shapes other than spherical or ellipsoid.[33]

The absorption and fluorescence studies were carried out in binary solvent mixtures of varying solvent polarity. The non-polar solvent toluene and polar solvent acetonitrile was selected and mixtures with varying weight fraction of acetonitrile were prepared. Solutions for spectral measurements were prepared by keeping the concentration of chromophores at a lower value to minimize interaction. The actual concentrations were in the range 3 x 10^{-5} mol/l to 8 x 10^{-5} mol/l. The dimensionless solvent polarity parameter E_T^N proposed by Reichardt was used for the analysis of various compositions.[34] The absorption maxima was red-shifted with increasing solvent polarity, thus the chromophores showed positive solvatochromism.

The accuracy of the estimation of the excited state dipole moment using solvatochromic method depends on the preciseness of the Onsager radii of the chromophores. The selection of the Onsager radius was a difficult problem in our case, since the chromophores under study were not absolutely spherical owing to the longer alkyl chains. The error related to the estimation of Onsager radius 'a' can be minimized by taking the ratio method as proposed by Ravi et al.[35] The dipole moment in the excited state was determined from the changes of Stoke's shift as a function of solvent polarity parameter E_T^N according to the following equation.

$$\upsilon_a - \upsilon_f = 11307.6 \left(\frac{\Delta\mu^2}{\Delta\mu_D^2} \right) \left(\frac{a_D^3}{a^3} \right) E_T^N + Constant \qquad (4.2)$$

In equation (2), $\upsilon_a - \upsilon_f$ is the Stoke's shift. $\Delta\mu$ and a are the difference between the ground and excited state dipole moments and Onsager cavity radius of the chromophore respectively. $\Delta\mu_D$ and a_D are those of the

betaine dye used to estimate the E_T^N scale of the binary solvent mixture. The Onsager cavity radius (a) of the synthesized molecule was calculated using the density (d) and molecular weight (M) from the relation $a^3 = (3M/4\pi dN_A)$.[29] The excited state dipole moment could be calculated from the plots of Stoke's shift versus E_T^N according to equation (2).

Table 4.2: UV-Vis absorption (λ_{abs}^{max}), Onsager cavity radius (a) and excited state dipole moment μ_e of chromophores (1a, 2a-d and 3a-d

Chromophores	λ_{abs}^{max} (nm)	a (A^o)	μ_e (D)
1a	388	4.71	14.53
2a	393	5.07	14.53
2b	395	5.23	14.55
2c	397	5.39	15.88
2d	399	5.67	19.07
3a	399	5.43	9.50
3b	400	5.58	17.58
3c	401	5.63	22.56
3d	402	5.97	14.67

The UV-Vis absorption (λ_{abs}^{max} nm), Onsager cavity radius (a), excited state dipole moment μ_e of chromophores are given in Table 4.2. The dipole moments are given in Debye (D). The excited state dipole moment value of chromophore **1a** is 14.96 Debye. The μ_e of the chromophores (**2a-d**) were between 14–19 Debye and chromophores (**3a-d**) were between 9–22 Debye. The higher dipole moment in the excited state indicates that the electronically excited charge transfer states were more stabilized than the ground state.[36]

4.3.6 First Hyperpolarizability

The different techniques employed for the experimental determination of β are electric field induced second harmonic generation (EFISH),[37] hyper-

rayleigh scattering (HRS)[38] and solvatochromic technique.[26] We have chosen the solvatochromic technique to calculate the β. The (β) was calculated using the expression based on quantum-mechanical two level microscopic model:[26]

$$\beta = \frac{3\omega_{eg}^2(\mu_e - \mu_g)\mu_{eg}^2}{2\hbar^2(\omega_{eg}^2 - 4\omega^2)(\omega_{eg}^2 - \omega^2)} \tag{4.3}$$

where, $(\mu_e - \mu_g)$ is the difference between the excited state and ground state dipole moments, $\omega_{eg} = 2\pi C/\lambda_{max}$ is the transition frequency was calculated from the area under the absorption band and μ_{eg} is the transition dipole moment between the ground and excited state.

Table 4.3: First hyperpolarizability β of chromophores (1a, 2a-d and 3a-d)

Chromophores	β (10^{-30}) esu	*Chromophores*	β (10^{-30}) esu
1a	3.32	3a	2.87
2a	2.57	3b	3.97
2b	2.17	3c	2.77
2c	2.42	3d	5.56
2d	4.07		

The β calculated for chromophore **1a** is $3.76 \times 10^{-30} esu$. The β of chromophores (**2a-3d**) were between $(2-6) \times 10^{-30} esu$ given in Table 4.3.

4.3.7 Electro-optic Properties

The second requirement for photorefractivity is electro-optic activity. The electro-optic coefficient can be determined by measuring the change in refractive index when a low frequency electric-field is applied across the sample. The transmission technique was employed for the measurement of electro-optic coefficient.[39] The technique involves the study of the state of polarization of a laser beam due to the electro-optic effect.

For electro-optic studies, we have selected molecules with large $\mu\beta$. The chromophores (**2d, 3b, 3c, 3d**) were embedded in optically transparent

PMMA matrix. DSC traces shown in Figure 4.13 exhibited glass transition temperature (T_g) of PMMA doped with the chromophores **2d, 3b, 3c** and **3d**. The T_g of **2d, 3b, 3c** and **3d** were found to be 100.80, 99.34, 99.04 and 101.85 ^{o}C.

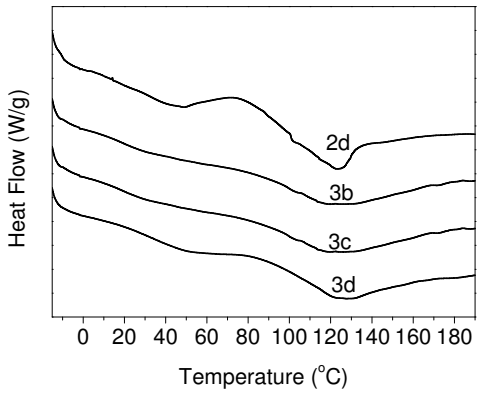

Figure 4.13: DSC thermogram of PMMA matrix doped with the chromopores 2d, 3b, 3c, 3d.

Electrical poling was performed at 100 ^{o}C by applying an electric field of 10 V/μm for 2 h. The sandwiched sample was placed between a polarizer and an analyzer. The light from a He-Ne laser (632.8nm) was polarized at 45 ^{o} with respect to the incidence plane of the sample so that the s component and p component of the light field have equal magnitude. The relative phase difference between both components can be adjusted with the Soliel Babinet Compensator (SBC-VIS, Thorlabs) placed before the sample. When a modulated voltage (221 Hz) was applied to the sample, the relative phase difference between both components caused a change in the intensity transmitted through the analyzer. The intensity modulation was detected with the photodiode (PDA55-EC, Thorlabs) and a lock-in-amplifier (SR830).

The electro-optic coefficient r_{33} was calculated according to the following equation:[39]

$$r_{33} = \frac{3I_m\lambda n[n^2 - sin^2(\alpha)]^{\frac{1}{2}}}{I_i\pi n^3 V_{ac} sin^2(\alpha)} \tag{4.4}$$

where, I_m is the modulated intensity, λ is the wavelength, n is the refractive index, I_i is the incident intensity and V_{ac} is the applied voltage.

The electro-optic coefficients are given in Table 4.2 along with the corresponding values of the figure of merit.

Table 4.4: Photorefractive Figure of Merits of the chromophores, Electro-optic Coefficients and glass transition temperatures of the matrix.

Chromophores	T_g (^{o}C)	r_{33} (pm/V)	FOM_{PEO} (10^{-46} esu)
2d	100.8	2.77	5.90
3b	99.3	1.73	5.30
3c	99.0	1.93	5.32
3d	101.8	1.42	4.73

4.4 Conclusions

A series of alkyl substituted para-nitroaniline derivatives were synthesized and characterized. The ground state dipole moment of the chromophores were determined using Debye-Guggenheim method and the excited state dipole moment by solvatochromic estimation. The excited state was found to be more polar indicating high degree of charge separation. All molecules exhibit positive solvatochromism. The chromophores with large figure of merit was selected and subjected to electro-optic studies. The guest-host system exhibited a maximum electro-optic coefficient of 2.8 pm/V. The maximum UV-Vis absorption (λ_{abs}^{max}) of all molecules was between 387-399 nm, which make them suitable for photorefractive composites, where absorption at the working wavelengths is not preferred.

References

[1] Y. Bai, N. Song, J. P. Gao, X. Sun, X. Wang, G. Yu, , Z. Y. Wang, J. Am. Chem. Soc. 127 (2005) 2060.

[2] Q. Pan, C. Fanga, Z. Zhangb, Z. Qina, F. Lid, Q. Gua, X. Wua, J. Yuc, Opt. Mater. 22 (2003) 45.

[3] F. Qiua, H. Xua, Y. Caoa, Y. Jianga, Y. Zhoub, J. Liub, X. Zhangc, Mater. Charact. 58 (2007) 275.

[4] T. K. Lim, S. H. Hong, M. Y. Jeong, , G. J. Lee, Macromolecules 32 (1999) 7051.

[5] L. Yu, Y. M. Chen, W. K. Chan, J. Phys. Chem. 99 (1995) 2797.

[6] Y. Qian, B. Lin, G. Xiao, H. Li, C. Yuan, Opt. Mater. 27 (2004) 125.

[7] J. Hwang, J. Sohn, S. Y. Park, Macromolecules 36 (2003) 7970.

[8] Y. Liao, C. A. Anderson, P. A. Sullivan, A. J. P. Akelaitis, B. H. Robinson, L. R. Dalton, Chem. Mater. 18 (2006) 1062.

[9] R. M. F. Batista, S. P. G. Costa, E. L. Malheiro, M. Belsleyb, M. M. M. Raposo, Tetrahedron: Asymmetry 63 (2007) 4258.

[10] D. R. Kanis, M. A. Ratner, T. J. Marks, Chem. Rev. 94 (1994) 195.

[11] R. Bavli, Y. B. Band, Phys. Rev. A 43 (1991) 5039.

[12] R. Bavli, D. F. Heller, Y. B. Band, Phys. Rev. A 41 (1990) 3960.

[13] W. J. Meath, E. A. Power, J. Phys. B: At. Mol. Phys. 17 (1984) 763.

[14] P. Gangopadhyay, S. Sharma, A. J. Rao, D. N. Rao, S. Cohen, I. Agranat, , T. P. Radhakrishnan, Chem. Mater. 11 (1991) 466.

[15] G. F. Lipscomb, A. F. Garito, R. S. Narang, J. Chem. Phys. 75 (1981) 1509.

[16] M. J. Prakash, T. P. Radhakrishnan, Cryst. Growth Des. 5 (2005) 1831.

[17] D. F. Eaton, Science 253 (1991) 281.

[18] W. Yang, S. Gong, Z. Xu, Opt. Express 14 (2006) 7216.

[19] Y.-J. Cheng, J. Luo, S. Hau, D. H. Bale, T.-D. Kim, Z. Shi, D. B. Lao, N. M. Tucker, Y. Tian, L. R. Dalton, P. J. Reid, A. K.-Y. Jen, Chem. Mater. 19 (2007) 1154.

[20] N. Tsutsumi, M. Morishima, W. Sakai, Macromolecules 31 (1998) 7764–7769.

[21] J. Kabatc, B. Ośmialowski, J. Paczkowski, Spectrochim. Acta, Part A 63 (2006) 524.

[22] M. Józefowicz, J. R. Heldt, Spectrochim. Acta, Part A 67 (2007) 316.

[23] W. Liptay, Angew. Chem. Int. Ed. 8 (1969) 177.

[24] A. I. Vogel, A Text-Book of Practical Organic Chemistry including Qualitative Organic Analysis, 3rd Edition, Longman, 1956.

[25] E. A. Guggenheim, Trans. Faraday Soc. 45 (1949) 714.

[26] C. Bosshard, G. Knöpfle, P. Prêtre, P. Günter, J. Appl. Phys. 71 (1992) 1594.

[27] V. C. Kishore, R. Dhanya, K. Sreekumar, R. Joseph, C. S. Kartha, On the dipole moments and first-order hyperpolarizability of n,n-bis(4-bromobutyl)-4-nitrobenzenamine, Spectrochim. Acta, Part A (2007) in press.

[28] M. S. Paley, J. M. Harris, J. Org. Chem. 54 (1989) 3774.

[29] P. Suppan, Chem. Phys. Lett. 94 (1983) 272.

[30] J. R. Lombardi, J. Phys. Chem. A 102 (1998) 2817.

[31] L. Onsager, J. Am. Chem. Soc. 58 (1936) 1486.

[32] Y. Luo, P. Norman, H. Ågren, K. O. Sylvester-Hvid, K. V. Mikkelsen, Phys. Rev. E 57 (1998) 4778.

[33] C. Dehu, F. Meyers, E. Hendrickx, K. Clays, A. Persoons, S. R. Marder, J. L. Brédas, J. Am. Chem. Soc. 117 (1995) 10127.

[34] C. Reichardt, Chem. Rev. 94 (1994) 2319.

[35] M. Ravi, A. Samanta, T. P. Radhakrishnan, J. Phys. Chem. 98 (1994) 9133.

[36] R. Ghazy, S. A. Azimb, M. Shaheena, F. El-Mekaweya, Spectrochim. Acta, Part A 60 (2004) 187.

[37] L.-T. Cheng, W. Tam, S. H. Stevenson, G. R. Meredith, G. Rikken, S. R. Marder, J. Phys. Chem. 95 (1991) 10631.

[38] S. Stadler, R. Dietrich, G. Bourhill, C. Brauchle, A. Pawlik, W. Grahn, Chem. Phys. Lett. 247 (1995) 271.

[39] Sandalphon, B. Kippelen, K. Meerholz, N. Peyghambarian, Appl. Opt. 35 (1996) 2346.

CHAPTER

FIVE

Synthesis and Characterization of Electro-Optic Poly(3-methacryloyl-1-(4'-nitro-4-azo- 1'-phenyl) phenylalanine-co-methyl methacrylate

5.1 Introduction

Non-linear optical chromophore functionalized polymers have greater advantages over the guest-host systems.[1,2] In guest-host systems, the NLO chromophore possessing high first hyperpolarizability are dispersed in an inert amorphous polymer matrix of high optical transparency.[3] However, guest-host systems are found to be of low NLO activity.[4] Orientational relaxation, poor solubility, thermal and environmental instability of chromophores in the host polymer matrix are major reasons behind low NLO activity.[5] In order to improve the above mentioned drawbacks, various designing methods were adopted to attach NLO chromophores into the polymer backbone.[6–8] The designing method involves NLO chromophore functionalized side-chain and main-chain polymers, chromophoric main-chain polymers with NLO-active side chains, crosslinked NLO polymers and ferroelectric polymers.[3,9–11]

In this chapter, the synthesis, characterization and electro-optic studies on a NLO-chromophore functionalized polymer are discussed. In NLO-chromophore functionalized polymers, the NLO chromophores are cova-

lently bonded to the polymer backbone via chemical modifications.[12] The advantages of NLO-chromophore functionalized polymers over guest-host systems are: high concentration of NLO chromophores can be introduced to the polymer backbone, absence of phase separation, greater stability towards orientational relaxation and they can be processed into thin films.[13–15] This class of polymers usually have polystyrene, poly(methyl methacrylate) and polyethylene type backbone.

The electro-optic polymer, poly(3-methacryloyl-1-(4'-nitro-4-azo-1'-phenyl)phenylalanine-co-methyl methacrylate) was synthesized via radical polymerization. It is a copolymer of methyl methacrylate and azo dye-substituted methacrylate. Azo-substituted polymers are receiving greater attention because of their potential applications in the field of non-linear optics, optical storage media, etc.[16,17] Azo polymers have good transparency and high non-linear optical susceptibility.[18–20] The presence of azo group in the chromophore results in extended conjugation.[21] The extended conjugation between donor and acceptor groups is responsible for enhanced NLO properties.

The synthesized polymer was characterized by NMR (^{1}H, ^{13}C) and FT-IR spectroscopy. The copolymer system showed an increased stability compared to the guest-host system studied in the previous chapter. The molecular weight was determined by SEC. The glass transition temperature, thermal stability and the degradation behavior was studied using DSC and TG analysis. The optical absorption spectrum of the copolymer was also studied. The electro-optic coefficient of the copolymer was measured using a transmission technique.

5.2 Experimental section

5.2.1 Materials

4-nitroaniline (98 %, Merck) was purified by recrystallization from ethanol. The following chemicals were used as received without further purification: concentrated hydrochloric acid (Merck, AR Grade), sodium nitrite (Merck, AR Grade), sodium hydroxide (Merck, AR Grade), L-phenyl alanine (Alfa

Aesar, 98 %), methacryloyl chloride (Alfa Aesar, 97 %), pyridine (Alfa Aesar, 97 %), benzoyl peroxide (Alfa Aesar, 97 %), chloroform (Merck, Spectroscopic Grade, 98 %), toluene (Merck, Spectroscopic Grade, 98 %) and methyl methacrylate (Alfa Aesar, 97 %). Methanol (Spectrochem, AR Grade) and THF (Rankem, AR Grade) were purified, dried and distilled by the standard procedures.[22]

5.2.2 Instrumentation

The instrumentation techniques employed for the study of molecules are described in detail in section 2.6.2.

5.2.3 Synthesis

5.2.3.1 Synthesis of p-Nitroazobenzene hydrochloride

p-Nitroaniline (30.2 g, 219.0 mmol) dissolved in hydrochloric acid (6 N) was cooled to 0 ^{o}C. The solution was kept in an ice-bath under magnetic stirring. The solution of sodium nitrite (16 g, 230.0 mmol) in water (75 mL) was cooled to 0 ^{o}C. This cold solution was added drop wise to p-nitroaniline hydrochloride solution. The temperature of the reaction was kept at 0 ^{o}C, upon which a yellow colored diazonium salt was obtained.

Yield: 92 %; mp: 98 ^{o}C. FTIR (KBr) ν cm^{-1}: 1341 (C-NO_2, sy st), 1516 (C-NO_2, ay st), 1448 (-N=N st), 3095 (aromatic C-H st), 1594, 1635 (aromatic C=C st). ^{1}H NMR (400 MHz $CDCl_3$) δ: 7.20- 7.59 (m, 4H). ^{13}C NMR (100 MHz $CDCl_3$) δ: 125, 126, 130, 115. Mass (m/e): 185 (molecular ion peak). Anal. Calcd for: $C_6H_4N_3O_2Cl$ - C, 38.83; H, 2.17 ; N, 22.64. Found: C, 38.86; H, 2.17; N, 22.61.

5.2.3.2 Synthesis of 1-(4'-nitro-4-azo-1'-phenyl)phenylalanine

L-phenyl alanine (7.8 g, 54.0 mmol) dissolved in 10 % sodium hydroxide solution (45 mL) was cooled to 0 ^{o}C. The solution was kept in an ice-bath under magnetic stirring. To this, cold p-nitroazobenzene hydrochloride (0 ^{o}C) solution was added drop wise with stirring. The reddish brown

precipitate obtained was filtered, washed with cold distilled water and dried. The compound was recrystallized from glacial acetic acid.

Yield: 64 %; mp: 128 ^{o}C. FTIR (KBr) ν cm^{-1}: 1516 (C-NO_2, ay st), 1341 (C-NO_2, sy st), 1448 (-N=N st), 3095 (aromatic C-H st), 1594, 1635 (aromatic C=C st), 2915 (aliphatic CH_2, ay st), 2843 (aliphatic CH_2, sy st), 2962 (aliphatic C-H, sy st), 3269, 3372 (NH_2 st), 1247 (aliphatic C-N st), 3428 (aliphatic O-H st), 1716 (aliphatic C=O st), 1742 (aliphatic C-O st). ^{1}H NMR (400 MHz $CDCl_3$) δ: 8.05-8.09 (m, 4H), 6.60-6.64 (m, 4H), 2.17 (d, 2H), 2.24 (t, 1H), 1.57 (s, 2H), 9.36 (s, 1H) . ^{13}C NMR (100 MHz $CDCl_3$) δ: 135, 125, 126, 141, 142, 113, 25, 77, 175. Mass (m/e): 314 (molecular ion peak). Anal. Calcd for: $C_{15}H_{14}N_4O_4$ - C, 57.32 ; H, 4.49 ; N, 17.83 . Found: C, 57.30 ; H, 4.51 ; N, 17.85 .

5.2.3.3 Synthesis of 3-methacryloyl-1-(4'-nitro-4-azo-1'-phenyl)-phenylalanine

1-(4'-nitro-4-azo-1'-phenyl)phenylalanine (3.0 g, 9.50 mmol) and methacryloyl chloride (1 mL, 10.26 mmol) dissolved in dry THF (25 mL) was cooled to 0 ^{o}C under N_2. To this mixture pyridine (0.1 g, 1.26 mmol) was added drop wise. The reaction was carried out for 36 h at reflux temperature. The reaction mixture was cooled and filtered. The brown solid obtained was purified by recrystallization from ethanol.

Yield: 58 %; mp: 135 ^{o}C. FTIR (KBr) ν cm^{-1}: 1516 (C-NO_2, ay st), 1341 (C-NO_2, sy st), 1448 (-N=N st), 3095 (aromatic C-H str.), 1594, 1635 (aromatic C=C str.), 2926 (aliphatic CH_2, ay st), 2962 (aliphatic C-H, sy st), 3369 (aliphatic N-H st), 1247 (aliphatic C-N st), 3428 (aliphatic O-H st), 1716 (aliphatic C=O st), 1742 (aliphatic C-O st), 1677 (C=C st), 3107, 3073 (aliphatic =C-H st), 2959 (aliphatic CH_3, sy C-H st), 2852 (aliphatic CH_3, ay C-H st). ^{1}H NMR (400 MHz $CDCl_3$) δ: 8.05-8.54 (m, 4H), 6.92-7.92 (m, 4H), 2.12 (d, 2H), 2.36 (t, 1H), 9.36 (s, 1H), 1.72 (s, 1H), 9.81 (s, 1H), 0.79 (s, 3H), 4.15 (s, 2H). ^{13}C NMR (100 MHz $CDCl_3$) δ: 145, 121, 123, 128, 129, 110, 23, 29.18, 172, 29.73, 10, 125. Mass (m/e): 382 (molecular ion peak). Anal. Calcd for: $C_{19}H_{18}N_4O_5$ - C, 59.68; H, 4.74; N, 14.65. Found: C, 59.64; H, 4.76 ; N, 14.65.

5.2.3.4 Polymerization

3-methacryloyl-1-(4'-nitro-4-azo-1'-phenyl)phenylalanine (1 g, 3.77 mmol), methyl methacrylate (0.39 g, 3.75 mmol) and benzoyl peroxide (2 g, 12.19 mmol) were dissolved in dry DMF (40 mL). The reaction was carried out at 110 ^{o}C for 78 h, under N_2. The resulting solid was dissolved in DMF and reprecipitated from methanol. The polymer was collected by filtration, dried under vacuum, and obtained as a dark brown powder.

Yield: 54 %; mp: 122 ^{o}C. FTIR (KBr) ν cm^{-1}: 1516 (aromatic C-NO_2, ay st), 1341 (aromatic C-NO_2, sy st), 1448 (-N=N st), 3095 (aromatic C-H st), 1594, 1635 (aromatic C=C st), 2944 (aliphatic CH_2, ay st), 2962 (aliphatic C-H, sy st), 3369 (aliphatic N-H st), 1247 (aliphatic C-N st), 3433 (aliphatic O-H st), 1721 (aliphatic C=O st), 1742 (aliphatic C-O st), 2959 (aliphatic CH_3, sy C-H st), 2852 (aliphatic CH_3, ay C-H st). ^{1}H NMR (400 MHz $CDCl_3$) δ: 7.07-7.51 (m, 4H), 6.91-6.99 (m, 4H), 2.12 (d, 2H), 2.36 (t, 1H), 9.38 (s, 1H), 1.74 (s, 1H), 9.81 (s, 1H), 3.53 (s, 3H), 1.87, 1.90 (s, 4H), 0.77, 0.95 (s, 6H). ^{13}C NMR (100 MHz $CDCl_3$) δ: 145, 121, 123, 128, 129, 110, 23, 51.06, 177, 178, 52.75, 16.47, 18.74, 54.46, 44.56, 44.90.

5.2.4 Sample Preparation

The samples for electro-optic studies were prepared as follows: 8 wt% solution eletro-optic polymer in chloroform was prepared. The solution was filtered through a 0.45 μm Nylon filter and deposited on patterned ITO coated glass substrates. The films were dried at room temperature (28 ^{0}C) for 12 h and then in vacuum chamber (at 10^{-2} Torr) for 24 h. The sample was heated to 100^{o}C and the second patterned ITO substrate was placed on top of the first. The film thickness was controlled by using a 48 μm Teflon spacer between the substrates. The sandwiched sample was cooled and the ITO's were glued together using a thermally stable adhesive. Refractive indices of the doped matrix were measured using an Atago DRM2 refractometer. A value of 1.673 was obtained at 590 nm.

5.3 Results and Discussion

5.3.1 Synthesis and Characterization

Azo polymers are of two types: Side chain and main chain azo polymers, based on the position of the -N=N- (azo) group.[23] The presence of azo group in the main chain and side chain polymers provides long conjugation between donor and acceptor groups.[23,24] Azo polymers generally have polystyrene, poly methacrylates, polyesters, polysiloxanes, polycarbonates, polysilanes etc. as polymer backbones. They are usually synthesized by polymerization and copolymerization of styrene, methacrylates, esters, silanes, siloxanes etc. with azo substituted monomers. The NLO properties of azo polymers have been investigated in detail.[25–28]

Copolymerization of 3-methacryloyl-1-(4'-nitro-4-azo-1'-phenyl)phenylalanine with methyl methacrylate is a two-step synthesis. Figure 5.1, Figure 5.2, Figure 5.3 and Figure 5.4 illustrate the multi-step synthesis of NLO molecule with methyl methacrylate. The first step involves preparation of NLO molecule. The synthesis of NLO molecule, 1-(4'-nitro-4-azo-1'-phenyl)phenylalanine, was carried out from L-phenyl alanine through coupling with p-nitroazobenzene hydrochloride. 1-(4'-nitro-4-azo-1'-phenyl)phenyl alanine was reacted with methacryloyl chloride in appropriate ratio to give 3-methacryloyl-1-(4'-nitro-4-azo-1'-phenyl) phenylalanine in 48 % yield. The structure of the monomers were confirmed by elemental analysis, NMR (^{1}H and ^{13}C) and mass spectral analysis.

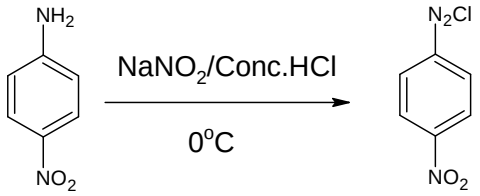

Figure 5.1: Synthesis Route of p-Nitroazobenzene hydrochloride.

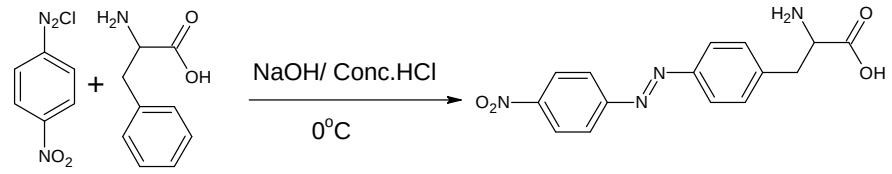

Figure 5.2: Synthesis Route of 1-(4'-nitro-4-azo-1'-phenyl)phenylalanine.

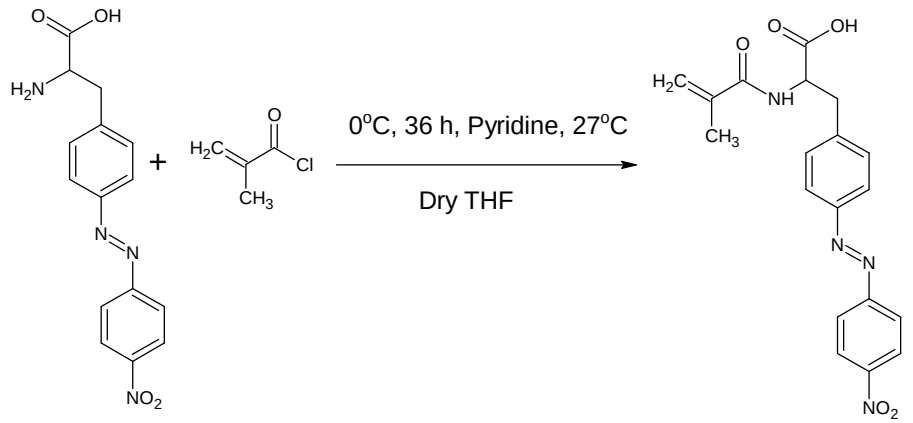

Figure 5.3: Synthesis Route of 3-methacryloyl-1-(4'-nitro-4-azo-1'-phenyl)-phenylalanine.

The second step is the radical polymerization of 3-methacryloyl-1-(4'-nitro-4-azo-1'-phenyl)phenylalanine with methyl methacrylate by using benzoyl peroxide as a thermal initiator. The reaction was carried out in dry DMF. The initiator was added to a prewarmed solution containing a mixture of x moles of NLO molecule and $(100 - x)$ moles of methyl methacrylate monomer. The polymerization was carried out at 110 ^{o}C in DMF for 8 h. The crude polymeric product was dissolved in DMF and precipitated by the addition of methanol. The polymer was obtained in acceptable (54%) yields. NMR (^{1}H and ^{13}C) and FT-IR spectral analysis confirms copolymerization. The glass transition temperature and the thermal stability of the copolymer was determined by DSC and TG analysis. The average molecular weight and polydispersity index of the copolymer was determined using SEC. The polymer can be processed into thin transparent

films. The copolymer has a reddish brown color.

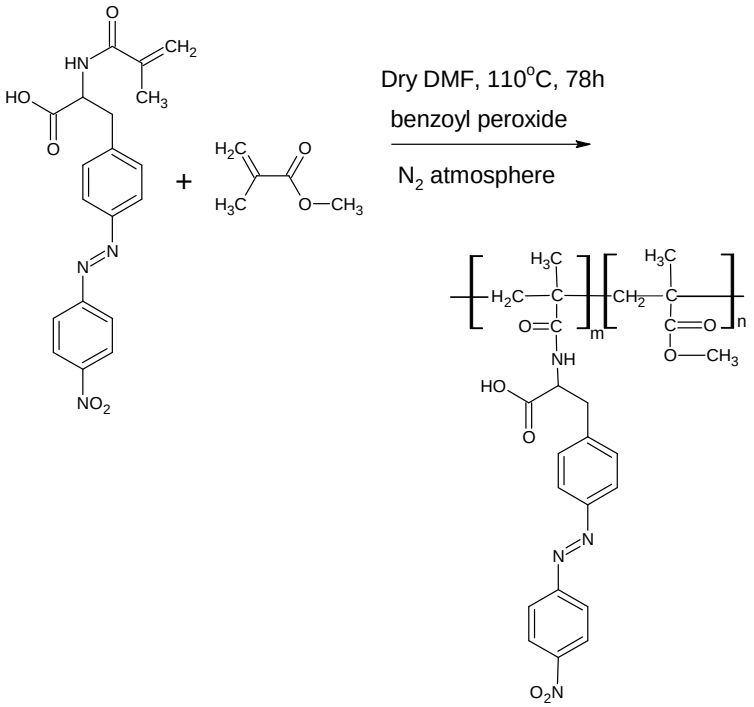

Figure 5.4: Synthesis Route of the Polymer.

The ^{1}H NMR spectrum of the copolymer is shown in Figure 5.5. The detailed spectral values of monomers and polymer are given in the experimental section. The resonance peak at 1.72 ppm corresponds to proton of the amino group. The peaks at 8.05-8.54 ppm and 6.92-7.92 ppm are assigned to the aromatic protons. The resonance at 4.15 ppm corresponds to vinyl proton (CH_2=C-) and the peak at 0.79 ppm to methyl proton of 3-methacryloyl-1-(4'-nitro-4-azo-1'-phenyl)phenylalanine. The absence of peak at 4.40 ppm and the appearance of two resonance peaks at 0.77 and 0.95 ppm (methyl proton) in the NMR spectrum of poly(3-methacryloyl-1-(4'-nitro-4-azo-1'-phenyl) phenylalanine-co-methyl methacrylate) indicated polymerization. In addition, the NMR spectrum of copolymer displayed peaks corresponding to methylene protons in the main chain (1.87 and 1.90 ppm).

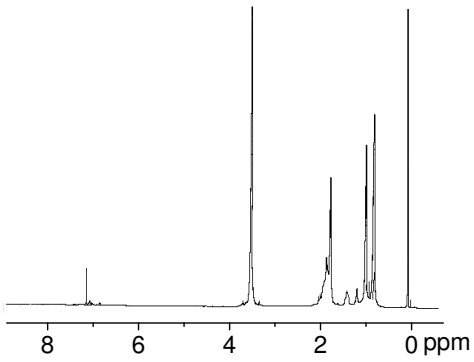

Figure 5.5: ^{1}H NMR Spectrum of the Polymer.

The structure of the copolymer was further confirmed by ^{13}C NMR. The ^{13}C NMR spectrum of the copolymer is shown in Figure 5.6. The resonance peaks at 145, 121, 123, 128 and 129 ppm are assigned to aromatic carbons. The resonance signal at 110 ppm corresponds to the aromatic carbon (C-N=N-C). The peak at 125 ppm due to vinyl carbon is absent in the NMR spectrum of the copolymer. The resonance peak at 16.47 and 18.74 ppm are of methyl carbon in the spectrum of poly(3-methacryloyl-1-(4'-nitro-4-azo-1'-phenyl) phenylalanine-co-methyl methacrylate). Two new peaks were found at 44.56 and 44.90 ppm in the spectrum, attributed to methylene carbon of 3-methacryloyl-1-(4'-nitro-4-azo-1'-phenyl)-phenylalanine and methyl methacrylate which confirmed copolymerization.

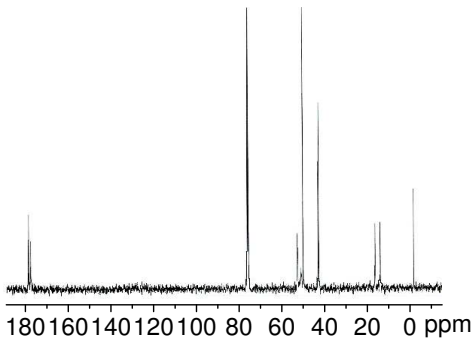

Figure 5.6: ^{13}C NMR Spectrum of the Polymer.

FT-IR spectrum of the copolymer is shown in Figure 5.7. The band at 3369 cm^{-1} was associated with N-H stretching vibration. The band at 1448 cm^{-1} was the symmetric stretching of N=N group.

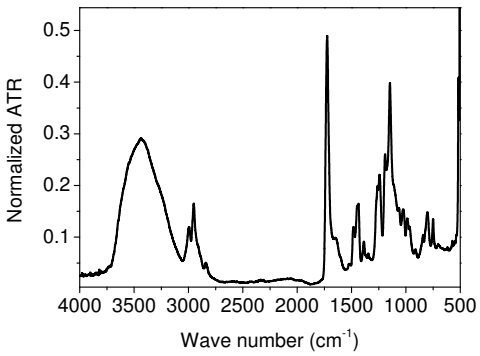

Figure 5.7: FT-IR Spectrum of the Polymer.

The disappearance of band around 3107, 3073 cm^{-1} (stretching vibration of aliphatic =C-H group) and 1677 cm^{-1} (stretching vibration of aliphatic double bond of the monomer) and the presence of new bands at 2857 and 3019 cm^{-1} indicate polymerization. The bands at 2857 and 3019 cm^{-1} are attributed to methylene aliphatic single bond asymmetric and symmetric C-H stretching vibration. The intense peak at 1721 cm^{-1} corresponds to aliphatic C=O stretching vibration.

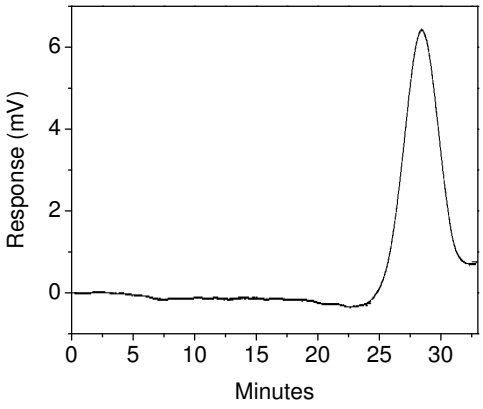

Figure 5.8: SEC Chromatogram of the Polymer.

Figure 5.8 shows SEC chromatogram of the copolymer. The number average molecular mass ($\overline{M}_n$) was 3175 and weight average molecular mass ($\overline{M}_w$) was 6408. The polydispersity index ($\overline{M}_w/\overline{M}_n$) obtained was 2.01.

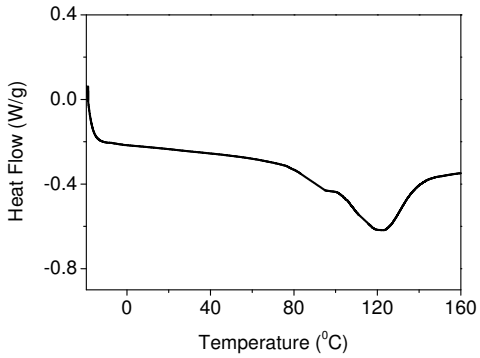

Figure 5.9: DSC curve of the Polymer.

The DSC thermogram of the copolymer is shown in Figure 5.9. The glass transition temperature (T_g) of the polymer is 96.75 ^{o}C. The polymer showed well defined melting point at 121.83 ^{o}C. The T_g of the side-chain polymer depends on the mole ratio of NLO molecules and methyl methacrylate molecules. T_g also depends on the structure of the NLO molecules and the spacer which links the NLO molecule to the polymer main chain.[29]

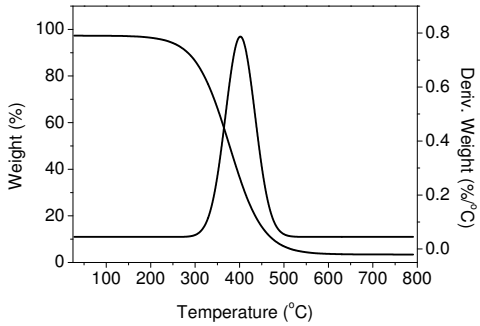

Figure 5.10: Thermogram of the Polymer.

The thermogram of the copolymer is shown in Figure 5.10. The degrada-

tion process started at around 298 ^{o}C and reached its maximum rate of 0.81 %/^{o}C at 401 ^{o}C was assigned as the degradation of C-C, C-O and C-N bonds. The polymer showed good thermal stability indicating occurrence of strong inter- and intramolecular dipolar interactions originated by the presence of high charge delocalization in the macromolecular side chain.[30]

5.3.2 Optical Properties

The UV-Vis spectra of copolymer is shown in Figure 5.11. Azo aromatic type molecules are characterized spectroscopically by a low-intensity n-$\pi*$ band in the visible region of the spectrum and a high intensity π-$\pi*$ band in the UV region of the electronic spectrum.[23]

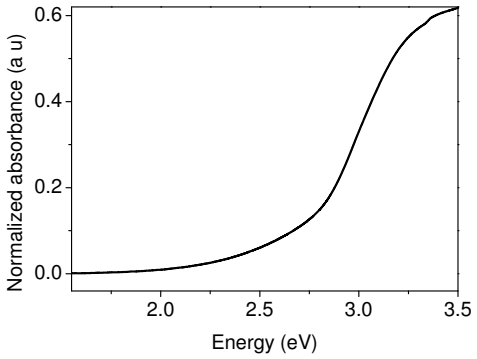

Figure 5.11: UV-Vis Spectrum of the Polymer.

The absorption spectrum of the polymer could be considered as a superposition of a low intensity band centered in the 3.45-1.72 eV region and a high intensity band in the 4.34-3.45 eV region. The intense band appeared in the low energy region is related to the combined contributions of the n-π^*, first π-π^* and internal charge transfer electronic transitions of azobenzene chromophores. The band in the high energy region corresponds to the π-π^* electronic transition of the aromatic ring.[31]

5.3.3 Electro-optic Properties

The electro-optic polymer, poly(3-methacryloyl-1-(4'-nitro-4-azo-1'-phenyl)-phenylalanine-co-methyl methacrylate), comes in the class of side-chain polymers. The transmission technique was employed for the measurement of electro-optic coefficient.[32] The method and experimental technique was described in detail in chapter **4**. The side-chain polymer exhibited a maximum electro-optic coefficient of 4.75 pm/V.

5.4 Conclusions

Poly (3-methacryloyl-1-(4'-nitro-4-azo-1'-phenyl) phenylalanine-co-methyl-methacrylate) was synthesized via radical initiated polymerization. It was a copolymer of 3-methacryloyl-1-(4'-nitro-4-azo-1'-phenyl)phenylalanine and methyl methacrylate. The structure of the polymer was confirmed by FT-IR and NMR (^{1}H and ^{13}C) analysis. The polymer showed good thermal stability. The polymer system exhibited a maximum electro-optic coefficient of 4.75 pm/V.

References

[1] C. Barrett, B. Choudhury, A. Natansohn, P. Rochon, Macromolecules 31 (1998) 4845.

[2] J. Park, T. J. Marks, Chem. Mater. 2 (1990) 229.

[3] D. M. Burland, R. D. Miller, C. A. Walsh, Chem. Rev. 94 (1984) 31.

[4] P. Qi-Wei, F. Chang-Shui, Q. Zhi-Hui, G. Qing-Tian, W. Xiang-Wen, S. Wei, Y. Jin-Zhong, Chin. Phys. Lett. 19 (2002) 1125.

[5] Y. Chen, B. Zhang, F. Wang, Opt. Commun. 228 (2003) 341.

[6] S. Song, S. J. Lee, B. R. Cho, Chem. Mater. 11 (1999) 1406.

[7] M. S. Ho, C. Barrett, J. Paterson, M. Esteghamatian, A. Natansohn, P. Rochon, Macromolecules 29 (1996) 4613.

[8] L. Dalton, A. Harper, A. Ren, F. Wang, G. Todorova, J. Chen, C. Zhang, M. Lee, Ind. Eng. Chem. Res. 38 (1999) 8.

[9] J. xin Lu, J. Yin, X. xu Deng, Q. shun Shen, Z. qi Cao, Opt. Mater. 25 (2004) 17.

[10] A. Hayashi, Y. Goto, M. Nakayama, K. Kaluzynski, H. Sato, T. Watanabe, S. Miyata, Chem. Mater. 4 (1992) 555.

[11] C. Xu, B. Wu, M. W. Becker, L. R. Dalton, Chem. Mater. 5 (1993) 1439.

[12] T. K. Lim, S. H. Hong, M. Y. Jeong, G. J. Lee, Macromolecules 32 (1999) 7051.

[13] D. H. Choi, H. M. Kim, W. M. K. P. Wijekoon, P. N. Prasad, Chem. Mater. 4 (1992) 1253.

[14] H. Ma, A. K.-Y. Jen, J. Wu, X. Wu, S. Liu, Chem. Mater. 11 (1999) 2218.

[15] D. H. Choi, W. M. K. P. Wijekoon, H. M. Kim, P. N. Prasad, Chem. Mater. 6 (1994) 234.

[16] I. P. Nikolaev, K. S. Nesterouk, A. V. Larichev, V. Wataghin, Laser Phys. 12 (2002) 978.

[17] G. Iftime, F. L. Labarthet, A. Natansohn, P. Rochon, K. Murti, Chem. Mater. 14 (2002) 168.

[18] I. McCulloch, H.-T. Man, B. Marr, C. C. Teng, Chem. Mater. 6 (1994) 611.

[19] C.-B. Yoon, K.-J. Moon, H.-K. Shim, Macromolecules 29 (1996) 5754.

[20] L. Brzozowski, E. H. Sargent, J. Mater. Sci.: Mater. Elec. 12 (2001) 483.

[21] J. L. Humphrey, K. M. Lott, M. E. Wright, D. Kuciauskas, J. Phys. Chem. B 109 (2005) 21496.

[22] A. I. Vogel, A Text-Book of Practical Organic Chemistry including Qualitative Organic Analysis, 3rd Edition, Longman, 1956.

[23] S. Xie, A. Natansohn, P. Rochon, Chem. Mater. 5 (1993) 403.

[24] L. Angiolini, D. Caretti, L. Giorgini, E. Salatelli, e-Polymers 021 (2001) 1.

[25] J.-H. Lee, K.-S. Lee, Bull. Korean Chem. Soc. 21 (2000) 847.

[26]

[27] C. Maertens, C. Detrembleur, P. Dubois, R. Jerome, P.-A. Blanche, P. C. Lemaire, Chem. Mater. 10 (1998) 1010.

[28] J. J. Kulig, W. J. Brittain, Macromolecules 27 (1994) 4838.

[29] H.-J. Lee, S.-J. Kang, H. K. Kim, H.-N. Cho, J. T. Park, S.-K. Choi, Macromolecules 28 (1995) 4638.

[30] L. Angiolini, T. Benelli, L. Giorgini, E. Salatelli, Polymer 46 (2005) 2424.

[31] L. Angiolini, D. Caretti, L. Giorgini, E. Salatelli, Polymer 42 (2001) 4005.

[32] Sandalphon, B. Kippelen, K. Meerholz, N. Peyghambarian, Appl. Opt. 35 (1996) 2346.

CHAPTER

SIX

Development of a Photorefractive System Based on Poly(6-tertiary-butyl-3-phenyl-3,4-dihydro-2H-1,3-benzoxazine)

6.1 Introduction

Over the past few decades, photorefractive polymers have attracted much attention due to their potential applications in real-time holographic display, high-density optical data storage, phase conjugation, optical computing, pattern recognition, etc.[1,2] Compared to inorganic crystals, photorefrative polymers possess several advantages such as high figure-of-merit, flexibility of the chemical structure, ease of synthesis, low dielectric constant, possibility of adjusting the properties by changing the polymer structure[3] and low cost.[4] The performance levels of photorefractive polymers were found to be comparable to that of the well known inorganic crystals.[5,6]

The two major requirements for photorefractivity are photoconductivity and electro-optic effect.[7] Most of the photorefractive polymer systems studied to-date consists of charge transporting polymer in which second-order non-linear optical chromophores, charge-generating molecules (sensitizers) and plasticizers are dispersed.[8] PVK based photorefractive systems have been investigated intensively because of their excellent film forming

properties and good photoconductivity.[9] The photogenerated charge carriers are provided by sensitizers. The sensitizers are usually added in small amounts to the system to provide minimum absorption.[10] The other components present in the system do not show notable absorption at the operating wavelength.[11] The electro-optic effect is offered by the addition of NLO chromophores. High concentration of NLO chromophores are required to produce large refractive index modulation. The addition of plasicizer reduces the glass transition temperature of the photorefractive system, thereby significantly increasing the photorefractive performance according to orientational enhancement effect. In 1994, Meerholz et al., reported a very large increase in diffraction efficiency and net two-beam coupling gain in a PVK based system after the incorporation of additional plasticizer molecules.[12] The monomer of PVK, i.e., N-ethylcarbazole is the most commonly used plasticizer. Phthalic acid derivatives such as DOP, butyl benzyl phthalate (BBP), etc., can also be used as plasticizers. The compatibility of the polymer matrix with the NLO chromophore and the plasticizer is an important factor to keep in mind since most of photorefractive systems suffer from phase separation and crystallization due to the presence of large amount of low molecular weight dopants.

The first photorefractive effect was observed in an electro-optic polymer doped with a hole transport agent.[13] After the discovery of photoconductivity in PVK, most of the photorefractive studies were done on systems based on PVK. Photorefractive two beam coupling gain was first observed in a system containing PVK as charge transporting polymer, 3-fluoro-4-N,N-diethylamino-β-nitrosyrene (F-DEANST) as second-order non-linear optical chromophore and 2,4,7-trinitrofluorenone as sensitizer.[14] Since then several high speed photorefractive polymer systems with PVK as photoconducting polymer matrix were reported.[12,15] Various photoconducting polymers other than PVK were designed, synthesized and are extensively used as hole transport conductors for the preparation of photorefractive systems. Among them are, poly(4-n-butoxyphenylethylsilane), poly (N,N'-diphenyl-N,N'-bis(3-methylphenyl)-[1,1'-biphenyl]-4,4'-diamine and some of its derivatives. Both polymers were found to be good charge

transport hosts for photorefractive systems.[16]

A photorefractive system containing poly(6-tertiary-butyl-3-phenyl-3,4-dihydro-2H-1,3-benzoxazine) (P3) as charge transporting polymer host was developed. The second-order nonlinear optical chromophore, disperse red 1 (DR1), the plasticizer, N-ethylcarbazole (ECZ) and the charge generator, C_{60} were dispersed into the charge transporting polymer host. DSC, optical absorption, photoconductivity, electro-optic and two-beam coupling results of the photorefractive system are presented in this Chapter.

6.2 Experimental Section

6.2.1 Materials

The synthesis route, purification and the complete structural characterization (FT-IR and NMR) of the charge-transporting polymer, poly(6-tertiary-butyl-3-phenyl-3,4-dihydro-2H-1,3-benzoxazine), P3, was given in Chapter 3. The following chemicals were used as received without further purification: DR1 (98 %, Aldrich), ECZ (98 %, Aldrich), buckminister fullerene (C_{60}) (98 %, Alfa Aesar) and chloroform (99 %, Merck, Spectroscopic Grade).

6.2.2 Sample Preparation

The photorefractive system was prepared according to the following procedure. P3 (1.13 g, 68.0 wt %), DR1 (0.20 g, 0.66 mmol, 12.5 wt %), ECZ, (0.31 g, 1.60 mmol, 18.9 wt %) and C_{60} (0.0099 g, 0.014 mmol, 0.6 wt %) was dissolved in 20 mL of chloroform for 30 minutes. The solution was filtered through a 0.45 μm Nylon filter into a 75 mL beaker. The beaker was covered with pierced aluminium foil and kept on a hotplate and heated to 40 ^{o}C to evaporate some of the solvent. After the volume was reduced to 5 mL, the beaker was placed in a vacuum oven. The remaining solvent was evaporated under reduced pressure and dried for 48 hours in the oven at 50 ^{o}C. The dried sample was ground to fine powder. The glass transition temperature of the photorefractive system was determined by DSC, (Q-

100, TA instruments), under nitrogen at heating rate of 10 ^{o}C/min. The absorption spectra of the film sample was recorded using a Jasco V-570 UV/VIS/NIR spectrophotometer.

6.2.3 Photorefractive Device Fabrication

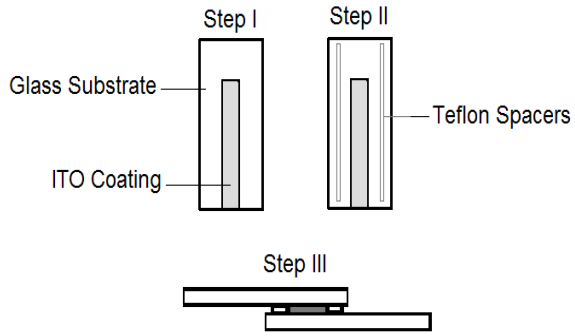

Figure 6.1: Photorefractive Device Construction.

The construction of the photorefractive device is shown in Figure 6.1. ITO coated glass substrates were cut into small pieces of desired size. The desired electrode area was masked with five coatings of ethylene-propylene diene monomer rubber (EPDM). The unmasked ITO surface was removed by etching in a mixture of 1 part nitric acid and 3 parts hydrochloric acid solution and then diluting with 1 (by volume) of water for 10 minutes.[17] The etched glass was then thoroughly washed with methanol, acetone and soap solution, followed by drying in an air oven at 100 ^{o}C. The photorefractive sample cell was constructed by clamping together two patterned ITO electrodes. The two electrodes are separated by a small gap of approximately 48 μm using Teflon spacers. The sample cell is placed on the hotplate maintained at a temperature near to the T_g of the photorefractive system. The dried powder is then placed halfway between the edge of the glass and the 48 μm gap. The melted photorefractive system was kept for several minutes on the glass edge to get a bubble free liquid. The liquid was then pushed into the gap through capillary action. Care must be taken that the liquid covers the whole electrode area, otherwise it will lead to

high-voltage breakdown. The sample cell was removed from the hot plate and rapidly transferred on to an ice cube. Thermally stable adhesive was used to glue together the ITO plates to complete the device fabrication. Transparent red colored films were obtained.

6.3 Results and Discussion

The primary and the most important process in a photorefractive system is the generation of mobile charge carriers. The charge carriers are usually generated by sensitizing with suitable electron acceptors. In this study, C_{60} was chosen as the electron acceptor to extend the photoconductivity to the red wavelength region.

The charge transport properties in a photorefractive system can be achieved either by the incorporation of a photoconducting molecule into an inert polymer matrix or by chemically attaching the photoconducting entity to the polymer backbone. We have developed two types of photoconducting systems. The first system comprise of aniline as electron donor, 2,4,6-trinitrophenol as electron acceptor and poly(methyl methacrylate) as inert polymer matrix. The photocurrent value was given in Chapter 2. The second one, comprise of poly(2-methacryloyl-1-(4-azo-1'-phenyl)aniline-co-styrene), poly (6-tertiary-butyl-3,4-dihydro-2H-1,3-benzoxazine), P1, poly (6-tertiary-butyl-3-methyl-3,4-dihydro-2H- 1,3-benzoxazine), P2 and poly (6-tertiary-butyl-3-phenyl-3,4-dihydro-2H- 1,3-benzoxazine), P3, as charge transporting polymer host. The detailed synthesis route, characterization and photoconducting properties of these polymers are discussed in Chapter 2 and Chapter 3. For the preparation of a photorefractive system, out of the above mentioned photoconducting polymers, we have selected the one with highest photoconductive sensitivity. The photoconductive sensitivity of P3 was higher compared to other three polymers. Hence, P3, was chosen as the charge transporting polymer host for the development of a photorefractive system.

The electro-optic effect was obtained in the photorefractive system by addition of second-order nonlinear optical chromophores to the charge-

transporting polymer host. The electro-optic molecules, N,N-bis(4-[(6-aminohexyl)amino]butyl)-4-nitro-benzenamine (2d), disperse red 1 (DR1) and a side-chain electro-optical copolymer, poly(3-methacryloyl-1-(4'-nitro-4-azo-1'-phenyl)phenylalanine-co-methyl methacrylate) was selected for the present study. The synthesis route, characterization and the electro-optic coefficients obtained are given in Chapter 4 and Chapter 5. The chromophore 2d contains $N(CH_2)_4NH(CH_2)_6NH_2$ group, DR1 contains $HOCH_2$-CH_2NCH_2C-H_3 group and the electro-optic polymer contains $C_6H_5CH_2CH$-$NHCOCCH_3$ group as electron donors and nitro group as electron acceptor. The electron donor group in 2d chromophore was connected to the electron acceptor group by a π-conjugated benzene ring and in DR1 and electro-optic polymer by an azobenzene group. We have tried to develop a photorefractive system using these three types of electro-optic molecules. The plasticizer, ECZ, was used to lower the glass transition temperature of the photorefractive system.

The first system studied consisted of 2d as a second order nonlinear optical chromophore, C_{60} as photosensitizing molecule, DOP as plasticizer and P3 as photoconducting polymer host matrix. The second system contained poly(3-methacryloyl-1-(4'-nitro-4-azo-1'-phenyl) phenylalanine-co-methyl methacrylate) as a second-order nonlinear optical polymer, C_{60} as sensitizer, ECZ as plasticizer and P3 as charge transporting polymer. During sample preparation, the major problem encountered with these systems was the incompatibility between the electro-optic molecules and the photoconducting polymer, thereby making the system opaque and hence unsuitable for further studies.

The third system studied consisted of P3 (as charge transporting moiety), DR1 (as NLO chromophore), ECZ (as plasticizer) and C_{60} (as charge generator). Different compositions were tried by varying the amount of NLO chromophore. The system with 68.0 wt % P3, 12.5 wt % DR1, 18.9 wt % ECZ and 0.6 wt % C_{60} was selected for photorefractive studies. Photocurrent and electro-optic measurements were done on the sample. The photorefractive properties of this system was characterized by two-beam coupling. The chemical structure of the molecules used in the photorefrac-

tive system (P3:DR1:ECZ:C_{60}) are shown in Figure 6.2.

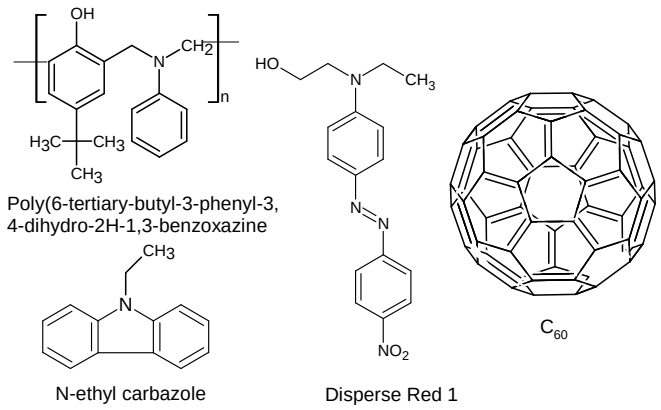

Figure 6.2: Chemical Structure of the Molecules.

The Tg of a photorefractive system can be lowered either by the addition of an inert plasticizer or by a charge transporting plasticizer. The advantage of using charge transporting plasticizer such as, ECZ, over inert plasticizer is the additional charge transport property shown by them.

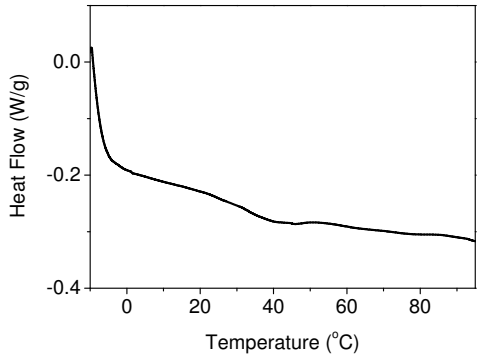

Figure 6.3: DSC Curve of P3:DR1:C_{60}:ECZ system.

A large increase in photorefractive performance was observed in PVK based photorefractive systems containing additional plasticizer molecules. This could be due to an increase in orientational mobility of the NLO chromophores.[18] The glass transition temperature of P3 is 52.45 ^{0}C. By

the addition of 18.9 wt % of ECZ, the T_g of the photorefractive system (P3:DR1:C_{60}) lowered to 33.28 ^oC. Figure 6.3 shows the DSC curve of the photorefractive system.

6.3.1 Optical Absorption

One of the important features of a photorefractive system is the optical absorption spectrum, since it determines the wavelength region in which the material can be used. The UV-Vis absorption spectrum of P3:DR1:ECZ:C_{60} photorefractive system is shown in Figure 6.4. The spectra was recorded on a film sample.

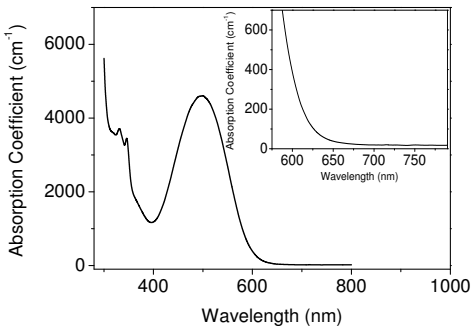

Figure 6.4: UV-Vis Absorption Spectrum of P3:DR1:C_{60}:ECZ System.

The absorption begins around 680 nm. The tail of absorption is due to the formation of a charge-transfer complex between P3 and C_{60}. The electro-optic molecule present in the photorefractive system should not absorb in the wavelength region of interest. The absorption spectra of the photorefractive system showed two bands, one in the low energy region and the other in the high energy region. The strong band at 497 nm (low energy region) was attributed to strong internal charge transfer electronic transitions of pseudo stillbene azobenzene dyes.[19] The n-π^* transitions of P3 and DR1 is not visible in the absorption spectrum of the system as it is hidden by the strong internal charge transfer band of DR1. The bands around 375, 345, 330, 275 nm corresponds to π-π^* transition of P3 and DR1. The absorption spectrum of DR1 is shown in Figure 6.5. The absorption coef-

ficient above 600 nm is low and is not due to the electro-optic molecule, DR1. Therefore, the electro-optic and photorefractive characterizations can safely be performed using a He-Ne laser which emits at 632 nm. The absorption coefficients at 632 nm of P3:DR1:ECZ:C_{60} is approximately 73 cm^{-1}.

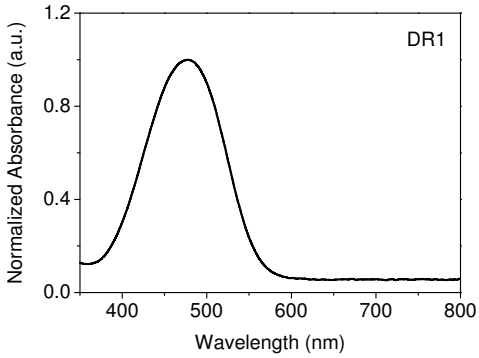

Figure 6.5: UV-Vis Absorption Spectrum of DR1 in Chloroform.

6.3.2 Photoconductivity Studies

The charge transporting polymer, P3 is made absorptive and photoconducting in the spectral region of He-Ne laser beam (632 nm) by the addition of small amount of C_{60} (wt %) as charge generator molecule.

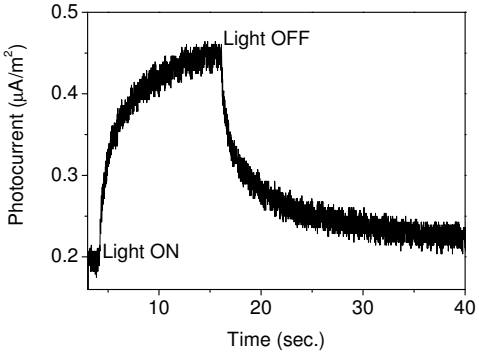

Figure 6.6: DC Conductivity of P3:DR1:C_{60}:ECZ System.

Figure 6.6 shows the photoconductivity graph of the photorefractive sys-

tem. The photocurrent of the photorefractive system was recorded using a Tektronix TDS 210 storage oscilloscope. The electric field was applied to the sample and the dark current (j_{dark}) was recorded for 5 seconds. Then the light source was turned on and the current under illumination (j_{light}) was measured for about 12 seconds. The photocurrent (j_{photo}) was calculated using, $j_{photo} = j_{light}$ - j_{dark}. The photorefractive system showed a photocurrent of 0.25 $\mu A/m^2$ at an electric field of 10 V/μm. The photoconductive sensitivity of the photorefractive system was found to be 1.25 x 10^{-10} S cm/W.

6.3.3 Electro-optic Properties

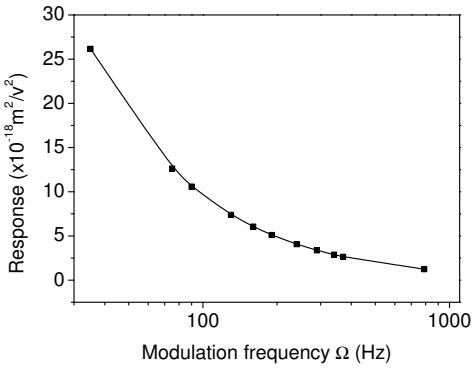

Figure 6.7: Frequency Response for P3:DR1:C_{60}:ECZ System.

In electrically poled high glass transition temperature photorefractive systems, the orientational freedom of electro-optic chromophores are generated at elevated temperature. On cooling down the system to room temperature with the poling field applied, the orientational freedom of the chromophores freeze. Hence, refractive index modulation in such systems is totally due to Pockels effect.[20] However, in low T_g photorefractive systems, the high index of modulation results from two contributions: the electro-optic (Pockels) contribution and the birefringent contribution.[21] The very high photorefractive performance observed in low T_g systems is primarily due to these two contributions. The electro-optic chromophores

present in the photorefractive system are oriented by both externally applied electric field and total internal space charge field and thus introduce spatially modulated birefringence.[22,23]

The electro-optic response function of the photorefractive system (P3: DR1:ECZ:C_{60}) was measured using the frequency dependent transmission ellipsometric technique.[24] The response function R(Ω) is calculated from the modulated intensity I_m by using the following equation:

$$R(\Omega) = \frac{3I_m(\Omega)\lambda G d}{I_i \pi n^3 V_B V_{AC}} \tag{6.1}$$

where, λ is the wavelength of the laser used, d is the sample thickness, I_i is the total intensity, n is the refractive index of the sample, V_B is the constant bias voltage applied over the sample, V_{AC} is the amplitude of modulated voltage superimposed on the bias voltage and G is the geometrical factor and is given by: $n(n^2\text{-}\mathrm{Sin}^2\ \theta)^{1/2}/\ \mathrm{Sin}^2\theta$. Figure 6.7 shows plot of R(Ω) versus frequency of the modulating field. A decrease in response function was observed with increase in the modulated frequency. This is because, at higher frequencies the electro-optic chromophores can no longer reorient in the polymer matrix.

6.3.4 Photorefractive Properties

To verify the photorefractivity of the low T_g composite, a two-beam coupling (2BC) measurement was performed. Because of the low T_g of the system, the electro-optic chromophores can be easily oriented by the applied electric field. A tilted sample geometry was employed to carry out the experiment. The sample was irradiated with two coherent laser beams from a He-Ne laser (632.8 nm) with an intensity of approximately 1 W/cm^2, at an incident angle of 25^0 and 55^0. The two beam coupling gain coefficient of the photorefractive composite was measured with the two beam coupling method.[25] Figure 4 shows an asymmetric energy transfer in a 2BC experiment at 62.5 V/μm.

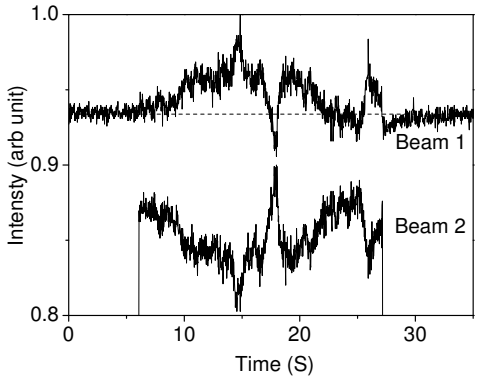

Figure 6.8: Two-Beam Coupling for P3:DR1:C_{60}:ECZ System.

The gain coefficient (Γ), employed as the measure of photorefractive performance was measured according to the following equation:

$$\Gamma = \frac{1}{L/Cos\theta}[ln(\beta I/I_0) - ln(\beta + 1 - I/I_0)] \tag{6.2}$$

where, L is the sample thickness, θ is the incident angle of the beam inside the sample, β is the intensity ratio of incident laser beams, I/I_0 is the beam coupling ratio where, I is the signal intensity with the pump beam on and I_0 is the signal intensity with the pump beam off. The calculated gain coefficient for the photorefractive system was 8.8 cm^{-1} at an electric field of 62.5 V/μm. No net gain was observed for the P3:DR1:ECZ:C_{60} photorefractive system due to the large absorption loss (73 cm^{-1}) at 632 nm .

The diffraction efficiency of the photorefractive grating was obtained from the degenerate four-wave mixing experiment. The efficiency is calculated using the following equation:

$$\eta = \frac{I_{diffracted}}{I_{incident}} \tag{6.3}$$

where, I_d is the intensity of the diffracted beam and I_t is the intensity of the incident beam. The maximum diffraction efficiency obtained was 0.002 % at an electric field of 62.5 V/μm. The diffraction efficiency measurements indicated the presence of non-photorefractive gratings.

6.4 Conclusions

A photorefractive system based on low cost charge transporting host polymer, poly(6-tertiary-butyl-3-phenyl-3,4-dihydro-2H- 1,3-benzoxazine), was developed. The second-order NLO chromophore, disperse red 1 and the charge generating molecule, C_{60} were dispersed into the host polymer. The glass transition of the composite was lowered near to room temperature by the addition of ECZ as charge transporting plasticizer. The photorefractive composite showed a gain coefficient of 8.8 cm^{-1} at an electric field of 63 V/μm. Non-photorefractive gratings were also detected in diffraction efficiency measurements.

References

[1] J. Hwang, J. Sohn, S. Y. Park, Macromolecules 36 (2003) 7970.

[2] H. Moon, J. Hwang, N. Kim, S. Y. Park, Macromolecules 33 (2000) 5116.

[3] C.-J. Chang, W.-T. Whang, C.-C. Hsu, Z.-Y. Ding, K.-Y. Hsu, S.-H. Lin, Macromolecules 32 (1999) 5637.

[4] J. Sohn, J. Hwang, S. Y. Park, G. J. Lee, Jpn. J. Appl. Phys. 40 (2001) 3301.

[5] K. Okamoto, T. Nomura, S.-H. Park, K. Ogino, H. Sato, Chem. Mater. 11 (1999) 3279.

[6] F. Wu1rthner, S. Yao, J. Schilling, R. Wortmann, M. Redi-Abshiro, E. Mecher, F. Gallego-Gomez, K. Meerholz, J. Am. Chem. Soc. 123 (2001) 2810.

[7] W. You, L. Wang, Q. Wang, L. Yu, Macromolecules 35 (2002) 4636.

[8] D. M. Burland, R. G. Devoe, C. Geletneky, Y. Jia, V. Y. Lee, P. M. Lundquist, C. R. Moylan, C. Pogay, R. J. Twieg, R. Wortmann, Pure Appl. Opt. 5 (1996) 513.

[9] W. G. Jun, M. J. Cho, D. H. Choi, J. Korean Phys. Soc. 47 (2005) 620.

[10] O. Ostroverkhova, K. D. Singer, J. Appl. Phys. 92 (2002) 1727.

[11] W. E. Moerner, S. M. Silence, Chem. Rev. 94 (1994) 127.

[12] K. Meerholz, B. L. Volodin, Sandalphon, B. Kippelen, N. Peyghambarian, Nature 371 (1994) 497.

[13] S. Ducharme, J. C. Scott, R. J. Twieg, W. E. Moerner, Phys. Rev. Lett. 66 (1991) 1846.

[14] M. C. J. M. Donckers, S. M. Silence, C. A. Walsh, F. Hache, D. M. Burland, W. E. Moerner, R. J. Twieg, Opt. Lett. 18 (1993) 1044.

[15] A. Gunnet-Jepsen, C. L. Thompson, R. J. Twieg, W. E. Moerner, Appl. Phys. Lett. 70 (1997) 1515.

[16] M. S. Bratcher, M. S. DeClue, A. Grunnet-Jepsen, D. Wright, B. R. Smith, W. E. Moerner, J. S. Siegel, J. Am. Chem. Soc. 120 (1998) 9680.

[17] C. J. Huang, Y. K. Su, S. L. Wu, Mater. Chem. Phys. 84 (2004) 146.

[18] H. J. Bolink, V. V. Krasnikov, G. G. Malliaras, G. Hadziioannou, J. Phys. Chem. 100 (1996) 16356.

[19] C. Toro, A. Thibert, L. D. Boni, A. E. Masunov, F. E. Hernandez, J. Phys. Chem. B 112 (2008) 929.

[20] E. Hattemer, R. Zentel, E. Mecher, K. Meerholz, Macromolecules 33 (2000) 1972.

[21] R. Wortmann, C. Poga, R. J. Twieg, C. Geletneky, C. R. Moylan, P. M. Lundquist, R. G. DeVoe, P. M. Cotts, H. Horn, J. E. Rice, D. M. Burland, J. Chem. Phys. 105 (1996) 10637.

[22] B. Kippelen, F. Meyers, N. Peyghambarian, S. R. Marder, J. Am. Chem. Soc. 119 (1997) 4559.

[23] J. Hwang, J. Sohn, J.-K. Lee, J.-H. Lee, J.-S. Chang, G. J. Lee, S. Y. Park, Macromolecules 34 (2001) 4656.

[24] Sandalphon, B. Kippelen, K. Meerholz, N. Peyghambarian, Appl. Opt. 35 (1996) 2346.

[25] V. C. Kishore, Development of photorefractive polymers: Evaluation of photoconducting and electro-optic properties, Ph.D. Thesis, Cochin University of Science and Technology, India, 2008.

CHAPTER

SEVEN

Summary

The discovery of photorefractive effect in $LiNbO_3$ created interest towards dynamic holographic optical devices with huge storage capacity. After the observation of photorefractive effect in polymers, considerable research effort has been devoted towards developing fully-functional and multi-functional polymeric photorefractive systems, since they offer many advantages over inorganic crystals such as low cost, low dielectric constant, structural flexibility and ease of synthesis. They have been a subject of considerable interest in the past few years due to potential applications in the field of real-time holographic display, high-density optical data storage, phase conjugation, optical computing, and pattern recognition.

Organic photorefractive systems are multifunctional in nature. The multifunctionality can be achieved by two design approaches: the guest-host approach and the fully functional polymer approach. Most of the photorefractive systems developed are based on guest-host approach, in which molecules responsible for charge generation and electro-optics are dispersed into a charge transporting polymer matrix. The second approach involves chemical attaching all these molecules into the polymer backbone, which was introduced to overcome the problems of phase separation. However, compared to fully functional systems, the guest-host systems were found to demonstrate high efficient photorefractive effects. The main advantage

with this approach over fully functional polymer approach is the ease of optimization of the photorefractive systems for high performance by varying the nature and concentration of each component. The target was to design and synthesize charge transporting host polymers and electro-optic molecules needed for photorefractivity. The main conclusions drawn from this study are discussed briefly in this chapter.

Chapter 2 and Chapter 3 discusses, synthesis, characterization, electrochemical studies on a series of photoconducting polymers. Molecularly doped system containing PMMA as inert host matrix, aniline as electron donor and 2,4,6-trinitrophenol as electron acceptor was developed. The photoconductive sensitivity of the molecularly doped system was found to be 10^{-14} S cm/W. But the major problem with this system is phase separation due to large amount of low molecular weight dopants. So a series of polymers with the charge transporting unit in the main chain and side chain were synthesized via free radical and cationic ring opening polymerization techniques. The structure of the polymers was confirmed by spectral and thermal analysis. The photoconducting nature of these polymers were investigated in undoped and C_{60} doped samples. The polymer with highest photoconductive sensitivity, was chosen as the charge transporting polymer host for the development of a photorefractive system.

Chapter 4 and Chapter 5, describes synthesis and characterization of electro-optic molecules. A series of alkyl substituted p-nitroaniline derivatives were synthesized and characterized. The ground state dipole moment of the synthesized chromophores was determined using Debye-Guggenheim method and the excited state dipole moment by solvatochromic estimation. The excited state was found to be more polar indicating high degree of charge separation. All molecules exhibit positive solvatochromism. The chromophores with comparatively large figure-of-merit were selected and subjected to electro-optic studies. The guest-host system exhibited a maximum electro-optic coefficient of 2.80 pm/V. Electro-optic polymer based on (3-methacryloyl-1-(4'-nitro-4-azo-1'-phenyl) phenylalanine-co-methyl-methacrylate), was synthesized via radical initiated polymerization. The structure of the polymer was confirmed by FT-IR and NMR

analysis. The polymer showed good thermal stability. The electro-optic coefficient was determined using transmission technique. The polymer system exhibited a maximum electro-optic coefficient of 4.75 pm/V.

In Chapter 6, different combinations of photoconducting and electro-optic molecules along with plasticizer molecules and charge generators were tried to develop a guest-host photorefractive system. The system containing poly (6-tertiary-butyl-3-phenyl-3,4-dihydro-2H- 1,3-benzoxazine) as charge transporting moiety, Disperse Red 1 (DR1) as electro-optic chromophore, N-ethyl carbazole (ECZ) as plasticizer and C_{60} as charge generator showed photorefractivity. The photorefractive properties of this system was characterized by two-beam coupling. The photorefractive composite showed a gain coefficient of 8.8 cm^{-1} at an electric field of 63 V/μm. The maximum diffraction efficiency obtained was 0.002 % at an electric field of 62.5 V/μm.

The thesis presented the synthesis, characterization and studies done on a variety of molecules which can also be considered for other applications such as organic solar cells, other organic electronic devices, electro-optic modulators, etc.

Publications in International Journals

1. Photoconductivity in molecularly doped poly(methyl methacrylate) sandwich cells, *V.C. Kishore, R. Dhanya, C Sudha Kartha, K Sreekumar and Rani Joseph*, Journal of Applied Physics **101**, 063102 (2007).

2. Ground state and excited state dipole moments of alkyl substituted p-nitroaniline derivatives, *R. Dhanya, V. C. Kishore, K. Sreekumar, Rani Joseph and C. Sudha Kartha*, Spectrochimica Acta Part A: Molecular and Bimolecular Spectroscopy (*in press*).

3. On the Dipole Moments and First-order hyperpolarizability of N, N-bis(4-bromobutyl) -4-nitrobenzenamine, *V.C. Kishore, R. Dhanya, C Sudha Kartha, K Sreekumar and Rani Joseph*, Spectrochimica Acta Part A: Molecular and Bimolecular Spectroscopy (*in press*).

4. Spectral distribution of photocurrent in poly(6-tert-butyl-3-methyl-3,4-dihydro-2H-1,3-benzoxazine), *V.C. Kishore, R. Dhanya, C Sudha Kartha, K Sreekumar and Rani Joseph*, Synthetic Metals (*in press*).

5. Photoconducting Polybenzoxazines: Synthesis, Optical and Electrochemical Studies, *R. Dhanya, V. C. Kishore, K. Sreekumar, Rani Joseph and C. Sudha Kartha*, Journal of Applied Polymer Science (Communicated).

6. Synthesis, electrochemical and photoconductivity studies on poly(6-t-butyl-3,4-dihydro-2H-1,3-benzoxazine), *R. Dhanya, V. C. Kishore, K. Sreekumar, Rani Joseph and C. Sudha Kartha*, European Polymer Journal (Communicated).

7. Alkyl substituted para-nitroaniline derivatives as electro-optic chromophores, *R. Dhanya, V. C. Kishore, Daly Davis, K. Sreekumar, Rani Joseph and C. Sudha Kartha*, Journal of Macromolecular Science, Part A: Pure and Applied Chemistry (Communicated).

Publications in Conferences

1. Photophysical and electrochemical investigations on photoconducting poly (6-tertiary-butyl-3, 4-dihydro-2h-1, 3-benzoxazine), *R. Dhanya, V. C. Kishore, C Sudha Kartha, K Sreekumar and Rani Joseph.* International conference, POLYCHAR-16, 17-21 February, 2008, Lucknow, India. (IUPAC and Prof. K. S. Brar Best Poster Award)

2. The photocurrent action spectrum of poly(6-tert-butyl-3-methyl-3,4-dihydro-2H-1,3-benzoxazine)/poly(methyl methacrylate) blend, *V. C. Kishore, R. Dhanya, K Sreekumar, Rani Joseph and C Sudha Kartha.* International conference POLYCHAR-16, 17-21 February, 2008, Lucknow, India

3. Electric field dependence of thermal activation energy in poly(4TBU)/ poly(methylmethacrylate) blend, *Kishore V. C., Dhanya R., Sreekumar K., Rani Joseph and C. Sudha Kartha.* International Workshop on the Physics of Semiconductor Devices, IWPSD, 16-20 December, 2007, Mumbai, India.

4. Synthesis, Characterization and Determination of First Hyperpolarizability of N, N-bis (4-(2-aminoethylamino) butyl)-4-nitrobenzenamine, *Dhanya R., Kishore V. C., Sreekumar K., Rani Joseph and C. Sudha Kartha*, National Conference OSI, 25-28 February, 2007, Baroda, India.

5. Photoconduction in Poly(methyl methacrylate)/4-tertiary butyl phenol formaldehyde resin blend. *R. Dhanya, V. C. Kishore, C Sudha Kartha, K Sreekumar and Rani Joseph.* International Conference Photonics 2006, 12-16 December 2006, Hyderabad, India.

6. Solvatochromatic Study of the Ground and Excited State Dipole Moments of N, N-bis(4-(2-ethylamino)butyl)-4-nitrobenzenamine. *V.C. Kishore, R. Dhanya, C Sudha Kartha, K Sreekumar and Rani Joseph.* International Conference Photonics 2006, 12-16 December 2006, Hyderabad, India.

7. Photoconductivity in molecularly doped PMMA at low electric fields. *V. C. Kishore, R. Dhanya, Cheranellore Sudha Kartha, Krishnapillai Sreekumar and Rani Joseph.* International Conference on Optoelectronic Materials and Thin films for Advanced Technology, OMTAT, 2005, Cochin, India.

8. Low field extrinsic photoconductivity in Aniline doped PMMA, *Kishore V.C., R. Dhanya., Cheranellore Sudha Kartha, Krishnapillai Sreekumar and Rani Joseph.* International Conference on Optics & Optoelectronics, ICOL, 2005, Dehradun, India.